CHALMERS
UNIVERSITY OF TECHNOLOGY

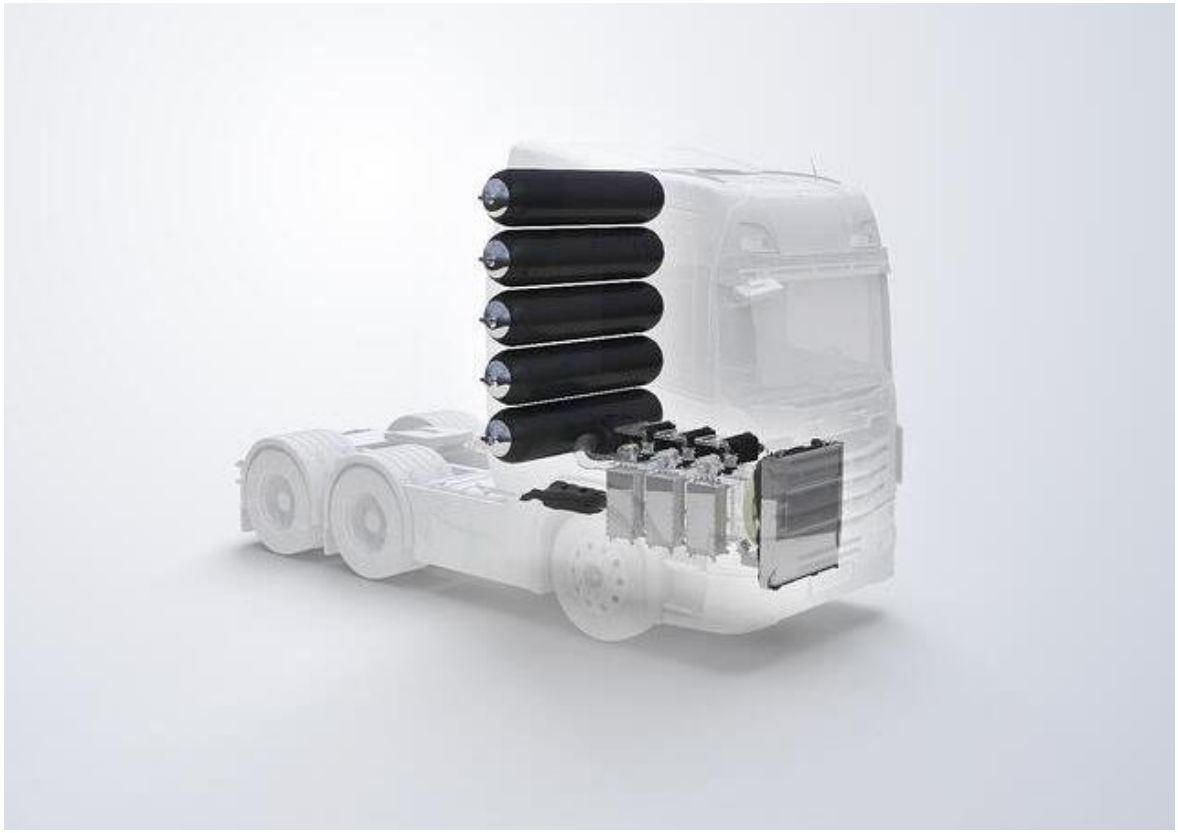

Life Cycle Assessment of Hydrogen Storage Systems for Trucks

An assessment of environmental impacts and recycling flows of carbon fiber

Master's thesis in Industrial Ecology

ELSA WEISZFLOG
MANAN ABBAS

DEPARTMENT OF TECHNOLOGY MANAGEMENT AND ECONOMICS
DIVISION OF ENVIRONMENTAL SYSTEMS ANALYSIS

CHALMERS UNIVERSITY OF TECHNOLOGY
Gothenburg, Sweden 2022
www.chalmers.se
Report No. E2022:089

REPORT NO. E2022:089

Life Cycle Assessment of Hydrogen Storage Systems for Trucks

An assessment of environmental impacts and recycling flows of carbon fiber

ELSA WEISZFLOG
MANAN ABBAS

Department of Technology Management and Economics
Division of Environmental Systems Analysis
Chalmers University of Technology
Gothenburg, Sweden 2022

Life Cycle Assessment of Hydrogen Storage Systems for Trucks
An assessment of environmental impacts and recycling flows of carbon fiber

ELSA WEISZFLOG
MANAN ABBAS

Chalmers supervisor: Anders Nordelöf, Department of Technology Management and Economics, Division of Environmental Systems Analysis

Company supervisors: Monica Johansson, Technology Strategy and Analysis, Volvo Group Trucks Technology

Examiner: Björn Sandén, Department of Technology Management and Economics, Division of Environmental Systems Analysis

Report no. E2022:089
Department of Technology Management and Economics
Chalmers University of Technology
SE-412 96 Göteborg
Sweden
Telephone +46 (0)31-772 1000

Cover: 3D prototype of a hydrogen fuel cell electric truck, sourced from Ballard.

Gothenburg, Sweden 2022

Life Cycle Assessment of Hydrogen Storage Systems for Trucks

An assessment of environmental impacts and recycling flows of carbon fiber

ELSA WEISZFLOG
MANAN ABBAS

Department of Technology Management and Economics
Chalmers University of Technology

Abstract

This thesis aims to extend the knowledge base regarding the life cycle environmental impacts of different hydrogen storage system (HSS) alternatives for fuel cell electric vehicles (FCEV). A Compressed Hydrogen (CH2) system was investigated and then used as the baseline for a comparison with a Liquid Hydrogen (LH2) storage system, and a Cryo-Compressed Hydrogen (CCH2) storage system. Further assessment was also made of the End-of-Life stage of CH2 system to capture how impacts alter if its most concerning material, Carbon Fiber Reinforced Polymer (CFRP), is recycled. The study was conducted in collaboration with Volvo Group.

As a result, two Life Cycle Assessment (LCA) case studies were conducted: one comparative of all HSSs; and one extended investigating aspects of CFRP recycling for the CH2 system. All HSS alternatives were modeled with a storage capacity of 80 kg of useable hydrogen. In both the studies, the life cycle processes were modeled in OpenLCA. The comparative LCA was modeled based on the cut-off approach, whereas the extended study credited recycling outputs back to the studied system.

The LCIA results of the CH2 system show high production related impacts, predominantly caused by the carbon fiber production. For global warming it represents almost 57% of the total impact. However, recycling CFRP shows potential to significantly reduce this life cycle impact. When comparing the CH2 system to the LH2 and CCH2 systems, both latter cause higher impacts in three out of four impact categories. This is mainly due to the use phase emissions, specifically due to the high energy demand of liquefying hydrogen compared to compressing it. Still, for global warming, the CH2 system causes a slightly higher impact.

Further research should be conducted for more detailed insights, especially regarding the utilization rate of the refueling infrastructure in the use phase. Due to the high impact of carbon fiber production, it is also proposed to evaluate a bio-based carbon fiber precursor input and study the life cycle impacts of long-term cyclic use of recycled carbon fibers.

Keywords: hydrogen storage, compressed hydrogen, liquid hydrogen, cryo-compressed hydrogen, carbon fiber, carbon fiber reinforced polymer, circular economy, life cycle assessment

Acknowledgments

We would like to extend our utmost and sincere gratitude to our supervisors, Anders Nordelöf (Researcher, Chalmers University of Technology) and Monica Johansson (Principal Energy and Fuel Analyst, Volvo Group Trucks Technology), for their continuous support throughout this thesis project. Our journey had not have been complete without their valued insights and guidance. A special thanks to our colleagues at Volvo, who were consistently flexible to our meeting requests and invested their precious time in helping us navigate and acquire the data needed.

We wish to thank Volvo and Chalmers University of Technology for this opportunity to exercise our knowledge. As we conclude our thesis, we feel we have gained more technical knowledge and the skills necessary for a thriving professional career in the corporate sector.

Finally, thanks to our families and friends for making this task easier for us with their incredible support.

Elsa Weiszflog and Manan Abbas,
Gothenburg, (20th of June, 2022)

Abbreviations

BEV	Battery Electric Vehicle
BoM	Bill of Materials
BoP	Balance of Plant
CCH2	Cryo-compressed Hydrogen
CE	Circular Economy
CFRP	Carbon Fiber Reinforced Polymer
CH2	Compressed Hydrogen
EoL	End of Life
EU	European Union
GH_2	Green Hydrogen
GHG	Greenhouse Gas
GWP	Global Warming Potential
HDPE	High Density Polyethylene
HDV	Heavy Duty Vehicle
FCEV	Fuel Cell Electric Vehicle
ILCD	International Reference Life Cycle Data System
IE	Industrial Ecology
IPCC	International Panel on Climate Change
LCA	Life Cycle Assessment
LCI	Life Cycle Inventory
LCIA	Life Cycle Impact Assessment
LH2	Liquid Hydrogen
OEM	Original Equipment Manufacturer
PM	Particulate Matter
RQ	Research Question
SOP	Surplus Ore Potential
Volvo	Volvo Group

Contents

Appendices

1 Introduction

1.1 Background

It is confirmed by the Intergovernmental Panel on Climate Change (IPCC) that global warming is one of the most urgent challenges of the 21st century (IPCC, 2021). The latest IPCC report confirms that human influence has contributed to climate change significantly. The continuous emission of greenhouse gases (GHGs), especially carbon dioxide (CO_2), has warmed the Earth's atmosphere and caused changes to the environment (IPCC, 2021). There is now an increasing global demand for action. In 2017, the transport sector alone was responsible for 27 % of the total European GHG emissions (European Environment Agency, 2019). Additionally, this sector poses significant challenges to human and environmental health through the pollution of air and the environment (Nowakowska-Grunt & Strzelczyk, 2019).

Road traffic has reached capacities at which it causes the largest share (70%) of the transport related GHG emissions in the European Union (EU) (European Environment Agency, 2021). Even if passenger vehicles are the most abundant, the small share of medium and heavy-duty trucks contributes significantly to transport-related emissions (Lee et al., 2018). In 2016, Heavy-Duty Vehicles (HDVs) were responsible for 27% of road transport CO_2 emissions, which will increase to 32% by 2030 if no actions are taken (European Environment Agency, 2018). The HDV sector is key to national economies and has a pivotal role in human society (Nowakowska-Grunt & Strzelczyk, 2019). Therefore, limiting road freight transport by reducing it is not a preferable option. Instead, other feasible alternatives must be explored and implemented.

The EU introduced a new regulation in 2019 due to the high emission levels of the HDV sector and its goal to create a safe and sustainable transport system. The target is to reduce average emissions from new HDVs. Targets are set for the manufacturers and their fleet-wide average CO_2 emissions of new trucks put on the market in a specific year. Targets are set as percentage reductions compared to the reference period in 2019/20. For 2025, a 15% reduction is set, and for 2030 the EU aims for a 30% reduction. This regulation also includes an incentive mechanism for zero and low-emission vehicles (European Union, 2019).

Currently, different options exist for manufacturing low or zero-emission HDVs. In late 2018, Volvo Group (Volvo) announced the first fully electric heavy-duty truck (AB Volvo, 2018). Other companies, such as Scania, have also pursued emissions reduction by introducing Battery Electric Vehicles (BEVs). According to Booto et al. (2021) , a BEV can cut up to about 70% of GHGs compared to combustion engine trucks, i.e., about 0.6 kg CO_2-eq per km. However, it depends on the carbon intensity of the fuel for the respective vehicles. Another alternative to produce low or zero-emission HDVs is Fuel Cell Electric Vehicles (FCEVs). In 2021, Hyundai already launched ten of its FCEVs in the Netherlands and Switzerland. However, these trucks currently have a driving range of 400 km per charge (HYUNDAI Truck & Bus, n.d.). The two leading European manufacturers, Volvo and Daimler, are currently working on an FCEV with a driving range of up to 1000 km and aim to launch them before 2030 (Daimler Truck, 2021, Volvo) . Compared to a combustion engine truck, an FCEV has the potential to cut up to half the amount of GHGs, which is 20% less than the reduction potential of a BEV (Booto et al., 2021). Nevertheless, this potential is dependent on the production methods of the hydrogen.

Essentially, the powertrain of an FCEV and that of a BEV are very similar. Both types of vehicles run on electric energy, and therefore both contain electric motors. The difference lies in the source of electric energy. For a BEV, the electricity is supplied only by batteries with capacities from 180 to 540 kWh, and it has a limited range of up to 300 km (Volvo Truck, n.d.). The FCEV, on the other hand, generates its electricity from hydrogen. This process takes place via a fuel cell system in which the hydrogen and oxygen convert into water and electric energy, which is then delivered to the electric

motor. However, fuel cells operate best in a steady state and respond slowly to the varying power demands of the FCEV. Therefore, the FCEVs entail a small battery as well. When the vehicle needs more power to increase speed or accelerate, the battery provides energy. The battery can also take up excess energy from the fuel cell or braking energy (J. Bergström, personal communication, February 16, 2022). For this vehicle, hydrogen fuel is stored in a tank system on the FCEV. The onboard storage of hydrogen allows for increased driving ranges and refueling speed compared to a BEV (M. Johansson, personal communication, January 28, 2022).

However, on-truck storage poses one of the biggest challenges for FCEVs. Hydrogen is an extremely light gas with a density lower than air, making gaseous hydrogen storage at normal atmospheric pressure (1 bar) very inefficient. Therefore, the hydrogen density must be increased significantly to make the tank systems space-efficient for FCEVs. This challenge of high-density hydrogen storage is subject to ongoing research in the scientific community and vehicle industry. At present, three systems are being discussed for hydrogen storage on trucks: Compressed Hydrogen (CH2), Liquid Hydrogen (LH2), and Cryo-Compressed Hydrogen (CCH2) storage systems (M., Johansson, personal communication, January 24, 2022). Since hydrogen-based freight transport is an emerging field, other technologies could become options for future implementation. However, currently, the CH2 system is the most developed technology.

Economic, engineering, and feasibility parameters are vital in choosing a hydrogen storage system (HSS). However, it is equally important to perform an environmental assessment of these emerging technologies. These technologies are in a formative phase, meaning they are not currently mature and produced at a large scale. Therefore, the possibility of environmental assessments influencing technology improvements is high (Arvidsson et al., 2018). These different hydrogen storage technologies are more complex than containing just a simple tank. They also have various other components that connect the tanks to the fuel cell. The production of different storage systems requires inputs of varying types and amounts of materials, involving clearly different processes. Therefore, they cause different environmental impacts. One of the main concerns about the most mature technology, the CH2 system, is its composition's high content of carbon fibers. According to Meng et al. (2018), carbon fibers production requires high energy inputs, which can cause relevant environmental burdens. Still, detailed environmental assessments of tank systems for this type of truck do not yet exist. This information gap poses a challenge for the ongoing development process of FCEVs which has important implications for the future environmental impacts of the HSSs.

1.2 Aim and Problem Formulation

This study aims to extend the knowledge base on the environmental impacts of HSSs. The objective is to assess and compare the environmental impact of the three most relevant HSSs for trucks: the CH2 system, LH2 system, and CCH2 system. It also aimed to analyze the material flows from a Circular Economy (CE) perspective to identify possible improvements. The overall research questions (RQs) investigated by this study are:

> *RQ1: What is the life cycle environmental impact of compressed hydrogen storage systems at 700 bars with storage capacity to enable a driving range of 1000 km?*
>
> *RQ2: How do the impacts of cryo-compressed and liquid storage tanks compare to those of a compressed system?*
>
> *RQ3: How can the recycling of carbon fiber affect the life cycle environmental impacts of the compressed system?*

Life Cycle Assessment (LCA) is applied to answer these research questions. The investigation also aims to identify steps in the life cycle of the HSSs causing most environmental impacts and identify the potential of change in impacts of the CH2 system by carbon fiber recycling.

Volvo is a major producer of trucks and holds a significant share in the HDV market of the EU (European Environment Agency, 2018). Its commitment pathway to reach the goals of the Paris agreement are validated by Science Based Targets initiative (SBTi) which drives its ambition to explore low/zero-emission technologies in manufacturing its trucks for the future (AB Volvo, 2021). This thesis project is conducted in collaboration with Volvo to examine the environmental impacts and compare them for three HSSs that could potentially be used in the upcoming FCEVs.

2 Theory

This section presents the theoretical frameworks, terms, and tools used in the study.

2.1 Principles and Framework for Life Cycle Assessment

LCA is a standardized tool for evaluating the environmental impacts of a product system over all stages of its life cycle. It can be used for general learning or, for example, to support decision-making, i.e., for policymakers, businesses, and consumers. The framework is illustrated in Figure 2.1 and shows the main steps of an LCA as per the International Organization of Standardization (ISO) 14040 standard guidelines: Goal and Scope, Inventory Analysis, Impact Assessment, and Interpretation.

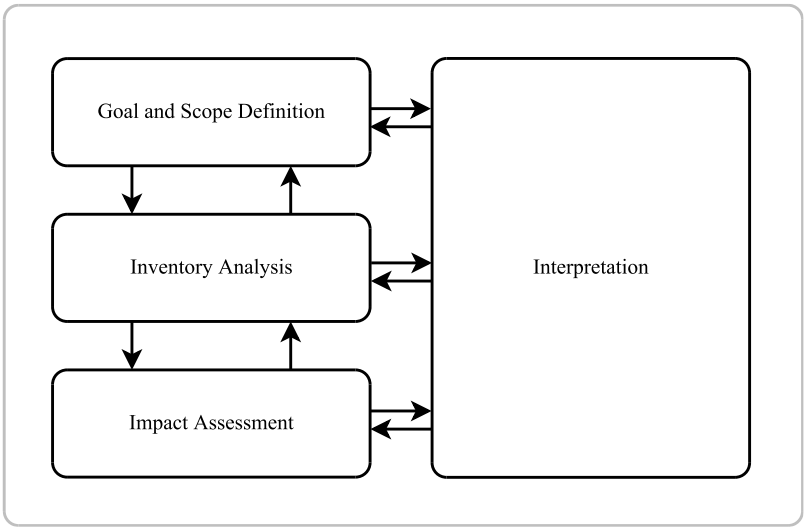

Figure 2.1. Life Cycle Assessment Framework

2.1.1 Goal and Scope Definition

The goal definition answers the following questions: What? Why? And for whom? The answers describe the intended application, reasons for conducting the research, and the intended audience. The system and its boundaries are determined by describing its temporal, geographical, and technical extent in a scope definition. The scope determines the width and depth with which the LCA is conducted. Deciding the primary function of the product system is another essential part of the scope. It defines the functional unit, which forms the reference for quantifying the product performance.

The approach for modeling the study system is selected in the goal and scope definition. There are two different modeling approaches: attributional and consequential modeling. The earlier accounts for steady-state environmental flows from the life cycle of a defined product system; the latter, however, depicts the direct consequences in response to changes in the existing product system (Finnveden et al., 2009). The attributional modeling is used to find improvement points, estimate different types of footprints, or compare environmental performance without any effects of interaction with other systems. The consequential modeling is used to assess the consequences of promoting one thing over the other, applying specific policies, or comparing the environmental performance of two products that would generate changes in the economy.

Furthermore, impact categories are chosen for the product assessment as a part of defining the system boundary between the technical system and the natural system and to determine which types of elementary flows to include in the modeling.

2.1.2 Inventory Analysis

In the inventory analysis, a chosen system is modeled. It includes all relevant system inputs and outputs in the form of resources and emissions to air, water, and land. This step entails the main data collection. Foreground and background data are researched in an iterative process. Furthermore, calculations include allocation procedures, where systems have multiple inputs or outputs. This step compiles the environmental flows per functional unit in a Life Cycle Inventory (LCI).

2.1.3 Impact Assessment

An impact category refers to a specific cause-effect chain linking emissions or resource use to represent a unique environmental problem. The impact categories applied in this study are defined as "midpoint" indicators which means that they represent a single environmental impact, such as climate change. This indicator reports how life cycle emissions of the product under study contribute to global warming by summing their Global Warming Potential (GWP), which is measured in CO_2-equivalents (eq). Non-CO_2 GHG emissions are converted to CO_2-eq to calculate a total global warming potential. In contrast to midpoint indicators, endpoint indicators characterize aggregated environmental effects on higher levels, for instance, impact on human health (Huijbregts et al., 2017). However, endpoint indicators are not included in this study. The midpoint impact categories applied in this study are described in sections 2.1.3.1 – 2.1.3.4 below. The relationship between these selected impact categories and the endpoint areas of protection is shown in Figure 2.2.

The compulsory steps of the Life Cycle Impact Assessment (LCIA) stage in LCA are the classification and characterization of the LCI results. These steps are performed for all selected impact categories. The characterization attempts to make sense of the environmental impacts and model them within their impact category. There exist different packages of methods that can be applied in this step. Commonly used such method packages are "CML" and "ReCiPe", where in each case all methods have been developed by the same group of researchers, or "ILCD", which is bundled set of methods from different sources, recommended by the International Reference Life Cycle Data System (ILCD) initiative (European Commission et al., 2010). The methods generally take different approaches to calculate the impact and include slightly different types of impact categories. When relevant, the LCIA can also include the steps of normalization, weighting, and sensitivity analysis.

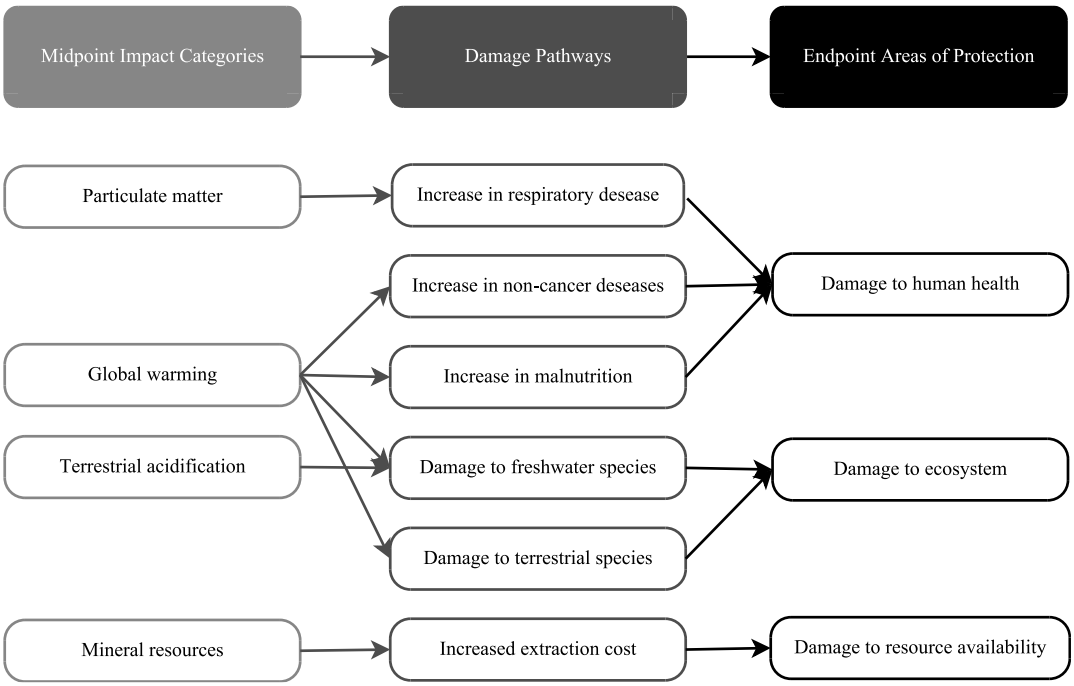

Figure 2.2. Relationship among impact categories, damage pathways, and endpoints.

2.1.3.1 Climate Change

Climate change and global warming are frequently used in similar contexts, but they have distinctive meanings. The long-term changes in average weather patterns define climate change, whereas global warming measures the heating of the Earth's climate since the pre-industrial era (NASA, n.d.). Global warming is indicated by the increase in the Earth's temperature triggered by increased infra-red radiative forcing (Huijbregts et al., 2017). This imbalance in radiative forcing is caused by the greenhouse effect of carbon dioxide (CO_2), methane (CH_4), chlorofluorocarbons (CFCs), and other GHG emissions to the atmosphere.

The role of emissions pollution in climate change is generally characterized by Global Warming Potential (GWP). GWP is measured in 'kg of CO_2-eq' emitted to the atmosphere and accounts for all GHGs. GWP is the ratio of additional radiative forcing integrated over time caused by the emission of 1 kg of GHGs relative to the additional radiative forcing integrated over the same time horizon caused by 1 kg of CO_2 release. In this study, the time horizon of 100 years is selected, which is regarded as a consistent choice owing to the varying atmospheric lifetimes of the GHG (Huijbregts et al., 2017).

2.1.3.2 Mineral Resource Scarcity

This impact category analyzes the future availability of the mineral resources such as iron, platinum, and cobalt. These abiotic resources are of instrumental value to humans and the survival of the Technosphere. The extraction of mineral resources deteriorates ore grade, and over time total ore extractions and their energy requirements increase, inducing surplus costs (Calvo et al., 2016).

As per the LCIA method applied in this study, the mineral resource scarcity is characterized by Surplus Ore Potential (SOP). SOP expresses the average extra ore to be produced in the future due to extraction of 1 kg of a particular resource 'x' relative to extra production of copper due to extraction of 1 kg of copper, considering all future extractions. SOP is measured in a unit of kg Cu-eq/kg x (Huijbregts et al., 2017).

2.1.3.3 Fine Particulate Matter Formation

This impact category calculates the potential air pollution caused by secondary aerosols. The Particulate Matter (PM), especially fine particles of size less than 2.5 microns, the PM2.5 are crucial to human health because they are linked to chronic public health impacts (Health Organization & Office for Europe, 2013). PM2.5 is formed in the atmosphere mainly due to precursor pollutants of ammonia (NH_3), sulfur dioxide (SO_2), and nitrogen oxides (NO_X) (Kim et al., 2015).

In the selected LCIA method, fine particulate matter formation is indicated by the increase in PM2.5 intake by population. It is characterized by Particulate Matter Formation Potential (PMFP) in the 'kg PM2.5 to air' unit. It is the ratio of PM2.5 intake per precursor 'x' in a particular region 'i' to the average global intake fraction of PM2.5. (Huijbregts et al., 2017).

2.1.3.4 Terrestrial Acidification

Terrestrial acidification describes the process of changes in acid levels in the ground caused by atmospheric deposition of inorganic substances and can have negative repercussions for plant life. The main emissions consist of nitrate oxide (NO_x), ammonia (NH_3), and sulfur dioxide (SO_2). The sulfates, nitrates, and phosphates are emitted into the air. Then these emissions move into the atmosphere before leaching into the ground due to acid rain. These emissions cause a change in the soil solution H^+ concentration, which is the indicator for acidification at a midpoint (Huijbregts et al., 2017).

The role of emission in terrestrial acidification is measured in acidification potential (AP). "The AP quantifies the increase in soil acidity by a substance emission relative to SO_2" and is measured in 'kg SO_2-eq' (Huijbregts et al., 2017, p. 58). The midpoint characterization factors are dependent on the changes in acid deposition and soil sensitivity. (Huijbregts et al., 2017).

2.1.4 Interpretation

The interpretation of the study takes place in close relation to all other phases of the LCA. Results are interpreted with consideration to the given limitations to reach conclusions and formulate recommendations. It is essential to revisit the goal, scope, key assumptions, inventory models, and allocation methods during this step. In the process, the results are checked for consistency and completeness. A contribution or dominance analysis can be performed to identify certain hotspots in a product life cycle. These show which part has the most significant environmental impact or show which elementary flows or impact categories contribute the most to the environmental impact.

2.2 Life Cycle Assessment Modeling Software

Multiple software tools support LCA studies involving complex networked and loop flows. Examples are OpenLCA, SimaPro, and GaBi, renowned among the LCA analysts in the educational and industrial sectors. These tools can model complex data and reproduce useful analytics in compliance with the ISO 14040 standard. If required, weighting methods can also be applied. They integrate inventory data for different upstream processes in the life cycle and impact assessment datasets. These computational and integration features render conducting LCA relatively simple, and they enable transparent assessments making the data quality and analysis open to reviews.

This study utilizes OpenLCA, which is open source and free software. OpenLCA requires the integration of an external database for inventory and impact assessment data. The Ecoinvent 3.7.1 cutoff database licensed for educational purposes was used in this study. The database accounts for the use of secondary raw materials inputs in the production phase of the product system.

The OpenLCA allows creating new processes or using those processes in the imported database. All processes in the LCA model are to be networked and may include all upstream activities according to the study scope and boundaries. Modeling a unit process in the OpenLCA requires defining the inputs and output flows based on a reference flow defined by the LCA analyst.

The software also enables analysis of the model and related computations. It identifies the main drivers of environmental impacts from processes and flows per impact category. OpenLCA also provides a visual representation of geographical locations where impacts occur. Other qualities include the import and export of results in spreadsheet formats which can be utilized to make select analyses. However, manual data processing concerning many flows and processes can be challenging. The data exported from OpenLCA can also be used for conducting dominance analysis.

2.3 Circular Economy and Circular Material Flows

According to Ellen McArthur Foundation, CE eliminates waste and pollution, circulates products and materials, and regenerates nature, in contrast to the take-make-waste model of the current economy. It works around two cycles, the technical and biological cycles. In the technical cycle, products are retained to circulate through reuse, repair, remanufacturing, and recycling. At the same time, the biological cycle aims to return the nutrients from biodegradable materials to the Earth. This concept of CE from Ellen McArthur Foundation is visualized in Figure 2.3. According to Bocken et al. (2014), the CE context revolves around closing, narrowing, and slowing the material loops. There are multiple evolving concepts of CE in the literature. However, the overall aim of the CE is to enable sustainable development and decouple economic growth from the environmental impacts (Millette et al., 2019).

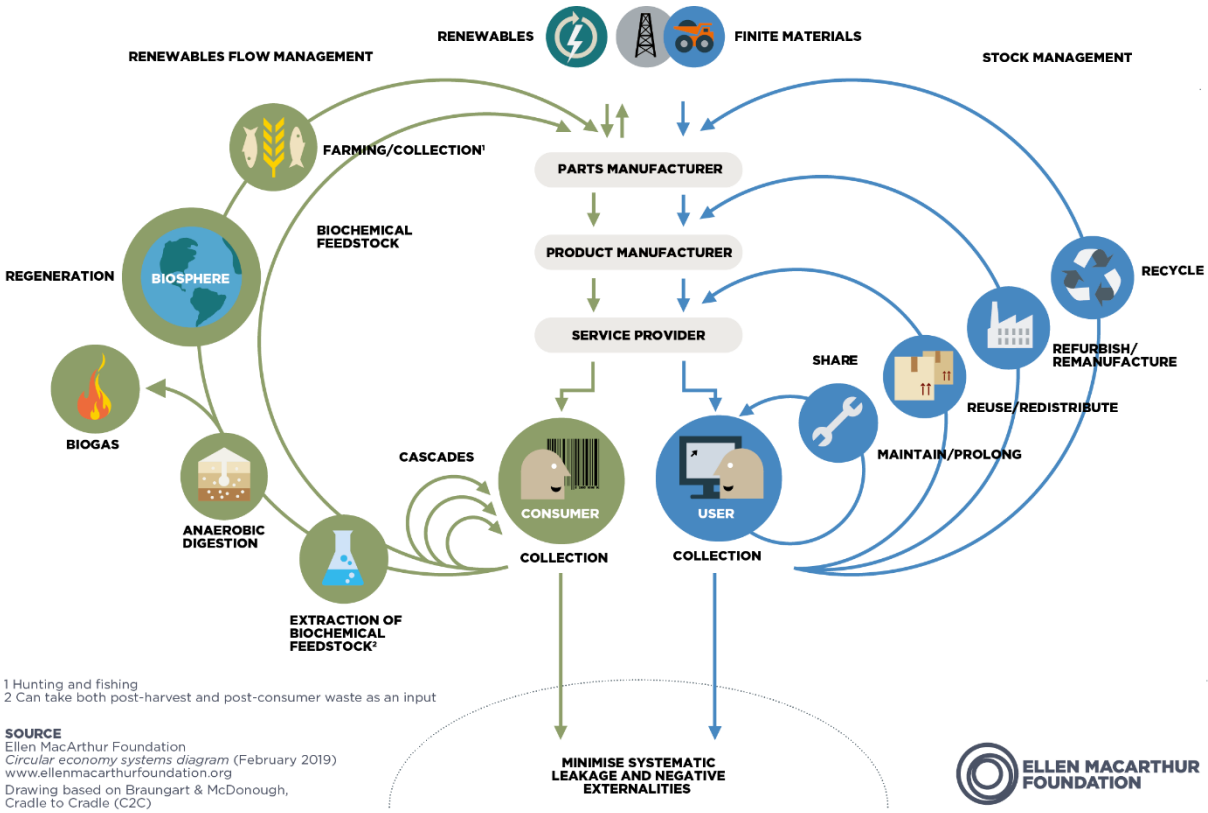

Figure 2.3 Circular economy systems diagram by Ellen McArthur Foundation

The drivers for businesses to achieve better CE are the value capture from materials, energy savings, and novel business opportunities, for example, remanufacturing, servitized business models, and enhanced customer interaction and loyalty. The CE strategies are implemented ideally within business models encompassing actors, networks, and consumers. CE improvements by businesses can be achieved from circular strategies which rightly match the product characteristics; otherwise, the environmental benefit can be risked, or other types of impact may emerge (Tillman et al., 2020). Therefore, multiple configurations of circular strategies must be assessed for environmental impacts (Blomsma & Brennan, 2017). LCA belongs to the set of Industrial Ecology (IE) tools that can be used for such assessments.

At the microlevel of a business, reducing primary resource and waste outputs is one of the CE aims. For instance, it promotes industrial symbiosis by using waste as input for other businesses enabling closed-loop material flows. Moreover, the closed-loop recycling of materials contributes to the circular economy by retaining the material flows within the economy (Hazell, 2017). However, it is crucial to understand the impact of circular material flows within a system. LCA is a helpful tool to assess the impacts of materials recycling and identify environmental opportunities for improved circularity within the studied system.

3 Technical Background

This section provides the technical description and functionality of the HSSs analyzed in the overall study. These are the CH2 system, LH2 system, and CCH2 system. Additionally, the primary material used in manufacturing the CH2 system tanks is also discussed.

3.1 Compressed Hydrogen Storage System

The CH2 system consists of several hydrogen storage tanks, various auxiliary components constituting its BoP, and a metal frame that mounts all the CH2 system parts together and attaches them to the truck. The CH2 system tanks store hydrogen in gaseous form with increased pressure. These tanks can be classified into different types (I, II, III, and IV). This study focuses on type IV tanks made for hydrogen compressed at 700 bars. The International Organization for Standardization (2009) defines type IV tanks as fuel tanks which fully wrapped with composite material and do not contain a metal liner.

The CH2 system collects hydrogen from the fuel station, stores it in tanks, and delivers it to the fuel cell system under optimal conditions. The hydrogen enters the CH2 system via a filling receptacle and makes its way to the tanks through a network of pipes and the on-tank valve. On its way to the fuel cell, hydrogen passes through one or two pressure regulators, which lower the pressure before the hydrogen enters the fuel cell. The first pressure regulator, the gas handling unit, mainly comprises of vent lines, valves, and gauges for checking the temperature and pressure of the system. It depressurizes the hydrogen and checks that the pressure does not exceed 30 bars. The hydrogen is further depressurized in the second pressure regulator to avoid damaging the fuel cell system. Typically, the minimum pressure is between 2-5 bar in fuel cell systems, and the maximum pressure is between 10-25 bar. If the maximum is exceeded, hydrogen is released from the CH2 system through valves. The system also contains an electronic control unit that continuously performs temperature and pressure checks. Its other processes include maintaining communication between the FCEV and the CH2 system, managing signals from sensors, and activating the on-tank valve (A. Hagby, personal communication, March 2, 2022).

3.1.1 Carbon Fiber Reinforced Polymer

The Carbon Fiber Reinforced Polymer (CFRP) is a significant material constituent of the type IV tanks used in the CH2 system. It is also used to manufacture tanks for the CCH2 systems. Apart from that, CFRP is also widely used to produce various high-performance products, for example, car and airplane bodies or sporting equipment. The demand for CFRP is proliferating in various industry sectors due to its unique properties, such as specific strength and low density (Zhang et al., 2020). According to a study by the Federation of Reinforced Plastics (2017), the compound annual growth rate of CFRP demand from 2010 to 2022 was projected at 11.98%. Carbon fibers are used as the primary material in the production of CFRP composites. Production of CFRP using virgin carbon fibers is very cost-intensive since virgin carbon fibers production requires significant amounts of energy (Meng et al., 2018). At EoL, the CFRP waste usually is landfilled or incinerated despite the existing commercial recycling methods. Instead, CFRP can be recycled to recover carbon fibers, potentially improving the circular economy.

3.2 Liquid Hydrogen Storage System

The LH2 system stores hydrogen in the liquid form rather than gaseous. It requires hydrogen cooling until -253 degrees Celsius (20 K). This liquefaction process involves compressors, heat exchangers, expansion engines, and throttle valves (Allevi & Collodi, 2017). The most significant advantage of liquid hydrogen is its high energy density, nearly twice as high as compressed hydrogen at 700 bars (Sheffield et al., 2014). The high energy density of hydrogen significantly reduces the space needed for storing it. However, the liquefication process is very energy intensive as it requires about 35% of the

lower heating value (LHV) energy content of the liquified hydrogen (Abdin & Khalilpour, 2019). Moreover, due to the very low boiling temperature of hydrogen, LH2 tanks require advanced insulation and cooling methods to avoid the gasification of hydrogen (Viswanathan, 2017).

In the LH2 tanks, hydrogen is stored as a cold gas and liquid mix. The liquid hydrogen is sprayed on the gas during refueling to cool it down further. Depending on the system and the supplier, the LH2 tanks run on about 6 bars when in operation. However, despite the insulation and careful management, a limited heat transfer between the liquid and the environment leads to slow gasification of hydrogen, which increases the pressure in the tanks. It does not create problems while the FCEV operates because hydrogen is removed continuously. However, the pressure can increase past the allowed maximum when the vehicle is parked. Therefore, a boil-off management system is in place that releases hydrogen in a controlled way once the upper-pressure limit is exceeded. These quick releases happen incrementally. Alternative to just releasing the hydrogen, it can be utilized to support other vehicle functions. The amount of hydrogen lost through boil-off depends on the filling level of the tank when parking the vehicle. The fuller the tank, the more likely that boil-off will occur due to less space for the gaseous hydrogen to expand.

Before hydrogen can enter the fuel cell, it must increase the temperature to at least -40°C. Therefore, LH2 tanks have a heat exchanger at the exit point. If too much hydrogen is removed from the tank, the pressure can drop below 6 bars. In such a case, heaters in the tank boil the hydrogen, which gasifies and again increases the tank pressure. The LH2 system is integrated with the cooling system of the FCEV, from where it gets most of the required heat. The warm hydrogen can then be fed back to the tank's heat exchanger.

3.3 Cryo-compressed Hydrogen Storage System

The CCH2 system combines the attributes of the technologies mentioned above, as this tank is designed to withstand high pressure and cryogenic temperatures. It means that the CCH2 tanks have higher storage capacity than the CH2 tanks and lower boil-off losses than the LH2 tanks. Since the tank must withhold lower pressures, it reduces the need for carbon fiber composites (Langmi et al., 2022).

In contrast to the LH2 system, hydrogen in the CCH2 tank is stored in gaseous form at low temperatures, called cryogas. However, there are two different ways to create cryogas during refueling. In the first method, liquid hydrogen is refueled in the CCH2 tanks, then cryo-compressed to 300-400 bars. This refueling technique delivers cryogas at 35-50K and has already been tested for technical viability. Another option is to create cryogas from cryo-cooling of compressed hydrogen and deliver cryogas at 70 – 80 K. This technique is still being researched and only theoretically proven. On the one hand, this method avoids the energy-intensive liquefication step. However, it also delivers slightly warmer cryogas, requiring more space than the cryogas from the first technique (F. Haberl, personal communication, April 15, 2022; Cryomotive GmbH, 2021).

The CCH2 system also contains a heat exchanger due to the low temperatures of cryogas. It is also integrated with the FCEV's cooling system to warm up the hydrogen. Additionally, the system also contains a pressure regulator to depressurize the gas. Together, these components regulate the hydrogen to be at least -40°C and in an acceptable pressure range before it enters the fuel cell (F. Haberl & P. Arya, personal communication, April 25, 2022).

4 Methods

This chapter is dedicated to describing the methods of conducting this study. It also includes discussions related to the modeling in OpenLCA and the procedure for verifying the robustness of results.

4.1 General Methodology

This study uses LCA as the principal method. Several iterative steps were needed in the modeling and data collection to answer the research questions. A numerical analysis was performed in Excel to estimate the weight and material of balance of plant (BoP) components in the HSSs. The weight-related hydrogen losses were modeled using Matlab and Excel. The results from these analyses were used as LCI data for the production and use phase.

The LCA was conducted in two stages to achieve the overall objectives. A comparative LCA study was conducted in the first stage, discussed in section 5. This case study defined the CH2 system as a baseline system and compared it with the LH2 and CCH2 systems. The EoL phase was modeled with the cutoff approach. Section 6 of this report describes the second stage, an extended LCA of the baseline system. In the extended study, an alternate EoL approach was modeled. The CFRP waste is recycled to recover carbon fibers as secondary raw material in this model version. The objective of this extension study was to assess the impacts of introducing the recycling of carbon fibers in the CH2 system life cycle.

The CH2 system was modeled to contain 50% CFRP by weight with carbon fibers to the epoxy ratio of 3:2. Therefore, CFRP was identified as crucial material and selected to be further studied for its recycling in the extension study. Various setups for CFRP recycling were developed and studied based on commercial and technically viable recycling methods presented by the scientific literature. The literature review and the studied recycling methods are discussed in section 6.

The modeled study system was divided into the foreground, background, and core systems, collectively referred to as the technical system in this study. The foreground system consisted of all those processes modeled with data acquired from literature studies or modified LCI datasets from Ecoinvent. The discussions and references to foreground data are presented in sections 5.2 and 6.4. In contrast to the foreground system, the background system consisted of processes that only used generic Ecoinvent data. A third subsystem, referred to as the core system, was also established. It contained only those system processes that were in the direct focus of Volvo by selecting the HSSs' design. The core system was modeled with the primary data provided by Volvo related to material compositions for all the HSSs. The mass balancing of material composition data is described in section 4.2. However, all the other data related to the core system, such as materials production, were sourced from the foreground and background systems. In the end, a sensitivity analysis was conducted for various parameters of the CH2 system, which included the weight of BoP components, tank production location, and the tanks' lifetime.

4.2 Mass Balancing of Hydrogen Storage Systems

The mass balancing was performed taking the top-down approach in which all the HSS components were categorized into three types overall. Each category was further investigated for its material type and corresponding weight based on Volvo's bill of materials (BoM) of the HSSs. These investigations comprised estimations to complete the mass balance of the HSSs.

4.2.1 CH2 System

The CH2 system consists of hydrogen storage tanks, a frame to attach the tanks to the vehicle, and BoP components. The material composition of the tanks was established through estimations with the support of Volvo experts. The numbers were further normalized for precisely 80kg of hydrogen storage.

The approximate weights of the materials for the CH2 tanks storing 80kg of usable hydrogen are presented in Table 4.1. The Volvo experts estimated the frame to weigh about 1120 kg for the CH2 system composed entirely of steel type S355 (S. Sonderegger, personal communication, April 4, 2022).

Table 4.1. The normalized weights of materials in CH2 tanks for storing 80 kg of usable hydrogen (Volvo, 2022)

Components	**Amount (kg)**	**Amount (%)**
Carbon fibers	810	55
Epoxy resin	540	36
High Density Polyethylene (HDPE) liner	120	8
Boss	10	1
Total	1480	100

The BoM for BoP components of 700 bar CH2 systems was not complete. Therefore, its material contents and mass balance were estimated using several sources of information and assumptions. These included the BoM of a 350-bar CH2 system storing 35 kg of usable hydrogen from a test vehicle, and a separate research study. In the latter study by Elgowainy et al. (2013), the BoP of a 350 and a 700 bar CH2 systems CCH2 systems are compared. The overall estimation was performed in three steps described below, and Volvo experts approved the results.

First, the BoP weight estimations were carried out for the 350-bar system since it had data for the total BoP mass available. According to Elgowainy et al. (2013), the BoP components can be divided into five categories: electronics, pipes, valves, instruments, and miscellaneous. The author analyzed a 350- and a 700-bar CH2 systems, which stored 6 and 5.8kg of hydrogen, assuming the same BoP categorization for both tanks. The BoP weights per category for one tank established by Elgowainy et al. (2013) are provided in column 2 of Table 4.2 below. The weight distribution in percent is reported in the subsequent column. The same distribution was then applied to the BoP weight of the 350-bar system in the test vehicle. The resulting masses of the parts in the 350-bar system are also reported in Table 4.2.

In the second step, the BoP category weights for the 350-bar system were upscaled to fit the 700-bar system. A higher BoP weight was assumed for two reasons. First, because the number of tanks is directly related to the number of specific BoP components, most components that depended on the number of tanks belonged to the valves and the miscellaneous category of the BoP. Since the 700-bar system contains more tanks, the components were scaled up accordingly. Secondly, the 700-bar system endures double the pressure as in the 350-bar system, which requires its components to be stronger and thicker. It required increasing the weight of the material content of the 700-bar system components. This increase was assumed to apply only to the BoP pipes and valves category, so their weight was scaled up by a factor of 1.5.

Table 4.2. The Weights of the Balance of Plants components from the paper, and for Volvo's 350- and 700-bar CH2 systems.

BoP categories	**Weight from** Elgowainy et al. (2013) **(kg)**	**BoP weight per category (%)**	**Weights for 350-bar tanks (kg)**	**Weights for 700-bar tanks (kg)**
Electronics	1	7%	6	6
Valves	3.4	25%	20	37
Instruments	3.3	24%	20	20
Piping	4	29%	24	36
Diverse	2	15%	12	14
Total	13.7	100%	82	113

Finally, the material composition of each category was determined by going through the BoM of the 350-bar systems and identifying the main materials used for the heaviest components of each category. Due to a lack of primary information, this was done in discussion with Volvo experts. All these steps resulted in estimating the overall weight contribution of tanks, frame, and BoP components in the CH2 system, as presented in Table 4.3.

Table 4.3. Weights of the CH2 system.

CH2 system	**Amount**	**Unit**
700-bar tanks	1480	kg
Frame	1120	kg
Balance of Plants	110	kg
Total weight	2710	kg

4.2.2 LH2 and CCH2 system

The LH2 and CCH2 systems also consist of tanks, BoP components, and a frame. However, much fewer data were available for these systems, especially the BoP components, than for the CH2 system. Therefore, the BoP components of these systems were not investigated and modeled in the baseline LCA study. Estimates of the weight and material composition of the LH2 and CCH2 tanks and their frame were provided by Volvo. The CCH2 system tank composition contains CFRP since it sustains high-pressure conditions, differing from the LH2 system. The materials mass balance for the tanks and frame for LH2 and CCH2 systems was performed in the same way as the CH2 system and based on Volvo data. The composition and weights for LH2 and CCH2 systems for 80 kg hydrogen storage are shown in Table 4.4 below.

Table 4.4. Normalized weight of components for LH2 and CCH2 systems, excluding the BoP (Volvo, 2022).

Components	**Amount LH2 tank**	**Amount CCH2 tank**	**Unit**
Inner Vessel (Liner)	320	350	kg
Boss	5	8	kg
CFRP	-	550	kg
Other steel	350	530	kg
Vacuum layer	10	20	kg
Frame	480	800	kg
Total	1165	2260	kg

A comparison of the life cycle impacts of three HSSs was performed in section 5 without including BoP components for the LH2 and CCH2 systems. The difference in environmental impacts can then be seen as an emissions budget for the BoP of each system and each impact category, representing the maximum burden of emissions that the BoP of the LH2 and CCH2 systems may cause before exceeding the burden caused by the CH2 system.

4.3 Hydrogen Loss Modeling

The use phase model of this LCA study accounts for the hydrogen use that can be assigned to the tank system, i.e., the amount of hydrogen it loses during FCEV operation. It required further analysis and estimation of hydrogen losses for all three HSS. Two types of losses were identified, the loss attributed to the tank weight and losses due to boil-off. The first type of hydrogen loss was shared among all HSSs, where hydrogen is lost in propelling the weight of the HSS. The second type of hydrogen loss is due to boil-off, which applies only to the LH2 and CCH2 systems.

The boil-off losses occur when liquid hydrogen turns back into gaseous form, expands in the tank, and must be released. According to Haberl (Personal communication, April 4, 2022), the boil-off losses were estimated between 1 and 10%; however, they are substantially lower for CCH2 than LH2.

The second type of hydrogen loss refers to the hydrogen allocated to propelling the HSS. It was modeled in Matlab, for which Volvo provided the code. To calculate the potential loss of hydrogen in propelling the HSS weight during the FCEV operation, other factors, such as rolling and grade resistance, needed to be eliminated. In the model, 20 standard trips in Europe are used for which the total energy use of the FCEV was known. The energy allocated to propelling the weight of the entire FCEV was calculated in Matlab by separating the energy used to overcome rolling and grade resistance. The results were exported to Excel, where the energy for propelling the HSS (E_{HSS}) was calculated for all three systems. The E_{HSS} calculation was based on the average energy used for the weight of the FCEV ($E_{FCEV,av}$) and the weight ratio from HSS to FCEV. It was performed using the following formula:

$$E_{HSS} = \frac{W_{HSS}}{W_{FCEV}} * E_{FCEV,av}$$

The results are shown in

Table 4.5 below. The rest of the hydrogen includes the hydrogen used for propelling the FCEV and overcoming resistance.

Table 4.5. Hydrogen division for propelling the HSS and the FCEV.

	H_2 for HSS	**Rest of the H_2**
	kg/kg H_2 to FC	*kg/kg H_2 to FC*
CH2	0.045	0.955
LH2	0.019	0.981
CCH2	0.030	0.970

4.4 Modeling in OpenLCA

The life cycle of the three HSSs was modeled in OpenLCA from the cradle to the grave. The life cycle model of the studied systems was developed by creating various interlinked processes from the core, foreground, and background systems.

The foreground system processes were modeled with LCI data from literature studies and modified Ecoinvent LCI datasets where required processes were unavailable. The background system was entirely modeled with the generic LCI data from Ecoinvent. The core system was modeled using LCI data from the foreground and background systems, except for the HSSs materials composition data. The LCI datasets for metals production in the core system were sourced from Ecoinvent and modified. The other production processes modeled in the core system used LCI data from the literature or generic Ecoinvent data. The modeled inventories for all life cycle processes and applicable assumptions are discussed in sections 5.2 and 6.4.

While modeling various system processes in OpenLCA, their flows were connected to a particular provider of the LCI dataset. The choice of data providers regarding geographical system boundaries is discussed in section 5.1.5. The selection of market processes was prioritized, representing the average consumption mix of a specific product for the entire market, including transport. However, if a market activity for a particular geographical region was unavailable, a similar production process from that region was selected.

4.5 Robustness of Results

The robustness of the results was checked by performing sensitivity and variation analyses. A sensitivity analysis was performed to investigate the LCA results' sensitivity against various modeling parameters. The selected parameters were the weights of BoP components and frame. Variation analyses were conducted for the lifetime of the CH2 system, the location of tank production, and the electricity demand to produce carbon fibers. These analyses were performed for the baseline CH2 system of the LCA study. An additional variation analysis was performed for all three HSSs on the utilization of the fueling station.

First, the variation in life cycle impacts was analyzed by changing the weight of the BoP components. It was done by parameterizing the BoP weight with a factor of 0.5 and 1.5 to get low and high range values, respectively. The BoP category was selected because its weight and material composition were estimated using several assumptions and the results were somewhat uncertain. The high sensitivity of results for different weights would mean that better data must be acquired, and additional research should focus on the BoP components. Like the BoP, the effect of variation in frame weight was also studied. It was done with a factor of 0.8 and 1.2 for a low and a high range value, respectively.

Second, the lifetime of the CH2 tanks was extended to two and three lifetimes. It was done to analyze how much the impact decreases if the tanks were reused in new trucks. It is relevant information for

Volvo, as this would decrease the HSSs' impact over its lifetime by reducing the demand for new tanks. The lifetime of the frame and the BoP components was kept constant.

Third, the location of the tank production was changed from Germany to Sweden for a greener electricity mix. This step included changing the electricity provider in every production step from the German market to the Swedish one and changing the transport distances accordingly. Sweden and Germany are merely representative countries for a fossil-intensive electricity mix and a fossil-free electricity mix.

Last, the electricity requirement for carbon fiber production was reduced by 25%. A study by Hermansson et al. (2019) suggests that using lignin-based carbon fibers could reduce energy requirements by about 25%. Since there is no LCA data available, this variation analysis gives a first indication of how this could affect the CH2 system's life cycle impacts.

The variation analysis for the fueling station utilization was conducted for all three HSSs. The fueling station inventory data was sourced from a study by Maack (2008). Even though not clearly stated in that study, the low production capacity of the electrolyzer likely limit the fueling station utilization. It means that the fueling station has a daily hydrogen throughput of about 130 kg, which can refuel only about 1.5 FCEVs. According to Volvo, the hydrogen throughput of a fueling station could be estimated at 1 to 2 tons per day (M. Johansson, personal communication, May 20, 2022). For this variation analysis, the fueling station's hydrogen throughput was raised to 1 and to 2 tons per day under the assumption that the previous output was 130 kg a day. This step was performed for all three HSSs.

5 Comparative LCA Study of HSSs

This section thoroughly explains the comparative LCA study conducted as the first of the two overall assessment stages. It includes descriptions of goal and scope, inventory analysis, LCIA results, and study-specific assumptions and limitations.

5.1 Goal and Scope Definition

This report section describes the reasons for conducting this comparative LCA study, its intended application, and the boundaries of the studied systems. It also presents the study system modeling requirements and suitable data-related choices.

5.1.1 Goal and Context

The aim of conducting the comparative LCA study is to explore and compare the environmental impacts of HSSs for use in FCEVs. These HSSs include the CH2 system, LH2 system, and CCH2 System. This LCA study answers the RQ1 and RQ2 from the overall research questions presented in section 1.2. It also provides a baseline to investigate further and compare the varied EoL approaches for the CH2 system to be able to answer the RQ3. The specific questions defining the purpose of this LCA study are:

(1) What are the environmental impacts of the CH2 system? How do the impacts differ per life cycle stage, and which components and processes contribute significantly to the impacts?
(2) How do the impacts of the LH2 and CCH2 systems compare to those of the CH2 system?
(3) How much will be the allowance of environmental impacts for the BoP components concerning the LH2 and CCH2 systems in relation to the CH2 system?
(4) How does the impact of hydrogen losses in the use phase compare to the HSSs' overall life cycle?

This LCA study is intended to guide the FCEV research and development based on a scientific basis. It is also to guide the improvement of the HSS supply chain for potential circular material flows. The results of this study will be used internally at Volvo as a basis to direct its further development and business strategy concerning FCEVs.

5.1.2 Scope

This attributional LCA study includes all life cycle stages ranging from raw material extraction to the EoL. The technical system is the HSSs for onboard use in an FCEV, as described in section 3. This study views and analyzes the HSSs in their current stage of development. The study systems' geographical boundaries are defined based on their life cycle phase. The EoL and use phases for all HSSs are restricted to Sweden only. Production and other upstream processes are referenced to the location of activities by the Original Equipment Manufacturers (OEM) and their suppliers, respectively. For one example, the geographical setting of the assembly of the CH2 system is Germany. The vehicle's lifetime is 10 years, and the HSSs are assumed to live as long, undergoing 3650 refueling cycles during their lifetime (M. Johansson, personal communication, April 6, 2022). The function of the study system is to provide hydrogen storage just enough to propel an FCEV for 1000 km along with the payload. According to Volvo experts, this target can be achieved by having an FCEV onboard HSS with 80 kg of useable hydrogen storage capacity. Therefore, the study system was modeled for HSSs with the capacity to store 80 kg of usable hydrogen. The functional unit of the study systems is the delivery of 1 kg of useable hydrogen to the fuel cell stack of an FCEV.

5.1.3 Study Systems and Modeling

The technical system under study is the HSSs for use in an FCEV. The descriptions of all the HSSs are given in section 3. The technical boundaries of the study system range from the hydrogen filling

receptacle of an HSS to the point where useable hydrogen is delivered to the fuel cell stack of an FCEV. The fuel cell stack and any other subsystems or components of the FCEV except the HSS are not included within the technical boundaries. The study system was modeled for three alternatives of HSSs which are: *(i) CH2 system, (ii) LH2 System, and (iii) CCH2 system.* Following the functional unit of this study, all the HSSs are modeled to have a storage capacity of 80 kg of useable hydrogen. The type, function, and materials of sub-components may vary among the HSSs; however overall function of all HSSs is modeled to be identical. The life cycle flow charts of all HSS indicating the system boundaries are given in sections 5.1.3.1, 5.1.3.2, and 5.1.3.3.

5.1.3.1 Compressed Hydrogen Storage System

In this study, the material representation of the entire CH2 system constituents is divided into three categories: hydrogen tank, frame, and the BoP components, which refers to all the other support or auxiliary components within the CH2 system. The BoP category is further categorized into pipes, valves, electronics, instruments, and miscellaneous parts. Table 5.1 shows the dominant materials contained in each category. Type IV tanks are made of an inner cylinder consisting of a plastic liner that acts as a hydrogen permeation barrier. This difference distinguishes these tanks from other types. The tank is then wrapped with carbon fibers in an epoxy matrix (Langmi et al., 2022).

Table 5.1. CH2 system components and dominant materials.

Component		**Dominant Material Content**
Tank		Carbon fibers, epoxy, HDPE
Frame		Steel
BoP	Pipes	Stainless steel
	Valves	Stainless steel, aluminum
	Electronics	Silicon
	Instruments	Stainless steel, aluminum
	Miscellaneous	Steel, stainless steel, aluminum

Figure 5.1 indicates the system boundaries of the CH2 system, its life cycle processes, and sub-components. All the components consist of a range of different materials. All these materials have different production processes before they are combined to form an HSS in the production phase. The system is then mounted to the FCEV and put to service in the use phase. In the use phase, the inputs for refueling and the loss of hydrogen are included. The tank system is dismantled at the end of its life, and materials are subject to EoL treatment.

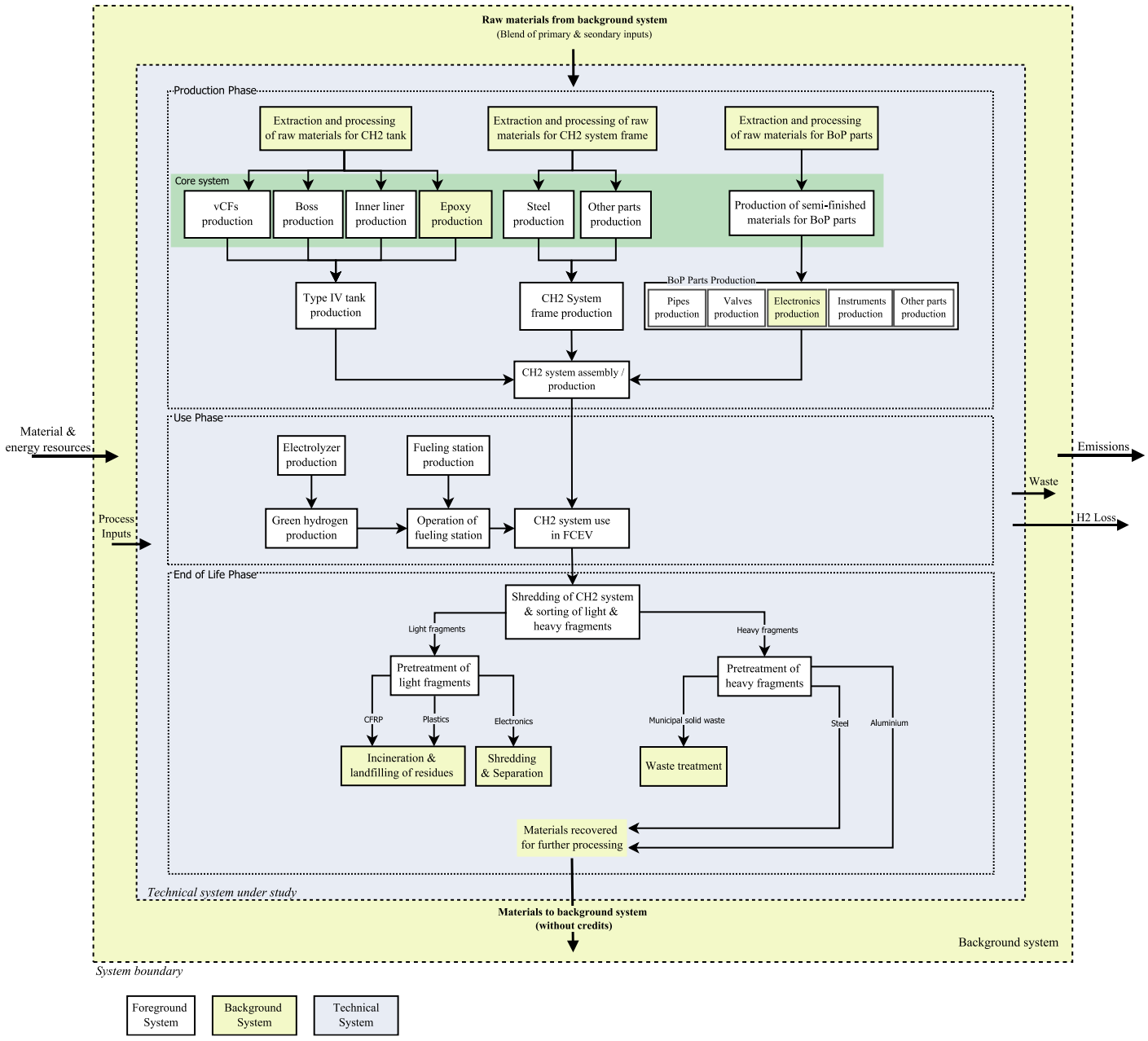

Figure 5.1. Life cycle flow chart of a CH2 Storage System.

5.1.3.2 Liquid Hydrogen Storage System

Figure 5.2 shows the system boundaries and life cycle of the LH2 system. As explained in section 4.2, LH2 tanks are primarily made from steel and do not require CFRP as they are not designed to withstand higher pressure. In addition to the inner vessel and the outer layer, they have a vacuum insulation layer made from aluminum layers. The BoP (e.g., heat exchangers and heater) was not modeled and therefore greyed out in the life cycle flow chart of the LH2 system.

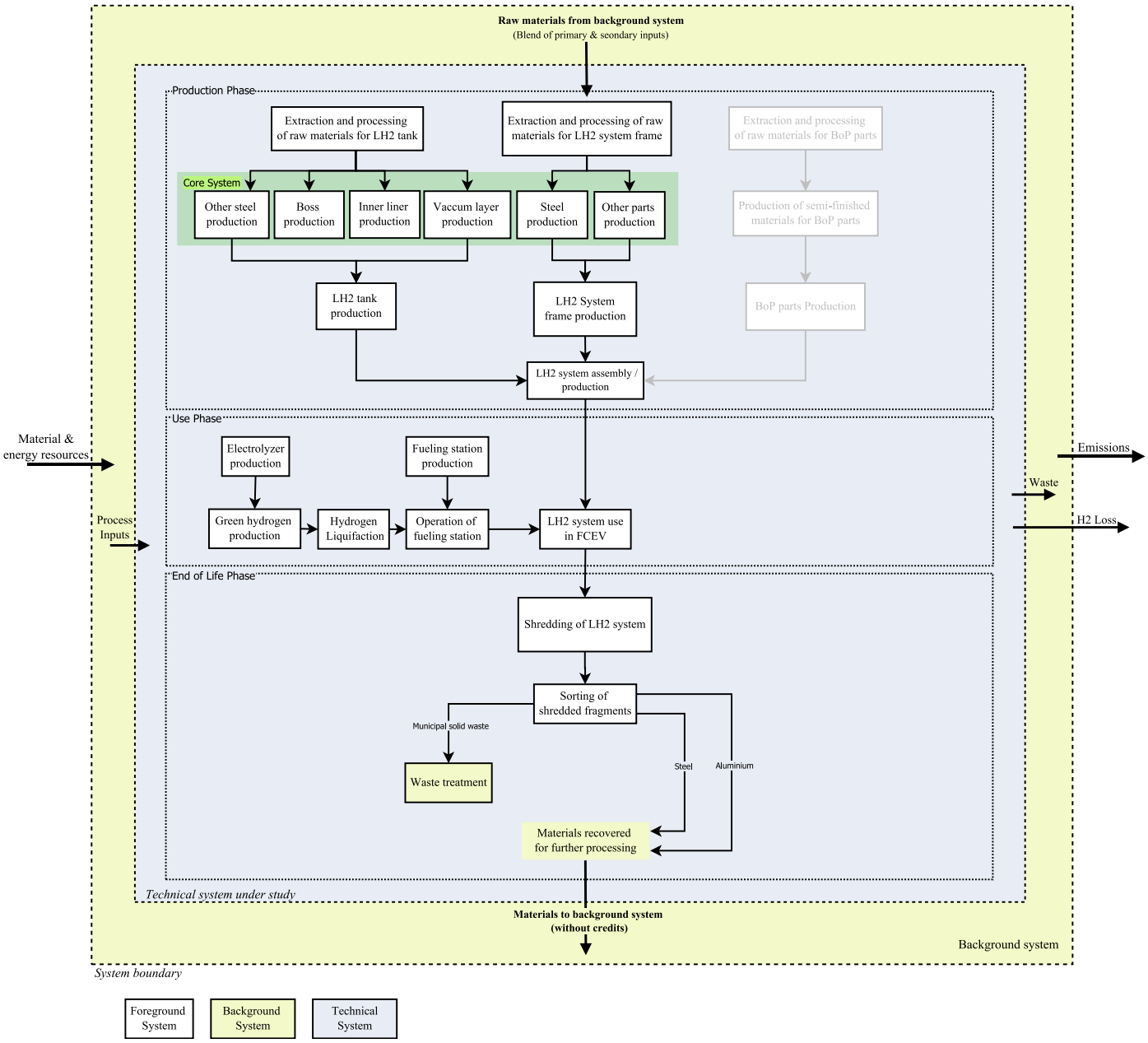

Figure 5.2. Life cycle flow chart of an LH2 Storage System.

5.1.3.3 Cryo-compressed Hydrogen Storage System

Figure 5.3 shows the system boundaries of the studied CCH2 system. It shows integration between the CH2 and LH2 system in terms of its production and material requirements as it combines the use of CFRP and steel components. Furthermore, the processes and flows throughout its life cycle are modeled similarly to the HSSs described above.

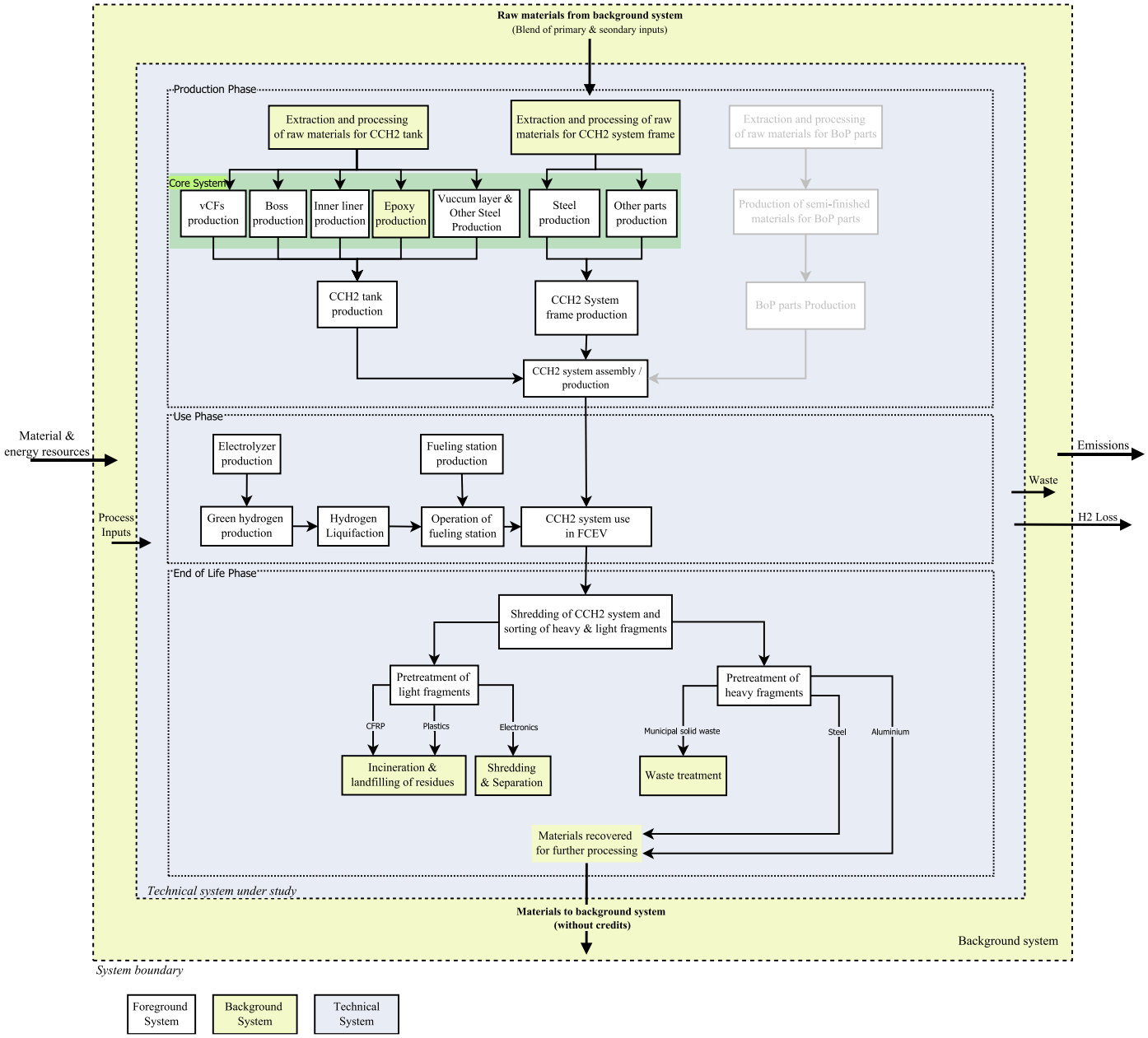

Figure 5.3. Lifecycle flow chart of a CCH2 Storage System.

5.1.4 Impact Categories

The transformation from diesel trucks to FCEVs and BEVs aims to contribute to environmental sustainability and combat climate change. Many studies synthesize or claim the environmental benefits of the shift to alternative powertrains (Nordelöf et al., 2014). Booto et al. (2021) studied that hydrogen fuel cell electric vehicles can reduce up to 48% of GHGs, and Lee et (2018) stressed the importance of choosing the electricity mix. Though extensive, these studies only emphasize the GHG emissions and

exclude impacts of material use. This LCA study strives to indicate key impact categories relevant to the HSSs. It is essential to include the impact of materials resource use concerning the EoL and production phase (Moberg et al., 2010).

ReCiPe 2016 method for LCIA was used in this study. This method provides characterization factors representing the global scales instead of the European (Huijbregts et al., 2017). This selection was made keeping in mind the global reach of Volvo products. Moreover, the Hierarchist (H) perspective of cultural theory was selected. It does not include any weighting since it is based on the most common policy principles concerning characterization factors and as required by the ISO standard (Mehmeti et al., 2018).

The midpoint impact categories selected for this study are: (i) Climate change, (ii) Mineral resource scarcity, (iii) Fine particulate matter formation, and (iv) Terrestrial acidification. The selection of impact categories is because the LCA system under study relies on the use of materials and subcomponents which are energy-intensive or complex to be produced. In a recent study conducted by Usai et al. (2021), carbon fibers and metals used in tank systems contributed significantly to the studied environmental impacts, especially the global warming and metal depletion potential. However, it is worth noting that the SOP method used for indicating metal depletion is valid only in the short term in terms of scarcity, as it represents economic allocation of minerals based on the market price data which is a time sensitive parameter and thus volatile (Arvidsson et al., 2020).

5.1.5 Data Quality

The HSSs under study were modeled based on the conceptual designs, so minimal primary data was available. The data for the tanks' composition and the frames of HSSs was taken directly from Volvo experts. Given the state of development of the HSSs, this data set was considered current, representative, and technology specific. However, the available data for BoP was not complete, and it was estimated using assumptions based on literature studies. The potential uncertainties in the BoP data estimations were attempted to be minimized by using assumptions only from peer-reviewed scientific studies. All such data interventions are given in section 5.1.6. The rest of the data used in this study was the secondary LCI data sourced from Ecoinvent and scientific literature.

All the studied systems had differences in their design and material contents, especially in the production phase. Therefore, the geographical coverage of the LCI data used in this study varies among the HSSs. Depending upon the geographical location of a particular life cycle process, country-specific average data was prioritized. However, the European regional or global averages were used for remote life cycle activities and activities where country-specific average data was absent. Moreover, this study prioritized using the latest data, but exceptions were made where the age of the data was traded off with its reliability. For instance, the LCI data for hydrogen production and energy use for compression and liquefication was sourced from relatively old reports by Maack (2008) and the U.S. Department of Energy (2009).

An HSS has specific material demands for parts in contact with hydrogen since hydrogen is highly reactive. To ensure these metals are included correctly in the model, data from Ecoinvent was modified based on the composition of the exact metal grades needed. The metal composition guidelines were gathered from different websites or datasheets (Aalco, 2019; Euro Inox, 2007; MEADinfo, 2015; Righton Blackburns, 2021).

5.1.6 Assumptions and Limitations

This section describes the main assumptions which were made in conducting this study. The additional assumptions related to LCA modeling are presented in sections 5.2 and 6.4. These assumptions were explained separately in conjunction with the description of modeling aspects for easier understanding.

In addition to the BoP components, the materials composition data for other parts of the CH2 system was incomplete. Therefore, the material composition data for the 700-bar system was based on a 350-bar system which was relatively mature in terms of design and data availability. The estimation methodology is discussed in section 4.2. Since the system information was even scarcer for the LH2 and CCH2 systems, the assumptions for the CH2 model were often expanded to the other two models. While this limits the comparability of the different HSSs, it was considered acceptable since the CH2 system is the baseline model.

The lifetime of the HSSs was assumed to depend on the operational lifetime of an FCEV which is 10 years. It was discussed with Volvo experts and estimated that the FCEV is refueled on average every day over its lifetime, resulting in 3650 refueling cycles. However, a discrepancy between the assumptions and design lifetime was identified in the literature. According to the studies by Villalonga et al. (2009; 2019), a CH2 type IV tank can sustain 15000 refueling cycles before it fails under extreme testing conditions. The possibility of extended refueling cycles for the CH2 system was further studied by conducting variation analyses. The effects of such changes on the life cycle impacts are discussed in section 5.3.1.2.

All hydrogen in the use phase is produced using wind power. This means the modelled hydrogen is always "green hydrogen" (GH_2) according to industrial terminology. This terminology does not contain strict definitions, but it categorizes hydrogen produced from various sources into color codes. Hence, hydrogen produced through electrolysis using renewable energy sources is categorized as green. Grey and blue hydrogen, on the other hand, are both produced from fossil fuels which cause relatively high CO_2 emissions. The difference between blue and grey hydrogen is that in the production of blue hydrogen, the CO_2 is captured and stored separately (Chocksey, 2021). Wind power was chosen since the use phase is modeled in Sweden where the share of wind power is already at 17% and set to increase further (Dellby, 2021). Any further energy requirements modeled in the use phase were also based on wind power.

The HSSs design specifications, especially for the CH2 and CCH2 systems, require that some hydrogen is retained in the tank to ensure its structural stability. This unusable hydrogen is entirely neglected from the use phase modeling, and it is assumed that the HSSs are refueled with 80kg of hydrogen every time. The FCEV completely consumes all the usable hydrogen before the next refueling.

Further, the maintenance and repair activities were entirely excluded from the use phase for all HSSs. In discussion with Volvo experts, it was determined that an HSS and its components are designed not to require any maintenance or repair during their lifetime. As per manufacturer specifications, the HSS would undergo routine visual inspections. However, the impacts from these inspections were deemed negligible. Additionally, all the potential repair activities resulting from abnormal operating events, such as accidents, were excluded.

5.2 Life Cycle Inventory Analysis

This section discusses the modeling and inventory development of the study systems in comparative LCA with cutoff EoL modeling. The life cycle model of the CH2 system was defined as the baseline model in this case study. The modeling of the LH2 and CCH2 systems was based on the CH2 system. The baseline model was adjusted for changed material inputs, processes, and flows, making it fit the other two systems. The methodology of performing materials balance for CH2, LH2, and CCH2 systems has been discussed and presented in section 4.2. In context to the study aims, the life cycle variation among all the HSSs was identified mainly in the production of tanks. The life cycle of the study system was categorized into three phases: production phase, use phase, and EoL phase.

5.2.1 Production Phase

The modeling and inventory aspects of producing all HSSs are described in this section. The HSS production is mainly concerned with the assembly of its constituent components. The production phase activities comprise of production of ancillary materials, HSS subcomponents, and their assembly. The subcomponents of an HSS were grouped into three categories for modeling purposes: tanks, frame, and BoP components. The inventory datasets for unit processes and flows in this phase are presented in Appendix A.1.

5.2.1.1 Tank Production

The inventory modeling for the tank production process was primarily based on the material composition of the tanks, as presented in section 4.2. The LCI datasets for metals in the tank were utilized from the Ecoinvent database and modified. The rest of the inventory data was either sourced from the literature or the generic Ecoinvent database.

The CH2 system contains Type IV tanks which comprise an inner liner, boss, and an external protective layer. The inner liner is made from HDPE using the injection molding technique, and the boss is made from aluminum. The most significant mass contributor to the tank composition is the external protective layer made from CFRP. The tank was modeled to be produced with a filament winding technique in which carbon fibers and epoxy resin are wound around the inner liner.

The carbon fibers production process was modeled in detail in OpenLCA based on inventory data from Benitez et al. (2021). This data is based on T700 G carbon fibers and includes the production of the carbon fibers precursor, their thermal treatments, and final processing. However, the production of carbon fibers can differ substantially, depending on the precursor material, precursor treatment methods, or changes in temperature in the production process. The exact production steps utilized in this report are described in Appendix A.1.1. Furthermore, Benitez et al. (2021) also provided the inventory data for the HDPE liner production and the manufacturing of the tanks.

The inventory data for the liner production and the manufacturing of the tanks was modeled per 102 kg of carbon fibers. The electricity and compressed air inputs were scaled according to the material content of carbon fibers in the CH2 system. The boss was assumed to be produced using Aluminum 6061-T6 alloy material; however, its production process model was proxied with a closely related process from Ecoinvent named *market for aluminium alloy, AlMg3 | aluminium alloy, AlMg3 | Cutoff, U – GLO*.

The LH2 and CCH2 tanks also consist of an inner liner, boss, and an external protective layer. Additionally, they contain insulation between the inner and outer vessel provided by a vacuum and aluminum layers. The material composition of LH2 tanks differs from CH2 tanks since the material for the inner liner, and the outer vessel is stainless steel-316. The CCH2 tank has similarities with both the CH2 and the LH2 tanks. Its outer protective layer contains CFRP composite material similar to the CH2 tanks. However, the inner liner of CCH2 tanks is made from stainless steel-316, and it includes a similar insulation layer as in LH2 tanks. The boss was modeled similarly to the CH2 system for both systems.

The materials for the stainless-steel components were modeled with the Ecoinvent production process *steel production, electric, chromium steel 18/8, Cutoff, U – RER.* To make it fit the required steel grade, the original process's ferronickel and iron scrap content were modified, and molybdenum was added (Euro Inox, 2007). Further, transport flows from a similar market process were added to account for the transportation of the product. The exact modifications of these and other metals can be referred to in Appendix A.1.2. The aluminum layers were assumed to be made from Aluminum 6061-T6. The CFRP for the CCH2 tanks was modeled similarly to the CH2 tanks. The energy and compressed air inputs for the LH2 and CCH2 systems tank manufacturing process were modeled based on Benitez et al. (2021) and per kg carbon fibers. However, LH2 and CCH2 tanks contain steel in the outer layer. It was assumed that the energy per kg of steel is half of the energy needed per kg of carbon fibers since manufacturing

carbon fibers is energy-intensive (Meng et al., 2018). The same modeling concept was applied to compressed air inputs as well. The inventory datasets for tank production for different HSSs, sub-components, and carbon fibers are provided in the Appendices A.1.1 – A.1.4

5.2.1.2 Frame Production

The frame production for all HSSs was modeled similarly. The frame was modeled to be produced from S355, a galvanized, powder-coated grade of low carbon steel. The steel input quantities were estimated to be different among all the HSSs, as discussed in section 4.2. The LCI dataset for steel production of S355 grade was not available in the Ecoinvent. The frame production was thus proxied with the Ecoinvent LCI production process dataset named *steel production, converter, unalloyed | steel, unalloyed | Cutoff, U – RER*. The ferromanganese and pig iron quantities in the original dataset were adjusted (MEADinfo, 2015). Additional transport flows were also added from a similar market process in Ecoinvent to account for material transport. The adjusted inventory datasets indicating the exact changes made in the steel production process and other production phase LCI datasets are presented in Appendix A.1.

5.2.1.3 Balance of Plant Production

In this case study, the BoP components were only modeled for the CH2 system since there was a significant data gap for the other HSSs. The methodology for categorizing and estimating material input requirements for all BoP components is presented in section 4.2. The BoP components consist of instruments, pipes, valves, electronics, and miscellaneous components. The instruments were modeled as composed of 50% stainless steel-316, 28% aluminum 6082/61-T6, and 16% stainless steel-316Ti. The pipes composition was modeled based on 100% stainless steel-316Ti. The valves were modeled with 75% stainless steel-316 and 25% aluminum 6082/61-T6. The electronics category was modeled with an Ecoinvent process *electronics production, for control units | electronics, for control units | Cutoff, U – RER*. The miscellaneous category was modeled to be containing 70% stainless steel 316, 25% stainless steel S355, and 5% polypropylene contribution by mass.

Stainless steel 316 was modeled as the steel used for the LH2 and CCH2 tanks. Stainless steel 316Ti was also modeled with the Ecoinvent production process, *steel production, electric, chromium steel 18/8, Cutoff, U – RER.* Molybdenum and titanium inputs were added, and ferronickel and iron scrap input values were adjusted (Righton Blackburns, 2021).

5.2.1.4 Transport

Additional transport processes were added for valves, tanks, and assembled HSSs. These distances were calculated using the environmental performance calculator tool available from the Network for Transport Measures (Network for Transport Measures, n.d.). The frame and other BoP components were assumed to be produced on the HSS assembly location site. The CH2 and CCH2 tanks production was assumed to be in Germany due to the country's fast development in hydrogen technology. LH2 tanks, however, were assumed to be produced in France. The CH2 system supplier also produces most of the BoP components in this study. However, the Valves are produced in Italy and transported to Germany. The tank is assembled in Germany and transported to Volvo in Göteborg, Sweden.

5.2.2 Use Phase

This section describes the modeling aspects of the use phase of all HSSs. As explained in section 5.1.6, the maintenance related activities had a minimal scope and data availability and were excluded from the model. Therefore, the use phase solely includes the hydrogen loss of the HSSs. The inventory datasets for unit processes and flows in this phase are presented in Appendix A.2.

5.2.2.1 Hydrogen Losses

The use phase of HSSs primarily accounts for the hydrogen losses. The production of the hydrogen needed to propel the FCEV and overcome the rolling and grade resistance was not modeled. The amount of hydrogen lost due to the HSSs' weight was modeled in Matlab, as explained in section 4.3. For the LH2 and CCH2 tanks, the losses for boil-off were estimated to be 4% and 1%, respectively. This estimate was based on the given range (1-10%), assuming that the HSSs would be handled relatively efficiently. The hydrogen production, compression and liquefaction, and dispensing processes were modeled for the lost hydrogen, including the fueling station infrastructure. The lost hydrogen was assumed to come from wind-powered electrolysis and modeled as presented in the following description.

First, the required inputs for hydrogen production were an electrolyzer, water, and electricity. The electrolyzer inventory data and required water amount was sourced from Maack (2008). The modeled electrolyzer had a 47250 kgH_2/year production capacity and 15 years of lifetime. Its water demand was 10L of water per kg of hydrogen. PEM water electrolyzers are assumed to have an efficiency of up to 80% (Shiva Kumar & Himabindu, 2019). Therefore, the electricity input for 1 kg of hydrogen was calculated to be 175 MJ/kg based on the higher heating value of hydrogen (140 MJ/kg). As the hydrogen is produced from wind power, the electricity input flow comes from the Ecoinvent process *electricity production, wind, 1-3MW turbine, onshore, U – SE*. Since the electrolyzer requires medium voltage electricity, the transformation was modeled based on the Ecoinvent process *electricity voltage transformation from high to medium voltage, U – SE*. The hydrogen production process was the same for all HSSs. It was assumed to take place at the location of the fueling station. Therefore, hydrogen transport was excluded from the model.

For the refueling process of the HSSs, the fueling infrastructure was modeled according to Maack (2008), including a compressor, fueling station, on-site storage, and the dispenser. The dataset accounted for the capital equipment such as the electrolyzer, compressor, fueling station, on-site storage, and dispenser. Further, the hydrogen was compressed for the CH2 and CCH2 systems, and an additional liquefaction process was modeled for the LH2 and CCH2 systems, which are assumed to be at the fueling station.

For the CH2 system, hydrogen was required to have an overpressure of 880 bar with pre-cooling up to -40°C for the refueling (R. Kvist, personal communication, March 30, 2022). According to the U.S. Department of Energy (2009), hydrogen compression to 880 bar requires electricity between 2.67 and 3.0 kWh/kgH_2. Due to the age of the reference study, lower energy consumption was used. The cooling requires an additional 0.2 kWh/kgH_2. The operation of the fueling station was modeled using hydrogen, energy for compression and pre-cooling, and the fueling station infrastructure.

For the LH2 system, the hydrogen needed to be liquified, but compression was not necessary. Due to a lack of inventory data for LH2 fueling stations, the fueling station infrastructure was also sourced from Maack (2008). However, it was modified not to include the compressor. The liquefaction infrastructure was also excluded. Energy requirements for liquefication could range from 10 to 13 kWh/kgH_2 (U.S. Department of Energy, 2009). The lowest value was chosen due to the research date and potential improvements since then. Furthermore, the liquefaction process is assumed to occur at the fueling station.

For the CCH2, refueling was modeled using the more mature technology where liquid hydrogen is compressed (F. Haberl, personal communication, April 25, 2022). The compression of liquid hydrogen to 300 – 400 bar requires less than 0.5 kWh/kg (Cryomotive GmbH, 2021). Therefore, it was assumed that the energy demand for compression and liquefication amounts to 10.4 kWh/kg. Besides the energy requirement, the fuel station operation was modeled similarly to the CH2 system. The liquefaction infrastructure was excluded for the CCH2 system as well. Lastly, the energy input for the compression

and liquefaction of hydrogen for all HSSs was assumed to come from the medium voltage wind power flow that was also used for the electrolyzer.

Even though the production of hydrogen used to propel the vehicle and overcome resistance is excluded from the model, the liquefaction or compression of this hydrogen is directly linked to the HSS and, therefore, highly relevant when comparing the HSSs. Therefore, the energy required for liquefaction or compression is added to the use phase in an additional modeling step for all HSSs. This electricity input is also based on medium voltage wind power.

5.2.3 End of Life

The EoL was modeled with the cutoff approach in the comparative LCA study. The EoL modeling for all HSSs was performed consistently. Due to a lack of EoL process information, it was assumed that the HSS reaches EoL along with the FCEV and is subject to industrial shredding, a process that also sorts the shredded materials. The LCI dataset for truck shredding was unavailable in the Ecoinvent; therefore, the proxy dataset *treatment of used glider, passenger car, shredding, Cutoff, U,* was selected.

It was assumed that the shredding process already sorts the inputs into heavy and light fragments, which are the two categories of output flows additionally created in the proxied dataset. The heavy shredded fragments consisted of waste metals, while the light fragments comprised CFRP, plastics, and electronics waste. Heavy fragments were further sorted into steel and aluminum. The model was then cutoff before the metals were modeled to be sent to the recycling facilities. The light fragments were sorted into electronic waste, CFRP, and plastic. While electronics were shredded further and then cutoff, the CFRP and plastic were modeled to be incinerated without energy recovery. The sorting process for heavy and light fragments was adapted from *treatment of metal scrap, mixed, for recycling, unsorted, sorting, Cutoff, U*. The LCI datasets for the EoL phase model are provided in Appendix A.3

5.3 Life Cycle Impact Assessment Results

This section presents the LCIA results of the baseline system, including robustness analyses. The comparison of CH2 system results with its alternatives, the LH2 and CCH2 systems, are also discussed. The LCIA results are presented in terms of life cycle phases. The production phase results include the impacts of tanks, frame, BoP, and the transport of HSSs from the OEM to the Volvo premises. The use phase impacts are caused by the electricity and infrastructure required to produce, compress, and dispense hydrogen into the HSS. The EoL phase impacts consist of waste management processes.

5.3.1 Baseline HSS

Figure 5.4 shows the contribution of the three life cycle stages to each impact category. Clearly, the production and use phases make up nearly all the impact of all categories. Especially the CFRP, the GH_2 production, and the fueling station operation cause most of the impact. The EoL stage is not visible in any impact category except global warming, where it contributes only about 4%. The use phase dominates all impact categories except global warming, where production causes most emissions.

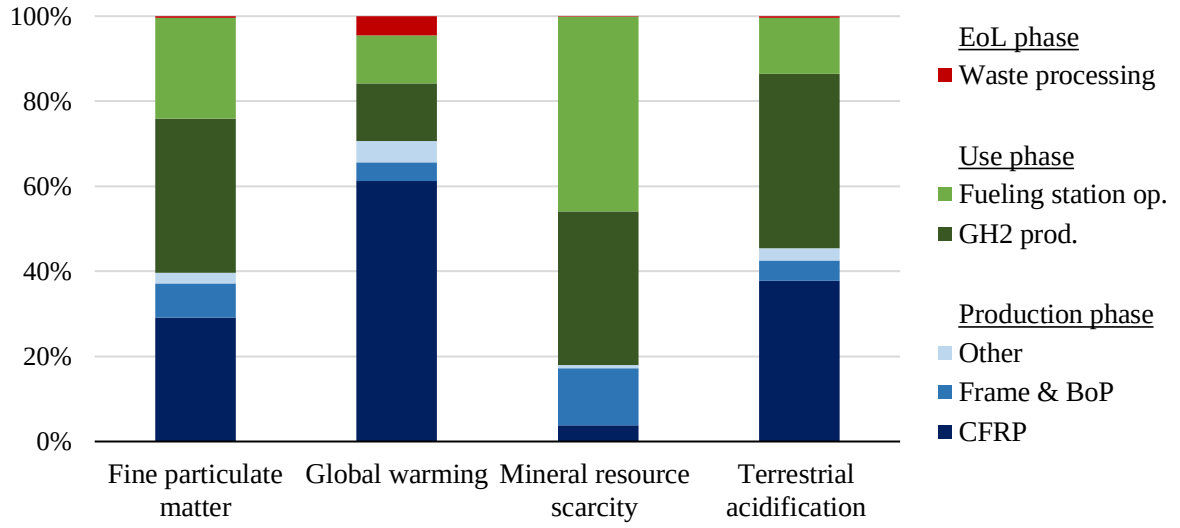

Figure 5.4. LCIA result of the CH2 system by life cycle stage.

Table 5.2 shows a more detailed overview of the impacts per category. The production of carbon fibers primarily causes fine particulate matter formation, closely followed by the production of the fueling station and the electrolyzer and the electricity and water input for the GH_2 production. For the carbon fibers, these emissions can be traced back to the first step of their production, the suspension polymerization process. The acrylonitrile and heat energy inputs in carbon fibers production are the underlying cause of the formation of fine particulate matter. As for the electrolyzer and the fueling station, the emissions can be traced back to the nickel and chromium steel input, respectively. Lastly, wind turbine construction also contributes significantly to this impact category.

The total global warming impact is around 0.26kg CO_2-eq per kg of hydrogen delivered to the FC. Around 70% comes from the production phase, mainly caused by carbon fibers production. Similar to the previous impact category, a significant part is caused by the acrylonitrile production and the heat inputs in the initial step of carbon fibers production. However, all processes in the carbon fibers production chain require electricity input, contributing to the global warming impact. This also shows in the carbonization steps of carbon fibers production. Besides that, the epoxy and the frame also contribute around 3% each to global warming. The main impact originates from electricity and water input for electrolysis in the use phase, followed by fuel station production. Despite the electricity for electrolysis coming from wind energy, the construction of the wind turbine contributes to global warming, primarily due to the input of energy-intensive materials. These material inputs are also the underlying cause of the impacts coming from the fueling station infrastructure. Lastly, nearly all the global warming impacts from the EoL phase are caused by CFRP and plastic incineration.

The CH2 system's effect on mineral resource scarcity derives from the infrastructure production in the use phase, specifically from the material resources utilized in the electrolyzer and fueling station production. Steel components are mainly responsible for these impacts. This is also why the BoP and the frame contribute to this impact category, despite their relatively lower weight. For the fueling station, which contributes about 45% to the impact of this category, ferronickel production is the underlying process that is mainly responsible, which is also the case for the BoP. Ferronickel is a component in chromium steel and this steel type is utilized in the fueling station. While the electrolyzer also contains a bit of chromium steel, the amount is less significant. Here, the impact is caused by cobalt production.

The terrestrial acidification is mainly caused by carbon fibers production and electrolyzer production, each causing around one-third of the impact. In the carbon fibers production chain, the acrylonitrile

production process and the heat input for the suspension polymerization step also cause a significant share of emissions. Next, the electricity input in several steps also causes terrestrial acidification, which can be traced back to the input of hard coal into the German electricity mix. The electrolyzer production causes impacts through its nickel demand, for which terrestrial acidification occurs during the metal mining operation. Further, electricity for electrolysis and the fuel station operation production causes their emissions of around 12% each. The emission originates from various materials required for manufacturing the wind turbine for electricity. Similarly, the material demand for the fueling station is responsible for the terrestrial acidification impact, primarily through ferronickel production, which is needed for manufacturing chromium steel.

Table 5.2. LCIA results of the CH2 system and its significant components.

Components	**Sub-processes**	**Fine particulate matter**	**Global warming**	**Mineral resource scarcity**	**Terrestrial acidification**
Unit		kg PM2.5 eq/kg H_2 at FC	kg CO_2 eq/kg H_2 at FC	kg Cu eq/kg H_2 at FC	kg SO_2 eq/kg H_2 at FC
Production phase					
Tanks	Carbon fiber	26%	57%	3%	35%
	Epoxy	3%	3%	~ 0%	3%
	Electricity	1%	2%	~ 0%	1%
	Other	1%	1%	~ 0%	1%
Frame		6%	3%	8%	3%
BoP		2%	1%	6%	2%
Transport HSS		1%	2%	~ 0%	1%
Total contribution		40%	71%	18%	45%
Use phase					
GH_2 production	Electrolyzer production	20%	2%	20%	29%
	Electricity & Water	16%	12%	16%	13%
Fueling station operation	Electricity compression	1%	1%	1%	1%
	Fueling station production	23%	11%	45%	12%
Total contribution		60%	25%	82%	54%
EoL phase					
Shredding	CFRP & Plastic incineration	~ 0%	4%	~ 0%	~ 0%
	Other	~ 0%	~ 0%	~ 0%	~ 0%
Total contribution		~ 0%	4%	~ 0%	~ 0%
Total life cycle impact		100%	100%	100%	100%

5.3.1.1 Sensitivity Analysis

In the first analysis, different weights of the HSS frame for the CH2 tanks were investigated. Figure 5.5 shows the impact results where the impact with the original frame weight is 100%. The lower and higher frame weight impacts are modeled in % in- or decrease. The graph shows that an in- or decrease of 20% of the frame weight shows only minor changes, about 1% in impact for all three categories. Only the mineral resource scarcity impact shows a change of 2% in both directions, caused by the frame being made of steel. These are very stable results.

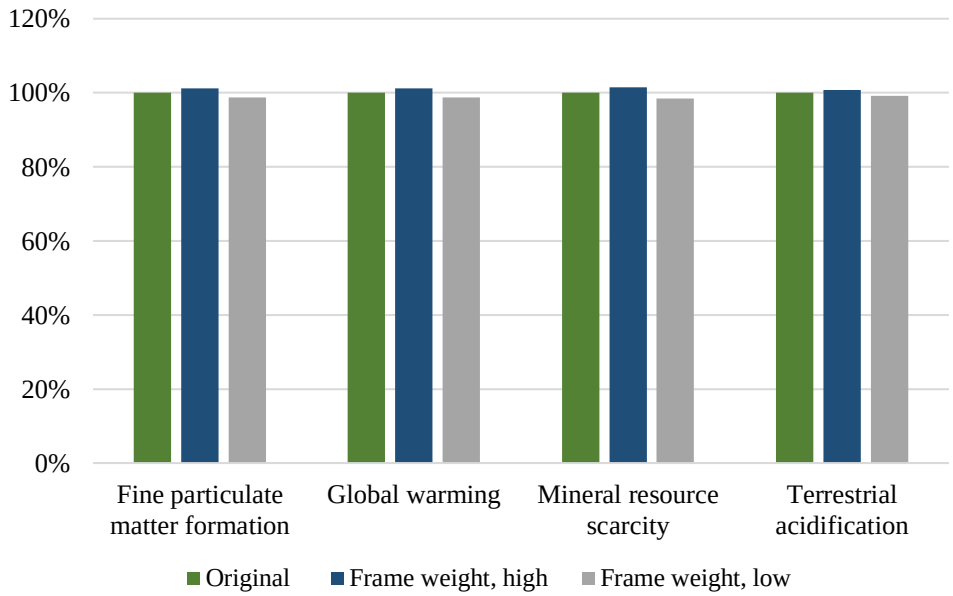

Figure 5.5. LCIA results for sensitivity of the frame weight.

The second analysis investigates the effect of changing the weight of the BoP components. The BoP weight was increased by 50% and decreased by 50% to test how sensitive the results are to the BoP weight. The graph below shows only a very small variation for all impact categories, indicating that the results are not sensitive to the BoP weight. The mineral resource scarcity impact is slightly more sensitive to these changes, showing a 3% change due to the stainless steel used for some BoP components. It entails ferronickel, which contributes significantly to this impact category.

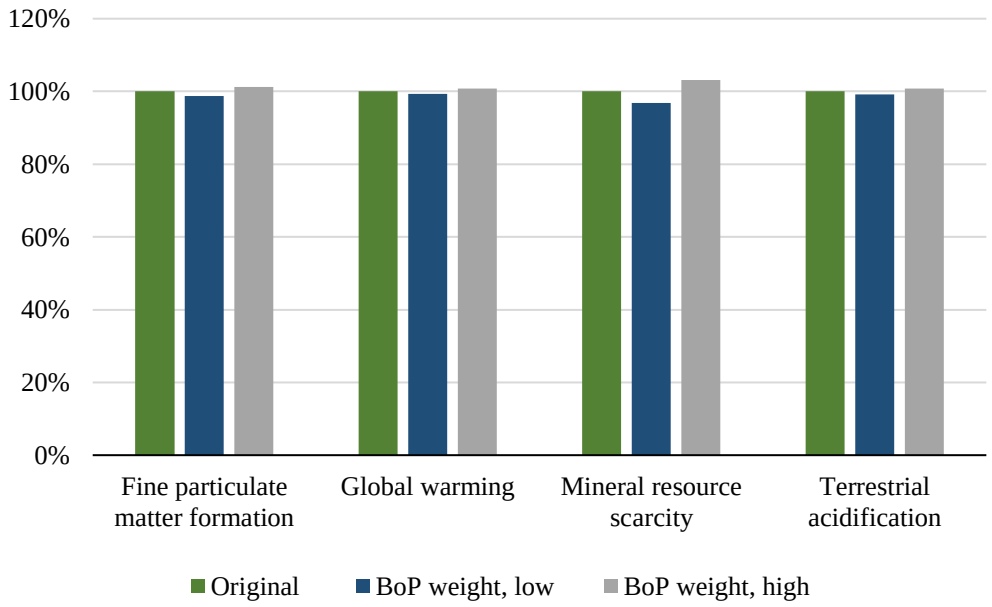

Figure 5.6. LCIA results for sensitivity of the BoP weight.

5.3.1.2 Sensitivity and Variation Analysis

The first variation analysis modified the lifetime of the tanks, extending it to two and three of its original lifetimes. Figure 5.7 shows the impacts of the CH2 system and the changes associated with modifying the CH2 tanks' lifetime. It shows that giving the CH2 tanks more lifetime decreases the impacts for all four impact categories, especially for global warming. Mineral resource scarcity is the least affected. In this scenario, the CH2 tank survives two FCEV lifetimes. However, all other components are assumed to be replaced, which means only the impact directly related to the tank is decreasing. Therefore, global warming impacts decreasing the most, and mineral resource scarcity the least is in line with previous findings since the tanks contributed most to the global warming impact category and least to the mineral resource scarcity.

Further, the graph shows that a third lifetime causes a less significant reduction than a second one. After the impacts have already been cut in half, a third lifetime reduces the impacts of the CH2 tanks only by one-sixths of their original impacts. However, for global warming, this means the impacts of the entire CH2 system can be reduced by almost 50%. Fine particulate matter formation and terrestrial acidification could decrease by more than 20%.

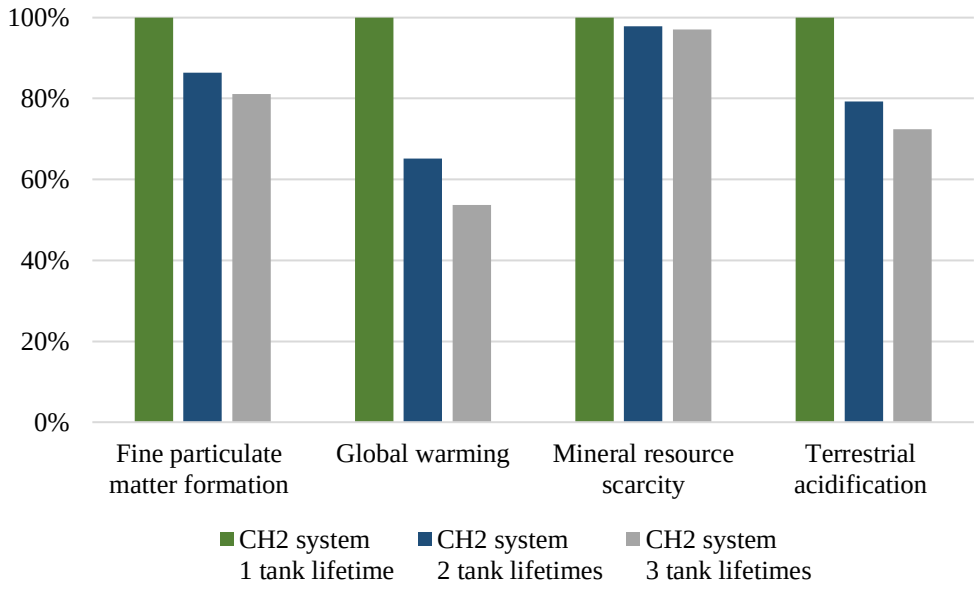

Figure 5.7. LCIA results comparing different lifetime extensions of CH2 tanks.

The second scenario analyzes the effect of moving the tank manufacturing to Sweden, changing the electricity mix and transport distances. Similar to extending the lifetime of the tanks, changing manufacturing location to Sweden mostly affects the global warming, but also the particulate matter formation and terrestrial acidification. However, the effect on mineral resource scarcity is negligible. This is in line with energy input in tank manufacturing playing a significant role in its environmental impact. Comparing Sweden's fossil free electricity mix with Germany's coal-dominated electricity mix explains these reductions. It shows that a change in electricity mix can reduce global warming impacts by more than 20%.

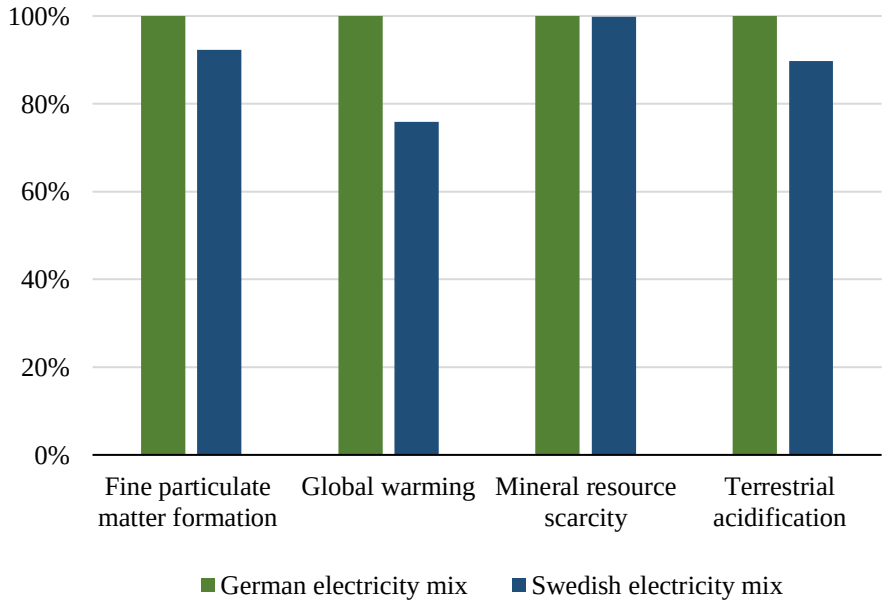

Figure 5.8. LCIA result comparison between the German and the Swedish electricity mix for the manufacturing of CH2 tanks.

The subsequent variation analysis is concerned with reducing the electricity input for tank manufacturing. Figure 5.9 shows that a 25% reduction of electricity input decreases the impact of the CH2 system by up to around 7% for global warming. For fine particulate matter formation and terrestrial acidification, the decrease is lower than 3%. For mineral resource scarcity, the decrease is minimal. It shows that the results are reasonably sensitive to the tank manufacturing electricity demand.

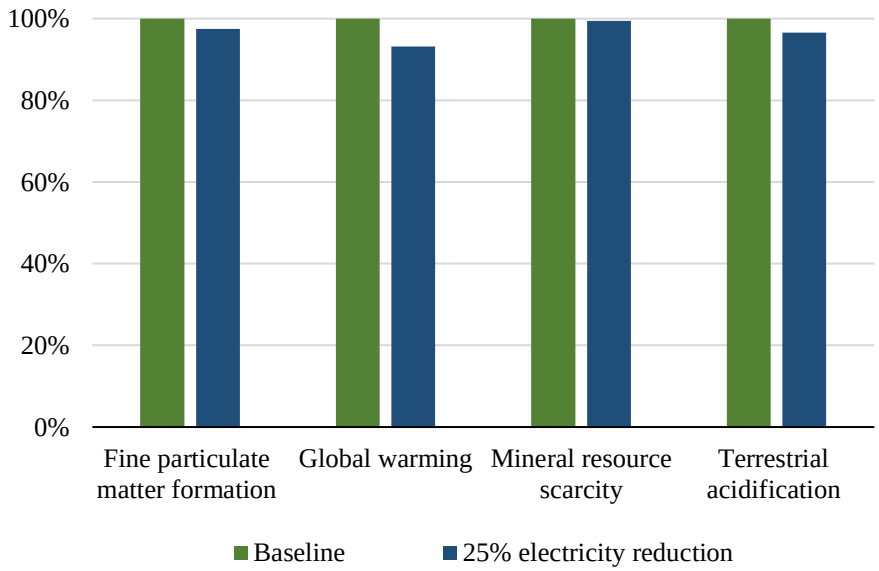

Figure 5.9. LCIA results of reduced electricity for carbon fibers production.

5.3.2 Comparison of HSSs

This section compares the LH2 and the CCH2 system impacts with those of the CH2 system. The impacts are illustrated per the main components of each life cycle phase. These are the tanks, frame, BoP components. In the use phase, impacts are divided into GH_2 production and its conversion of physical state, and the fueling station production. Since the LH2 and the CCH2 system were modeled without the BoP components, the difference in total life cycle impacts of the LH2 and CCH2 systems compared to the CH2 system is referred to as the BoP allowance.

5.3.2.1 Fine Particulate Matter Formation

The LCIA results for the impact category of particulate matter formation are presented in Figure 5.10. It shows that fine particulate matter formation does not significantly differ between all three HSSs. The CH2 system causes the highest emissions of PM2.5-eq, closely followed by the LH2 system. The CCH2 system causes the lowest burden.

The graph shows that a large share of the burden comes from the use phase for all HSSs, especially for the LH2 system, for which the use phase accounts for about 80% of the impact. This can be explained by the boil-off losses and the high energy demand for hydrogen liquefaction. The CH2 system requires relatively less energy for compression, but it has the highest weight-related hydrogen loss. The lower impact of the CCH2 system can be traced back to having the lowest hydrogen losses, and therefore least impacts from the fueling station production. Another significant share of fine particulate matter formation stems from tank production, which is especially high for the CH2 and CCH2 systems due to the CFRP content. Since the CCH2 system requires a relatively lesser amount of CFRP, its production-related emissions are lower, setting it apart from the other two systems. The EoL phase does not contribute significantly to impacts for any HSSs. Compared to the CH2 system, the LH2 and CCH2 systems have BoP allowance of about 4% and 16%, respectively. For the LH2 system, this is close to the BoP impact of the CH2 system, whereas it is visibly bigger for the CCH2 system.

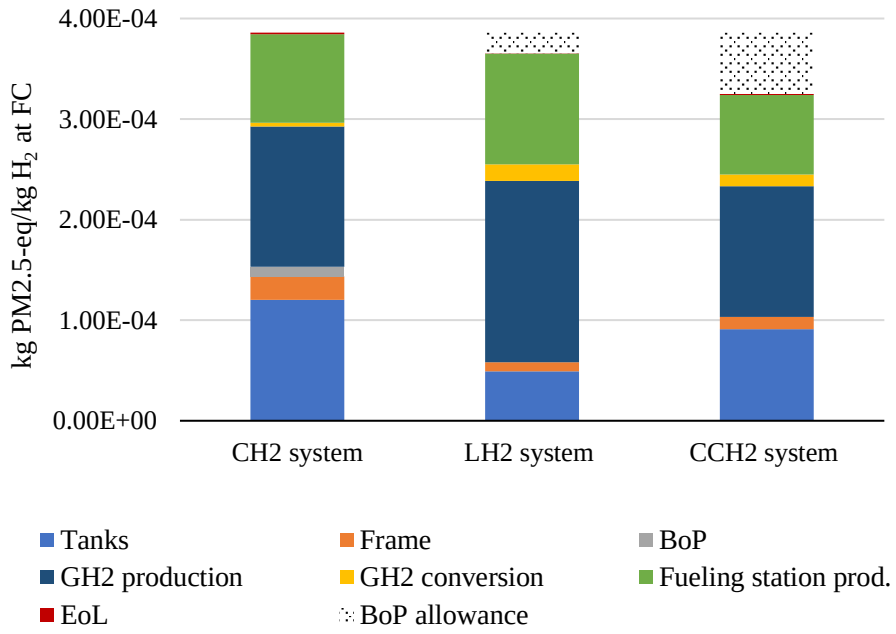

Figure 5.10. LCIA results for fine particulate matter formation.

5.3.2.2 Global Warming

The LCIA results for the impact category of global warming are presented in Figure 5.11. It shows that the CH2 system has the highest life cycle environmental impacts relative to the LH2 and the CCH2 system. However, the LH2 system causes the least global warming.

For the CH2 system, the largest share of life cycle impacts is caused by the production phase. As discussed in section 5.3.1, this is primarily due to the CFRP in the tank production process, causing around 65% of the HSS's burden. The CCH2 system has about half the production related impact since it requires significantly less CFRP. The LH2 system has the lowest production impact since it does not require CFRP at all. For the LH2 system, the emissions mainly stem from the use phase. The high hydrogen loss and energy-intensive production of liquid hydrogen cause the burden. Compared to the LH2 system, the CH2 and CCH2 systems have a lower use phase impact due to lower hydrogen losses of the CCH2 system and lower energy requirements for the CH2 system.

The EoL impact of the CH2 and CCH2 systems is closely related to the incineration of the CFRP, which causes a significant burden for this impact category. The LH2 system causes negligible emissions in the EoL since it does not contain CFRP. Compared to the CH2 system, the LH2 and CCH2 systems have BoP allowance of about 135% and 70%, respectively.

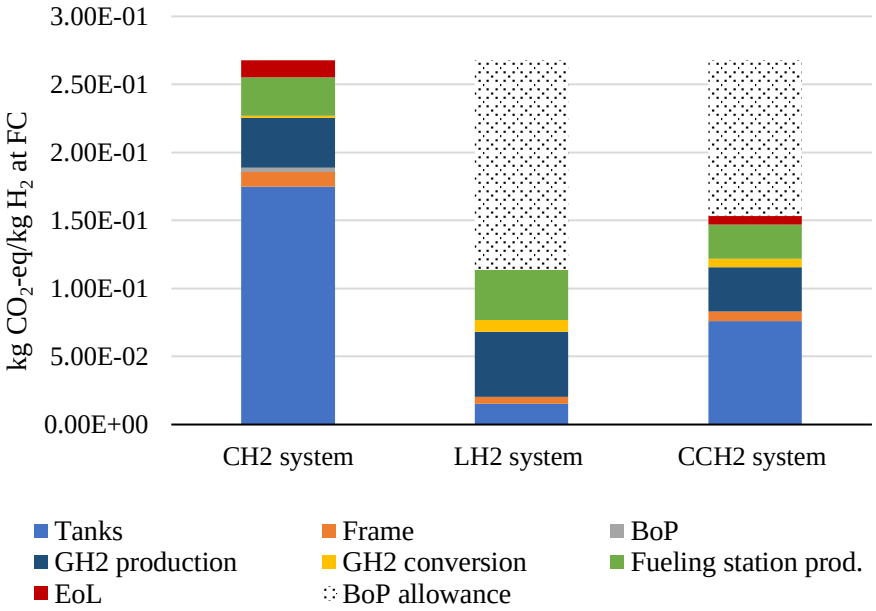

Figure 5.11. LCIA results for global warming.

5.3.2.3 Mineral Resource Scarcity

The LCIA results for the impact category of mineral resource scarcity are presented in Figure 5.12. The results show that the LH2 system causes the most impact compared to the CCH2 system and CH2 system. This impact category is dominated by the use phase of the HSSs, specifically the fueling station infrastructure and GH_2 production.

Mineral resource scarcity is closely related to the use of steel elements. Therefore, the production phase impacts, especially from tanks of the LH2 and CCH2 are significantly higher than those of the CH2 system. For the CH2 system, the main impact stems from the frame production. The impacts from the tank production are nearly the same for the LH2 and CCH2 systems. The latter weighs more, but the outer layer is composed of CFRP instead of steel. However, the bigger tank requires a more oversized frame, so the frame production has a higher impact on the CCH2 system.

The use phase impact looks almost the same for the CH2 and CCH2 systems, while the LH2 system shows a higher impact for the use phase overall. It comes from the fueling station infrastructure production, as well as the GH_2 production. The LH2 system has high hydrogen losses and a high energy demand for liquefaction like the other impact categories. These are also here the underlying causes for higher burdens. The contribution of the EoL phase of HSSs is negligible compared to the production and use phases. Compared to the CH2 system, the LH2 and CCH2 systems have BoP allowance of about -35% and -19%, respectively. It means that the BoP allowance is already exceeded.

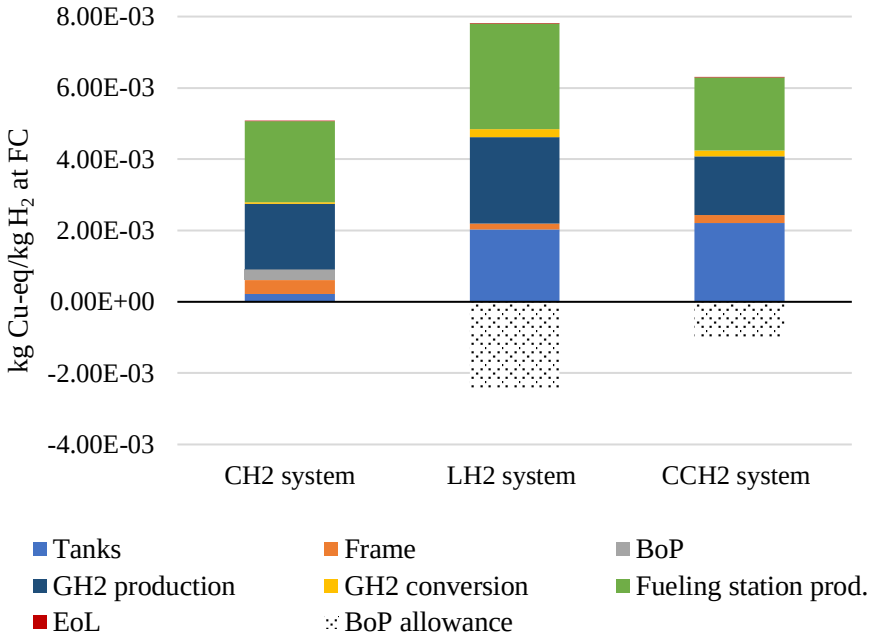

Figure 5.12. LCIA results for mineral resource scarcity.

5.3.2.4 Terrestrial Acidification

The LCIA results for the impact category of terrestrial acidification are presented in Figure 5.13. The CH2 system shows the highest impact in this category, followed by the LH2 system. The CCH2 system causes the lowest impact.

The use phase also dominates this impact category. Especially the GH_2 production causes a lot of emissions. As explained in the previous section, this is due to the high nickel content in the electrolyzer production. Since the LH2 system has the highest hydrogen losses, the impact from the GH_2 production is higher than for the other two systems, and so is the impact of the production of fueling station infrastructure. The use phase emissions for the CCH2 and CH2 systems are similar, the latter causing a little higher impact due to its higher weight-related hydrogen loss.

The production phase impact is highest for the CH2 system, followed by the CCH2 system. As discussed earlier, this is due to the suspension polymerization process in the carbon fibers production, which also explains the comparatively low impact of the LH2 system. Similar to previous impact categories, the EoL impact is negligible for all three HSSs. Compared to the CH2 system, the LH2 and CCH2 systems have a BoP allowance of about 19% and 35%, respectively, significantly higher than the impact of the CH2 system's BoP.

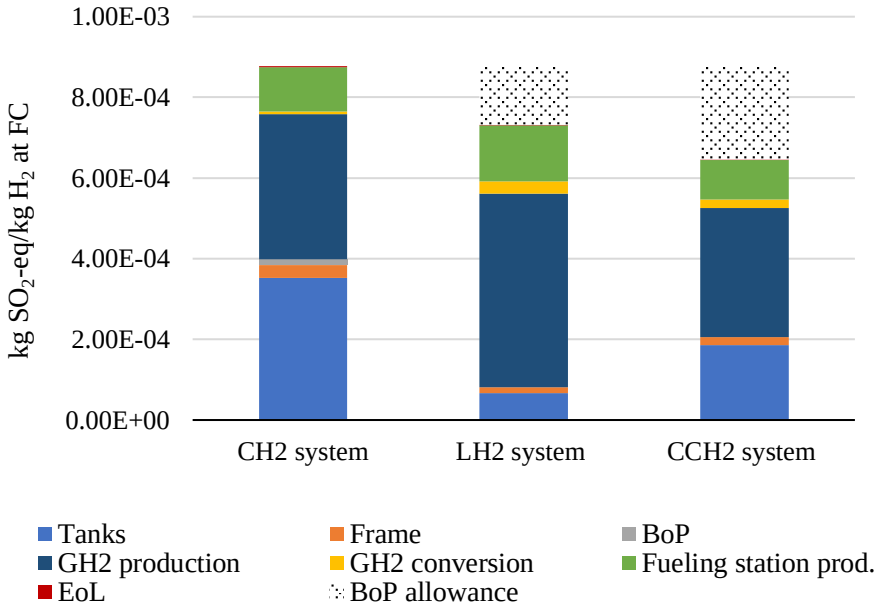

Figure 5.13. LCIA results for terrestrial acidification.

5.3.2.5 Hydrogen Compression and Liquefaction

This section presents the additional impacts of the liquefying and compressing the hydrogen used in propelling FCEV and overcoming rolling and grade resistance. These impacts are from the energy used by these processes for all the hydrogen that is delivered to the fuel cell. Figure 5.14 below shows these impacts relative to the comparative impacts presented and discussed above.

The graphs show that the impact of liquefying and compressing the hydrogen used by FCEV is quite high when comparing against the impact of the HSSs. This is especially significant for the LH2 and CCH2 systems and changes the outcome of the comparative LCA study. The CH2 system causes the lowest impact in all impact categories except global warming with these added impacts. Based on the results below, the LH2 system causes the highest environmental impacts among all the HSSs.

Consequently, this also affects the BoP allowance of the LH2 and the CCH2 system. The BoP allowance is now negative for three of the impact categories. Even though the BoP allowance for global warming is still positive, it has shrunk significantly, so it could be at risk of being exceeded.

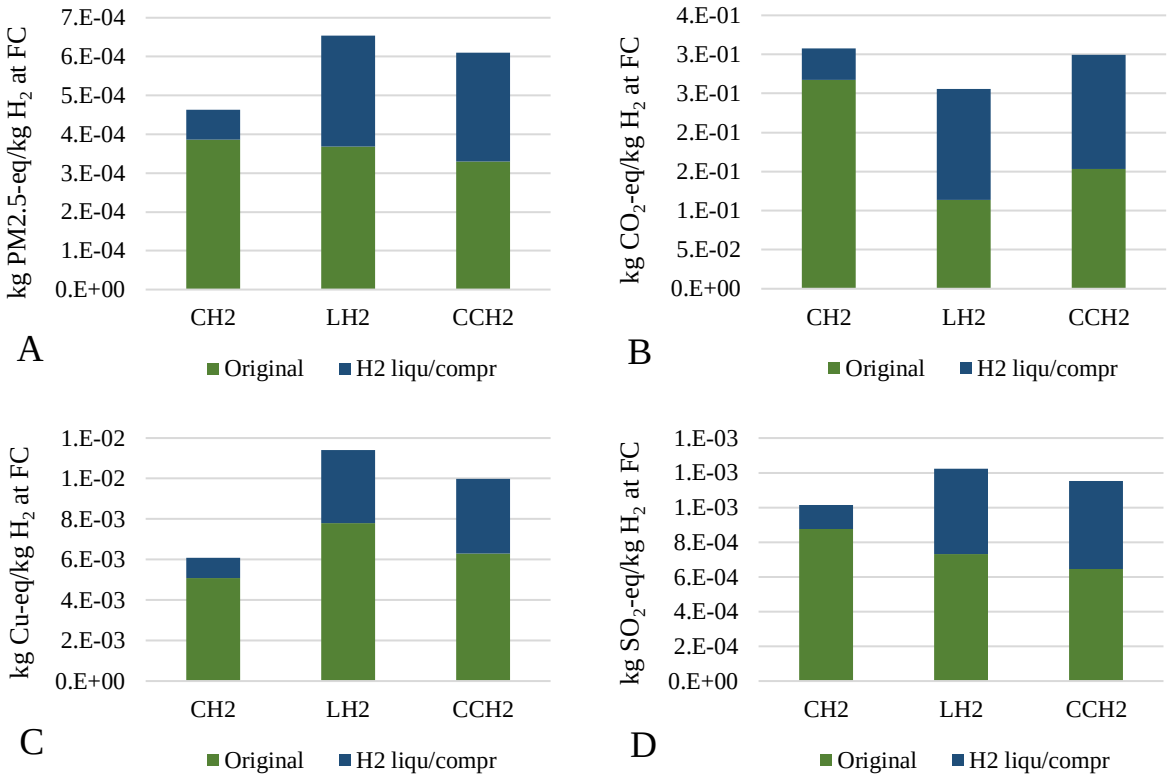

Figure 5.14. LCIA results showing the additional impacts of including the liquefaction and compression of all the hydrogen for the impact categories (A) fine particulate matter formation, (B) global warming, (C) mineral resource scarcity, and (D) terrestrial acidification.

5.3.2.6 Variation Analysis for Refueling Station Infrastructure

The hydrogen throughput of the fueling station is estimated to be too low, leading to its high share in the impacts shown in the results comparison of the HSSs. This analysis was conducted for the model that includes the additional liquefication and compression impacts to see whether a smaller fueling station utilization affects the overall outcome. As shown in the table below, increasing the daily hydrogen throughput from 130 kg to 1000 kg has a notable effect on the overall lifecycle impact in all four impact categories for all HSSs. However, increasing it further to 2000 kg does not decrease the impacts by a lot.

The increased utilization of the fueling station has decreased the overall lifecycle impacts of the LH2 system a little more than for the other two HSSs. However, the variation analysis shows that the lower fueling station impact does not change the overall results of the HSSs compared to each other.

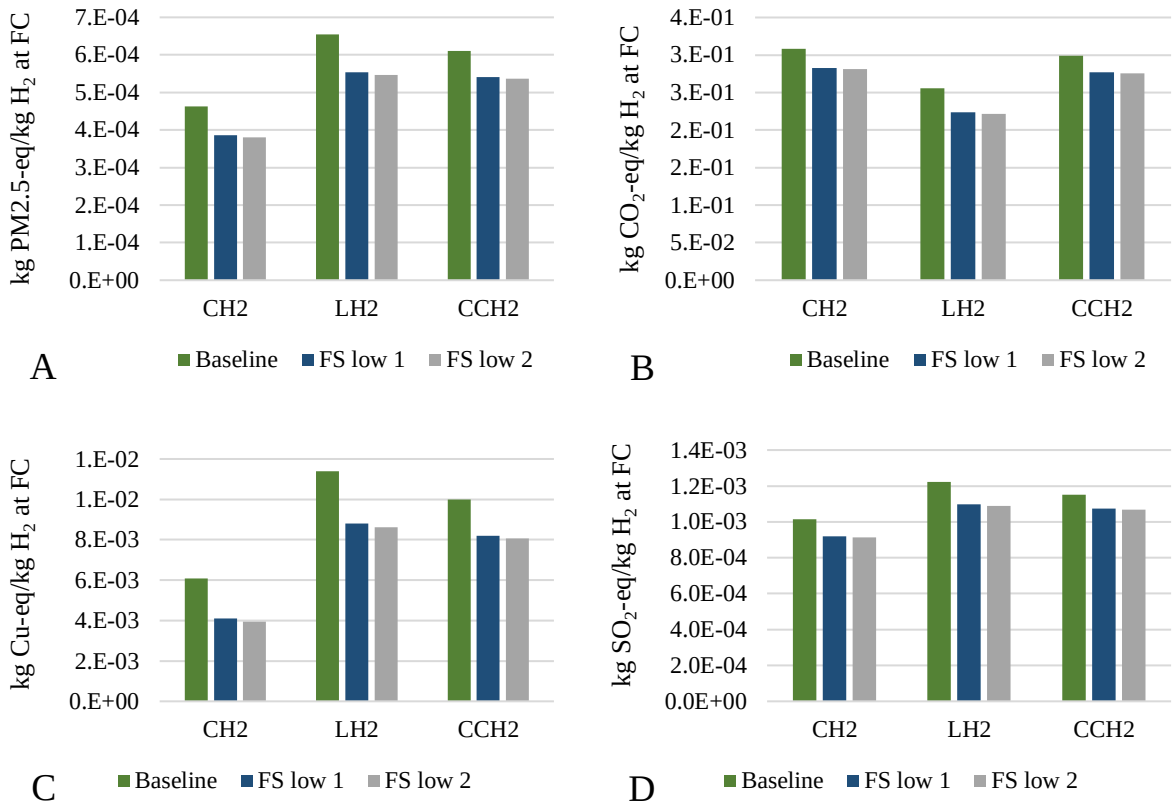

Figure 5.15. LCIA results for the variation analysis on the hydrogen throughput of the fueling station for the impact categories (A) fine particulate matter formation, (B) global warming, (C) mineral resource scarcity, and (D) terrestrial acidification.

6 Extended LCA Study of the Baseline HSS

This section extends the LCA case study for the CH2 system presented in section 5. The goal and scope, modeling aspects, and life cycle impacts of different CFRP recycling methods are presented.

6.1 Goal and Scope of Extension Study

This extension study aims to evaluate how the CH2 system is impacted if the CFRP waste is recycled for recovering carbon fibers, and the study system is credited with the recovered secondary raw material. The technical system and scope of the study are the same as described for the baseline CH2 system in section 5, except for the changed EoL phase. This study modeled the recycling EoL approach using various CFRP recycling methods compared to the cutoff EoL approach in the baseline CH2 system. This study aims to answer the RQ3 from the overall study research questions by assessing the potential effect of recycling CFRP waste on the overall life cycle impacts of the CH2 system. The specific questions answered by this study are:

(1) What is the net impact of introducing recycling of CFRP in the EoL phase of the CH2 system?
(2) How do different CFRP recycling methods compare environmental burdens and carbon fibers crediting?

6.2 Modeling of CH2 System EoL with Recycling

The EoL phase with the recycling approach was modeled to assess the effect on environmental burdens by displacing virgin carbon fibers used as primary raw material in the production phase, i.e., a closed-loop approximation modeling setup. In the EoL recycling model, the HSS was manually dismantled and separated from the FCEV. After dismantling, the tanks were separated from the HSS and then shredded. The shredded CFRP was modeled to be recycled using various recycling methods to recover carbon fiber. These carbon fibers were modeled as an avoided amount of virgin carbon fibers, which means the avoided emissions of virgin carbon fiber production were credited to the studied system. The life cycle flow chart of the CH2 system modeled with the EoL recycling approach is presented in Figure 6.1.

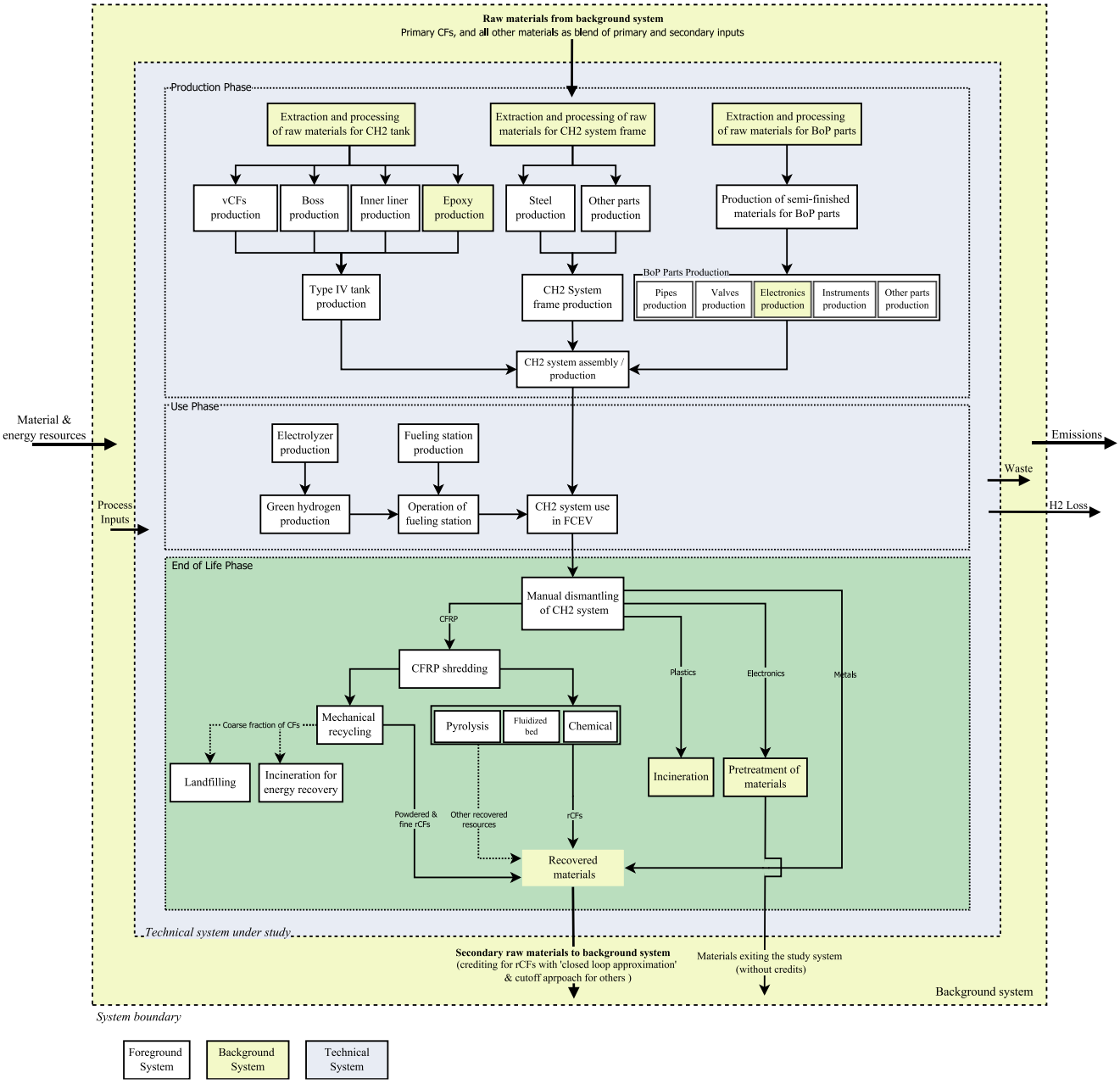

Figure 6.1. Life cycle flow chart of a CH2 Storage System including different EoL recycling process for CFRP.

6.3 CFRP Recycling Methods

Generally, the CFRP recycling methods are mechanical, thermal, and chemical (Zhang et al., 2020). These were the recycling methods investigated in this extension study to assess the impact of circular flows of carbon fibers. All the recycling methods require CFRP to be cut into smaller fragments. Among all, mechanical recycling is the most mature technology. The CFRP is either ground or milled in this method to recover carbon fibers. These carbon fibers from this method can only be downcycled to replace the use of glass fibers in manufacturing other products (Zhang et al., 2020). The carbon fibers recovered from this method are short, and their tensile strength is reduced by 35-50% compared to virgin carbon fibers (Zhu et al., 2019).

Thermal recycling can be further categorized into pyrolysis and fluidized bed recycling. In the most commercialized pyrolysis recycling, the shredded CFRP waste is thermally decomposed under inert conditions. The recovered carbon fibers lose 15-50% of their tensile strength, but the fibers are longer than those produced by the mechanical recycling method (Zhu et al., 2019). Moreover, the epoxy-based matrix is also recovered in the form of hydrocarbons, for instance, liquid benzene (Meng et al., 2018). According to Zhang et al., (2020), the pyrolysis method's technology readiness level (TRL) is '8', meaning its technology is relatively well developed and mature. CFRP waste is fed into the fluidized bed reactor in fluidized bed recycling. The epoxy content of the CFRP is decomposed in the reactor by a silica bed to release carbon fibers. The released carbon fibers are then separated by upward airflow (Meng et al., 2018). The carbon fibers recovered from this process lose their tensile strength by 25-90% (Zhu et al., 2019).

Lastly, the chemical recycling process applies the solvolysis technique using either supercritical or sub-critical solvents. This technique uses a liquid solvent and alcohol to decompose epoxy resin by inducing a depolymerization reaction. The carbon fibers are then released and separated. This method also recovers the epoxy resin (Meng et al., 2018). This method is most efficient in retaining the tensile strength of the recycled carbon fibers with losses of only about 2-15%. However, this process involves using toxic substances (Zhu et al., 2019). Moreover, the technology for this method is immature and is currently in the development stage (Zhang et al., 2020).

Except for the mechanical recycling method, the recovered carbon fibers from three methods can be used as a secondary raw material to replace virgin carbon fibers if a closed-loop recycling approach was taken. However, the mechanical properties of the carbon fibers in the recycled fibers are degraded in comparison to the virgin fibers. Therefore, to match these properties, a relatively higher weight fraction of recycled carbon fibers is required to replace the virgin carbon fibers (Meng et al., 2018). This is accounted for in the modeling of the LCA extension study and discussed in section 6.4.

6.4 LCI Analysis of EoL with Recycling

The modeling and EoL inventory aspects for recycling CFRP are discussed in this section. The recycling process was modeled with four different techniques as described above. The CH2 system was modeled to be dismounted from the FCEV and dismantled manually for its components. These steps are assumed negligible in terms of losses and energy consumption. The dismantled components are then sorted based on the type of dominant material content as described in section 0. The segregated materials are CFRP, steel, aluminum, electronics, and plastics. All the material outflows from the manual dismantling process except CFRP are modeled precisely as the EoL cutoff model. The non-shredded CFRP waste was modeled as input to the recycling process for recovering carbon fibers and then return them as secondary raw material to the background system. The LCI datasets for alternate CFRP recycling techniques were based on a study conducted by Meng et al. (2018). The original LCI datasets assumed the CFRP waste with 55 wt.% carbon fibers content for chemical and fluidized bed recycling methods. However, this study neglects the minor differences in wt.% between the carbon fibers from the tanks.

All recycling methods include a preprocess in which the CFRP is cut up into smaller pieces. In mechanical recycling, 1 kg of recycled CFRP was modeled to produce 0.24 kg of recovered carbon fibers, 0.19 kg of a fine powder, and 0.285 kg of the coarse fraction. The combination of recycled carbon fibers and fine powder was modeled as infeed to virgin glass fibers production process in the background system. The coarse fraction outflow was subject to landfilling and energy recovery in equal weight proportions. The recycled carbon fibers and coarse fraction outputs were allocated to avoid burdens in the study system. The second CFRP recycling model was based on the fluidized bed recycling technique. In addition to the environmental flows, this method was modeled to produce outputs of 0.55 kg of recycled carbon fibers per kg of CFRP waste. The third method modeled to recycle CFRP waste was based on the chemical recycling technique. 1 kg of CFRP waste recycled using this technique produced 0.55 kg of recycled carbon fibers and 0.35 kg of epoxy resin which is also a vital

material feed to the tank production process. Finally, the pyrolysis technique for recycling CFRP waste was modeled. This recycling process resulted in a throughput of 0.55 kg of recycled carbon fibers for 1 kg of CFRP waste. It also generated specific amounts of benzene, ethyl acetate, methanol, and pentane, among other outflows.

The LCI datasets representing modeling of all alternative techniques for recycling CFRP are included in the Appendix B. In addition to the main products generated by these methods, flows related to auxiliary materials and direct emissions have also been added to the annexed LCI datasets.

6.5 Extension Study Impact Assessment Results

This section presents the change in EoL impacts for different CFRP recycling methods. The results are presented in comparison to the cutoff model. In all impact categories, the production and use phase impacts stay constant for all recycling methods, while the EoL impact change due to different types of recycling. Further, the crediting of useful outputs results in negative impacts. The net life cycle impacts of studied recycling methods and the cutoff model are compared.

6.5.1 Fine particulate matter formation

Figure 6.2 shows LCIA results for fine particulate matter formation of different CFRP recycling methods It shows the differences in fine particulate matter formation impact for all EoL setups. First, the EoL impacts from direct emissions, losses and energy use caused by the different recycling routes are slightly higher than that in the baseline model. This difference is barely noticeable for mechanical and fluidized bed recycling. However, the impacts from chemical and pyrolysis recycling are higher which are triggered by toxic chemicals and higher energy inputs.

While the EoL impacts increase with recycling methods, their recyclates reduce impact as their primary production is avoided. Mechanical recycling causes the smallest credit since the low quality of recycled carbon fibers allows it to be downcycled only, replacing glass fibers with significantly lower production burdens than that of carbon fibers. The impact reduction of the other three recycling methods is larger since the recycled carbon fibers then can replace virgin carbon fibers. Fluidized bed recycling has the largest credit because it has the highest recycling efficiency. On the other hand, chemical and pyrolysis recycling increases their negative impact by recovering by-products. In chemical recycling, epoxy resin is recovered. The pyrolysis method generates numerous by-products, such as benzene, ethane, and methanol.

The increases in EoL impact and credit for material recovery are combined to get the net impacts for each recycling method. It shows that pyrolysis, chemical recycling, and fluidized bed recycling reduce fine particulate matter formation by about 20% compared to the baseline system cutoff model. These three methods only show slight variations from each other. Fluidized bed recycling showed the most significant reduction, followed by chemical and pyrolysis recycling. Mechanical recycling also decreases net impact, but by only about 2%.

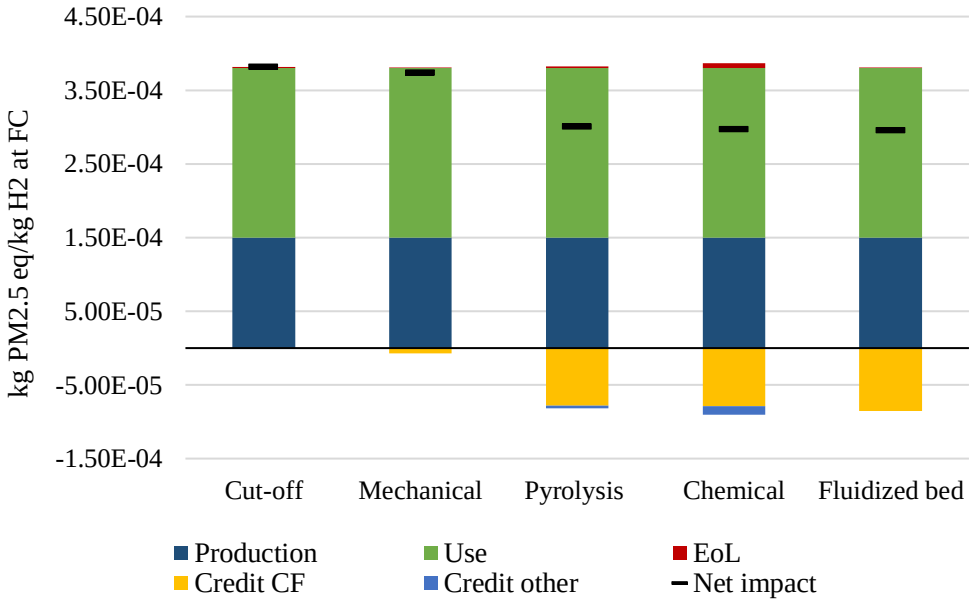

Figure 6.2. LCIA results for fine particulate matter formation of different CFRP recycling scenarios.

6.5.2 Global Warming

The comparison of the global warming impacts of recycling methods and the cutoff model is presented in Figure 6.3. The EoL processing impacts of all recycling methods against the cutoff model are relatively higher. The chemical recycling method causes the most EoL impact. The underlying process responsible for it is the production of acetic acid. It is followed by pyrolysis and mechanical recycling, causing almost similar burdens. However, the EoL phase of the fluidized bed method affects global warming by the least.

In terms of benefits from recovered materials, the fluidized bed method causes the largest credit among all recycling methods. It is followed by almost comparable credits from the chemical and pyrolysis methods. The smallest credit arises from mechanical recycling.

All the recycling methods induce lesser net life cycle impacts than the cutoff model of the baseline system. The net impacts of the fluidized bed, chemical, and pyrolysis method are around 50% less compared to the cutoff model. Among all these methods, the fluidized bed recycling method causes the least net impacts. The net impacts from chemical and pyrolysis recycling methods are comparable, however, more significant than the fluidized bed recycling. The mechanical recycling method performs worst among all the methods, and its net impacts are almost comparable to the cutoff model of baseline system.

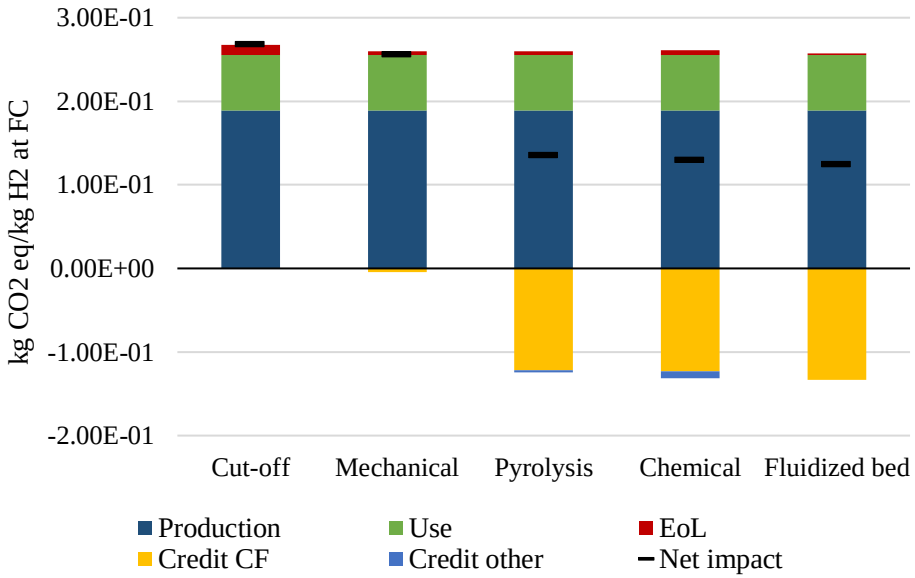

Figure 6.3. LCIA results for global warming of different CFRP recycling scenarios.

6.5.3 Mineral Resource Scarcity

The comparison of impact results for all the recycling methods and cutoff models for the mineral resource scarcity category is presented in Figure 6.4. The graph shows no visible difference in EoL processing impacts for all recycling methods compared to the cutoff model. The EoL phase of all recycling methods also reduces impacts on mineral resource scarcity. The chemical method has the highest credit among all the methods. It is followed by the fluidized bed and pyrolysis methods with comparable credit. The mechanical recycling method has the least credit. Similarly, as the above impact categories result, the fluidized bed, chemical, and pyrolysis recycling methods perform the best causing about 3% lesser net life cycle impacts than the cutoff model.

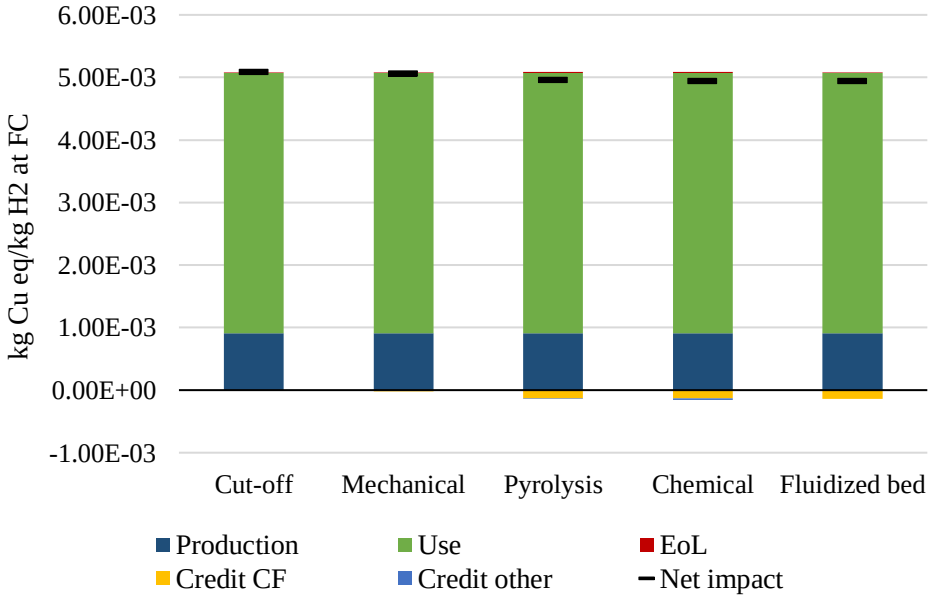

Figure 6.4. LCIA results for mineral resource scarcity of different CFRP recycling scenarios.

6.5.4 Terrestrial Acidification

Figure 6.5 presents the comparative results of all recycling methods against the cutoff model for terrestrial acidification. It can be seen from the graph that the EoL processing impacts from the chemical recycling method are significantly larger than the cutoff model. It is mostly caused by the production of acetic acid utilized as input material by this method. The impacts of the pyrolysis method are also more significant than the cutoff model. However, the EoL processing impacts from the other methods are minor and less than the cutoff model.

As for the other impact categories, the recycling methods also reduces burdens due to crediting of their outputs. The largest credit arises from chemical recycling, closely followed by the fluidized bed method. The pyrolysis method stands third in place, with mechanical recycling causing the smallest benefit in terms of avoided impact.

The CFRP recycling via fluidized bed, chemical, and pyrolysis methods cause significantly lesser net life cycle impacts. All these methods reduce the overall life cycle impacts by about 30% compared to the cutoff model. However, the mechanical recycling method reduces the overall life cycle impacts only by about 3%.

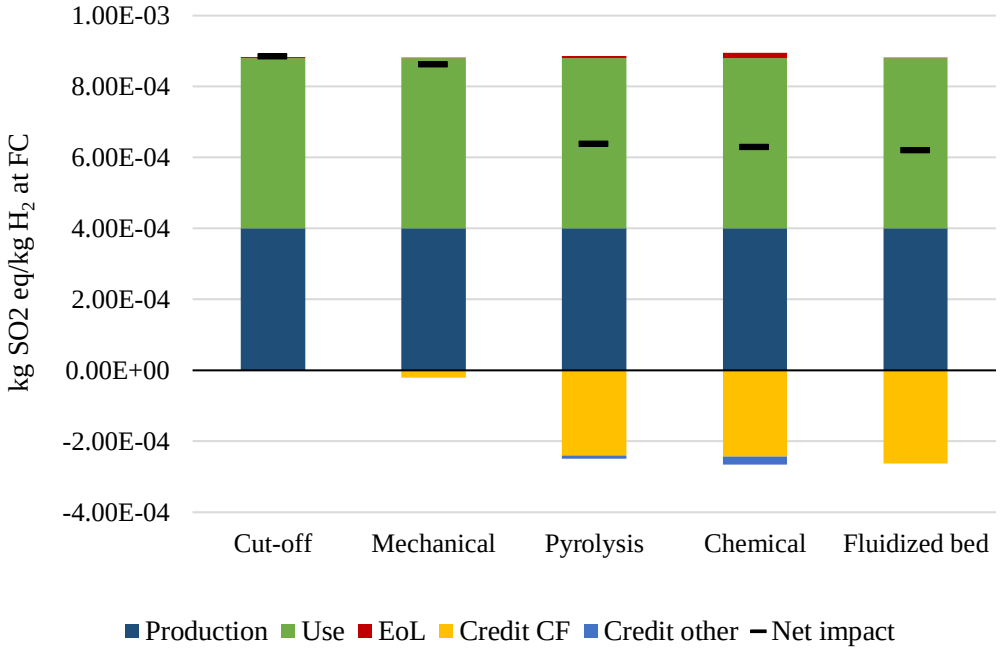

Figure 6.5. LCIA results for terrestrial acidification of different CFRP recycling scenarios.

7 Discussion

This chapter discusses the results and relates them to the research questions. The first section aims to answer what the life cycle environmental impacts of the CH2 system are, followed by the section comparing the CH2 system with the LH2 and CCH2 systems. Lastly, the third section discusses how circular material flows can be improved for the CH2 system, focusing specifically on CFRP.

7.1 Baseline HSS

The CH2 system causes emissions contributing 0.37 g of PM2.5-eq to fine particulate matter formation, 265 g of CO_2-eq to global warming, 4.85 g of Cu-eq to mineral resource scarcity, and 0.85 g of SO_2-eq to terrestrial acidification. These impacts are per kg of hydrogen delivered to the FC of an FCEV. The CH2 system delivers about 292 tons of hydrogen to the FC over its lifetime, making its full-scale impacts much higher. Considering the ambition of introducing hydrogen as a low carbon fuel option for trucks, it is notable that for every kg of hydrogen delivered to the fuel cell, a quarter of a kg of CO_2-eq is emitted by the HSS.

This comparative LCA study confirms the existing concerns in the literature regarding the potential of high impacts from carbon fibers production. This study identifies carbon fibers causing the largest share of the environmental burdens for all impact categories, except the mineral resource scarcity as the selected ReCiPe method does not include carbon-based materials in its characterization factors. Even if including them would not have significantly altered the outcomes for the mineral resource scarcity. It is because the extraction and processing of abundant fossil carbon-based materials is rather advanced, and very cost and energy efficient. For the affected impact categories, the acrylonitrile in the initial carbon fibers production step was the cause behind a significant share of the emissions. This process produces acrylonitrile which is the precursor material for carbon fibers. The acrylonitrile should be in focus when improving the CH2 system value chain. As mentioned before, other materials can also serve as a precursor, potentially reducing the impact caused by the first step of producing carbon fibers. Mineral resource scarcity is the only impact category in which the tank does not contribute the most in the production phase. Instead, a significant share is caused by the frame and the BoP components, more specifically, the valves and pipes.

As per the LCIA result, the infrastructure contributes mainly to the use phase impacts. Since the electrolyzer and the fueling station were modeled with a high level of uncertainty, their impacts could have been overestimated. As mentioned in section 5.2.2.1, the electrolyzer only produces about 130 kg of hydrogen in a day, which is very low as it would mean only about 1.6 trucks could be refueled with it daily. Moreover, the impacts from the production of fueling station infrastructure are allocated to only one FCEV refueled at the station per day. However, in real-life scenarios, the fueling station utilization is more efficient in terms of capacity for serving a relatively larger number of FCEVs. Therefore, further research with more precise data concerning the utilization rate of refueling infrastructure was required. A variation analysis for the fueling station utilization was conducted in the comparative LCA.

Additionally, the hydrogen economy will likely grow in the future. With large-scale infrastructure, the potential output would most likely increase exponentially. The contribution of infrastructure-related impacts to 1 kg of hydrogen would decrease accordingly. The EoL impact was less than 1% for all impact categories except the global warming, where it was 4%. The primary data for the EoL phase was not available and, therefore, entirely based on literature studies and assumptions. The pathway of shredding the CH2 system with the vehicle was based on assumptions. Therefore, it is possible that the impact of waste treatment was underestimated. However, due to the high production process impacts upstream of the life cycle, the EoL phase becomes relevant in material recovery rather than being a significant cause of emissions.

7.1.1 Sensitivity Analyses

The BoP and the frame of the CH2 system were both modeled based on estimates with relatively high uncertainty regarding their weight. However, the robustness check of the results has shown that their weight did not play a critical role. Changes in weight for the frame and BoP only caused a change in the impact of around 2-3% for mineral resource scarcity and 1% for the other three impact categories. It indicates that the weight of the frame and BoP components does not significantly alter the overall impact results.

7.1.2 Variation Analyses

The first variation analysis was conducted for the lifetime extension of the CH2 tanks. The maximum lifetime of a 700-bar CH2 tank could potentially be up to 15000 refueling cycles, as mentioned in section 5.1.6. Since the baseline study assumes that the tank is disposed of along with the FCEV, this scenario explored the impact change if the lifetime were extended once, and then twice. As described in the results, the first decrease in impact is relatively high for all impact categories, and however, with a second lifetime, the additional decrease is a lot less significant. It indicates that a second lifetime of the tank can be highly beneficial. Extending the lifetime further will decrease the impacts but less and less with every added lifetime. Lastly, there might be other steps involved when implementing an existing tank into a new FCEV. This could mean additional processes that would need to be included, such as transport distances. These are not included in this model. Therefore, the impacts will decrease less.

The second and third variation analysis investigated changes in the electricity input for carbon fibers production steps. Like carbon fibers production, the suspension polymerization caused significant burdens, especially in the global warming and terrestrial acidification impact categories. The high electricity demand also plays an important role. Since the tanks are manufactured in Germany, the coal-heavy electricity mix is responsible for a part of the emissions. The two electricity scenarios show how impacts could be reduced by changing the electricity mix. First, manufacturing the tanks in Sweden, where the electricity mix is less fossil-fuels dependent, can create an opportunity to reduce the burden of the tanks. The results show that this especially affects the global warming category.

The second scenario has shown the change in impacts for a 25% reduction in electricity use. The reduction also decreased the impacts, especially global warming. However, the changes are only half of what can be achieved by changing the electricity mix. It indicates that efforts should be made to increase the share of fossil-free electricity for tank manufacturing rather than focusing on reducing electricity demand. While a reduction of electricity demand can be beneficial, it should be noted that the impact reduction due to lower electricity demand will decrease if the tanks are already produced with fossil-free electricity.

7.2 HSS Comparison

As per the LCIA results, the CH2 system clearly causes the most overall life cycle impacts compared to other HSSs in three out of the four impact categories. The production of CH2 tanks using carbon fibers becomes a critical choice for environmental sustainability. However, the mineral resource scarcity is important in producing LH2 and CCH2 systems since metallic liners mostly or entirely replace the carbon fibers. However, global warming is a particularly urgent impact, making the CH2 system the least preferable choice.

The LH2 and CCH2 systems were modeled, excluding the BoP components. The difference of their impacts against the CH2 system was an emission budget for their BoP components. For most of the impact categories, the CH2 system has the most noticeable impacts, and its difference with LH2 and CCH2 systems' impacts, herein referred to as the emission budget, is very high. Adding the BoP in LH2 and CCH2 systems would cause little increments in their overall impacts. Therefore, they are very far

from exceeding their BoP emission budget. One exception is fine particulate matter formation, where the LH2 system's impact is slightly lower than that of the CH2 system. In this case, adding the BoP to the LH2 system could cause its impact to exceed that of the CH2 system. However, it is unlikely that the addition of the BoP causes significant changes in the model or significantly affects the conclusions drawn from it.

The key factors which cause the high overall use phase impacts of the LH2 system among the HSSs are the relatively higher hydrogen loss and high energy consumption in liquifying hydrogen. Especially, the higher hydrogen loss causes higher impacts. These impacts are underpinned by the increased use of refueling station infrastructure by a large amount of lost hydrogen by the LH2 system. While the LH2 system already shows significantly higher use phase emissions, these might still be underestimated. The assumption that the hydrogen is liquefied on-site is unlikely to be accurate, which means there will be further boil-off losses down the supply chain.

Additionally, the fueling station infrastructure is based on a compression system. Therefore, there might be relevant differences that affect the impact results. It also includes the modeling of the liquefaction infrastructure. On the other hand, the potential overestimate of the infrastructure's impact explained in section 7.1 also applies here and would lower the LH2 systems use phase impact. Furthermore, the hydrogen boil-off losses are highly related to the FCEV management and cannot be predicted accurately for an average HSS. The losses might be over- or underestimated depending on how the vehicle is used.

The CCH2 system can be considered a combination of the other HSSs, which is mirrored in the results. The reduced CFRP content of its tanks decreases its production phase impacts compared to the CH2 system, and lesser boil-off losses decrease its use phase impacts compared to the LH2 system. Since the CCH2 system is based on a liquid hydrogen refueling system, the limitations of the LH2 system regarding infrastructure and liquefaction also apply here.

However, it should be highlighted that the hydrogen used to propel the vehicle and overcome resistance was excluded here. However, adding the energy for liquefication and compression of all hydrogen to the model has changed the results significantly. It has increased the use phase impacts that are significantly higher for the LH2 and CCH2 systems since liquefaction takes a lot more energy than compression. Therefore, it has also changed the overall results for two of the four impact categories. Under these conditions, the LH2 system shows the largest burden in the fine particulate matter formation and terrestrial acidification impact categories, followed by the CCH2 system. It means that the CH2 system might be the preferable choice. However, it is important to discuss which of the impact categories are important in selecting an HSS. The CH2 system still has the highest global warming impact among all HSSs, and while the difference to the other systems has shrunk, this category might still be the most relevant one.

However, the energy flows in the use phase were modeled to come entirely from wind power. If instead, the energy source was fossil-based, it would have an important effect on the discrepancies between the different HSSs. Especially the energy from liquefaction and compression of the hydrogen plays a big role, and since LH2 and CCH2 systems need a lot of energy for the liquefaction, their impact would increase disproportionally to that of the CH2 system. Moreover, the increasing production of renewable electricity would also affect the production phase as energy comes from renewable sources. It would decrease the overall impacts and the focus might shift to material related impacts.

Furthermore, since wind power is the only energy source in the use phase, the hydrogen that is produced is considered "green hydrogen", which creates a much lower impact than grey hydrogen production. Even though grey hydrogen is more common as of now, the hydrogen economy is evolving with the goal to make hydrogen less impactful. Even though the use phase impacts of all the HSSs are high, it is yet undefined how these impacts will unfold in the future, since it is dependent on the hydrogen production, and therefore on the hydrogen economy. The future development of the hydrogen economy

will be crucial in defining the environmental profile of the HSSs. Various hydrogen value chain elements, such as the dominant hydrogen production pathway, distribution method, and related infrastructure will be crucial in defining the future of the HSS alternatives. For example, the potential transition from grey to either green or blue hydrogen is a relevant factor for future analysis.

7.3 Extension Study

The EoL phase of all HSSs causes the most negligible environmental impacts. However, it is equally vital when recycling of EoL waste materials is considered, especially for the CH2 system. It can be inferred from the extension study results that CFRP recycling significantly reduces the net life cycle impacts of the baseline system, making EoL a crucial life cycle phase. However, it is only possible if the FCEV is disassembled, and its waste materials are well sorted at its EoL. The manufacturer can support the disassembly by designing the FCEV to promote this EoL step and make it as easy and cost-efficient as possible.

The potential of impact reduction varies with each impact category. These variations are in line with the aforementioned impacts of carbon fibers production. The higher the impact of carbon fibers, the higher the potential reduction. It means global warming decreases the most when recycling methods are implemented. As per the results, it is preferable to recycle CFRP using any of the investigated methods, i.e., fluidized bed, chemical, or pyrolysis recycling but not the mechanical method. The pyrolysis method becomes the first choice for Volvo if only the technology readiness level is considered an important benchmark. However, the fluidized bed method shows the best results regarding recovered carbon fibers output efficiencies.

A limitation of this extension study is that the inventory data for the different recycling methods were sourced from the same scientific study, which assumes a very high efficiency. Therefore, the recycling methods may potentially vary more in their impact than represented in the LCIA results. The variation may depend on a range of different factors.

Furthermore, this study solely assesses the one-time recycling of virgin carbon fibers, while its cyclic use as a secondary raw material is excluded. However, it needs to be considered that there are potential limitations to repeated recycling of carbon fibers, such as small but continuous losses of fibers strength with every cycle. Since the recycling of carbon fibers is not yet a widely applied method, there is a lack of research regarding the retention of carbon fibers' residual quality at each recycling level. However, this topic becomes increasingly important with the rising demand for carbon fibers and as it starts to be recycled more frequently.

Moreover, the modeled CH2 system utilizes acrylonitrile precursor material to manufacture carbon fibers in an energy-intensive production chain. Advancements in alternative bio-based precursor materials, such as lignin, have been made, requiring lesser energy to manufacture carbon fibers, as mentioned in section 4.5. As observed in the variation analysis, a reduction in energy requirement can have a notable effect on the impacts, especially for global warming. Therefore, it is recommended to conduct further research to develop lignin-based carbon fibers and assess their environmental impacts.

8 Conclusion

This study has provided an extended knowledge base concerning the environmental impacts of three different HSSs: CH2 system, LH2 System, and CCH2 System, especially the CH2 system. The study findings indicate that the CH2 system, among all HSSs, causes the most significant environmental burdens, especially when it comes to global warming. The carbon fibers content of the tank was identified as the leading cause behind the environmental impacts. Variation analyses have shown that the impacts can be significantly reduced by extending the tank lifetime and shifting away from a fossil-based electricity mix.

Compared to the CH2 system, the LH2 and CCH2 systems have lower impacts except for mineral resource scarcity, where both HSSs score higher, especially the LH2 system. However, these results change when the liquefaction and compression energy for all the hydrogen is included. It shows that the high energy demand of liquefying hydrogen significantly affects the HSSs overall environmental impact. While the CH2 system now only causes the highest impact in the global warming category and the difference to the other two HSSs is a lot smaller, it is essential to acknowledge the relevance of this specific impact category.

The CH2 system is a critical option in terms of environmental impacts, mostly due to the energy-intensive carbon fiber production. In the LH2 and CCH2 systems, the use phase triggers the largest impacts due to hydrogen losses. The prominent impacts of all the HSSs are primarily rooted in the consumption of energy in their respective life cycles. It is imperative that the impacts analyzed in this study are likely to vary with further diffusion of hydrogen and other renewable energy resources within the HSS value chain. Therefore, the future selection of an HSS alternative must take place while closely considering the development of the hydrogen economy and penetration of other renewable energy resources in the energy market.

The EoL stage of the CH2 system does not add environmental burdens of significance compared to the production and use phases of the CH2 system. However, the extension study results show that if EoL waste CFRPs are recycled, it significantly reduces the net life cycle impacts of the CH2 system.

Due to the uncertainty of the underlying assumptions of this study, further research is essential to draw more concrete conclusions regarding the environmental burden of the three HSSs. The CH2 system only shows the largest global warming burden, but in combination with CFRP recycling, the CH2 system could be considered the most reasonable choice.

It is recommended to acquire primary LCI data from relevant OEMs to enable more precise results. It is vital that future LCA studies use the latest and scaled data for modeling hydrogen production and transportation, and the utilization of the refueling station infrastructure. Additionally, it is recommended to study the use of bio-based precursors for producing carbon fibers and the quality aspects of recycled carbon fibers. Finally, it is proposed that a prospective LCA is conducted with explorative scenarios, especially concerning the future hydrogen value chain and infrastructure.

9 Personal Communication

Volvo experts:

Arya, Pranav – Lead Simulation Engineer

Bergström, Johanna – Lead Research Engineer

Johansson, Monica – Principal Energy and Fuel Analyst

Haberl, Felix – Principal Concept Architect

Hagby, Anton – Lead Analysis Engineer

Kvist, Roland – Manager Product Platform Hauler

Sonderegger, Sigurd – Senior Principal Engineer, Hydrogen Storage System

10 References

Aalco. (2019, July 18). *Aluminium Alloy - Commercial Alloy - 6082 - T6~T651 Plate*. https://www.aalco.co.uk/datasheets/Aluminium-Alloy_6082-T6~T651_148.ashx#:~:text=Aluminium%20Alloy%20%2D%20Commercial%20Alloy%20%2D%206082%20%2D%20T6~T651%20Plate,-6082%20%2D%20T6~T651&text=Aluminium%20alloy%206082%20is%20a,most%20commonly%20used%20for%20machining.

AB Volvo. (2018, December 4). *Premiere for Volvo Trucks' first all-electric truck*. https://www.volvogroup.com/en/news-and-media/news/2018/apr/news-2879838.html

AB Volvo. (2021, June 8). *SBTi-approval of Volvo Group's industry-leading climate targets*. Press Release. https://www.volvogroup.com/en/news-and-media/news/2021/jun/news-3994597.html

Abdin, Z., & Khalilpour, K. R. (2019). Single and Polystorage Technologies for Renewable-Based Hybrid Energy Systems. In *Polygeneration with Polystorage: For Chemical and Energy Hubs* (pp. 77–131). Academic Press. https://doi.org/10.1016/B978-0-12-813306-4.00004-5

Allevi, C., & Collodi, G. (2017). Hydrogen production in IGCC systems. In *Integrated Gasification Combined Cycle (IGCC) Technologies* (pp. 419–443). Woodhead Publishing. https://doi.org/10.1016/B978-0-08-100167-7.00012-3

Arvidsson, R., Söderman, M. L., Sandén, B. A., Nordelöf, A., André, H., & Tillman, A. M. (2020). A crustal scarcity indicator for long-term global elemental resource assessment in LCA. *International Journal of Life Cycle Assessment*, *25*(9), 1805–1817. https://doi.org/10.1007/S11367-020-01781-1/FIGURES/6

Arvidsson, R., Tillman, A. M., Sandén, B. A., Janssen, M., Nordelöf, A., Kushnir, D., & Molander, S. (2018). Environmental Assessment of Emerging Technologies: Recommendations for Prospective LCA. *Journal of Industrial Ecology*, *22*(6), 1286–1294. https://doi.org/10.1111/JIEC.12690

Benitez, A., Wulf, C., de Palmenaer, A., Lengersdorf, M., Röding, T., Grube, T., Robinius, M., Stolten, D., & Kuckshinrichs, W. (2021). Ecological assessment of fuel cell electric vehicles with special focus on type IV carbon fiber hydrogen tank. *Journal of Cleaner Production*, *278*, 123277. https://doi.org/10.1016/J.JCLEPRO.2020.123277

Blomsma, F., & Brennan, G. (2017). The Emergence of Circular Economy: A New Framing Around Prolonging Resource Productivity. *Journal of Industrial Ecology*, *21*(3), 603–614. https://doi.org/10.1111/JIEC.12603

Bocken, N. M. P., Short, S. W., Rana, P., & Evans, S. (2014). A literature and practice review to develop sustainable business model archetypes. *Journal of Cleaner Production*, *65*, 42–56. https://doi.org/10.1016/J.JCLEPRO.2013.11.039

Booto, G. K., Aamodt Espegren, K., & Hancke, R. (2021). Comparative life cycle assessment of heavy-duty drivetrains: A Norwegian study case. *Transportation Research Part D: Transport and Environment*, *95*, 102836. https://doi.org/10.1016/J.TRD.2021.102836

Calvo, G., Mudd, G., Valero, A., & Valero, A. (2016). Decreasing Ore Grades in Global Metallic Mining: A Theoretical Issue or a Global Reality? *Resources 2016, Vol. 5, Page 36*, *5*(4), 36. https://doi.org/10.3390/RESOURCES5040036

Choksey, J. S. (2021, September 27). What's the Difference Between Gray, Blue, and Green Hydrogen? J.D. Power. https://www.jdpower.com/cars/shopping-guides/whats-the-difference-between-gray-blue-and-green-hydrogen

Cryomotive GmbH. (2021). *Cryomotive and Cryogas Technology: Introduction to RCS Pathways - Strategic Baselines and Technical Directions*.

Daimler Truck. (2021). *Daimler Truck's hydrogen-based fuel-cell truck receives license for road use*. https://media.daimlertruck.com/marsMediaSite/en/instance/ko/Daimler-Trucks-hydrogen-based-fuel-cell-truck-receives-license-for-road-use.xhtml?oid=51714040&ls=L2VuL2luc3RhbmNlL2tvLnhodG1sP29pZD05MjY1NzgyJnJlbElkPTYwODI5JmZyb21PaWQ9OTI2NTc4MiZyZXN1bHRJbmZvVHlwZUlkPTQwNjI2JnZpZXdUeXBlPXRodW1icyZzb3J0RGVmaW5pdGlvbj1QVUJMSVNIRURfQVQtMiZ0aHVtYlNjYWxlSW5kZXg9MSZyb3dDb3VudHNJbmRleD01JmZyb21JbmZvVHlwZUlkPTQwNjI4&rs=0

Dellby, C. (2021, February 10). *Ökning av förnybar elproduktion under 2020*. https://www.energimyndigheten.se/nyhetsarkiv/2021/okning-av-fornybar-elproduktion-under-2020/

Elgowainy, A., Reddi, K., & Wang, M. (2013). *Life-Cycle Analysis of Hydrogen On-Board Storage Options The 2013 DOE Fuel Cell Technologies Program Annual Merit Review and Peer Evaluation Meeting*.

Euro Inox. (2007). Stainless steel: tables of technical properties. *Stainless Steel:Tables of Technical PropertiesMaterials and Applications Series*, *5*.

European Commission, Joint Research Centre, & Institute for Environment and Sustainability. (2010). *Analysis of existing Environmental Impact Assessment methodologies for use in Life Cycle Assessment*. *1*. http://lct.jrc.ec.europa.eu/

European Environment Agency. (2018). *Carbon dioxide emissions from Europe's heavy-duty vehicles*. https://www.eea.europa.eu/themes/transport/heavy-duty-vehicles

European Environment Agency. (2019). *Greenhouse gas emissions from transport in Europe*. https://www.eea.europa.eu/data-and-maps/indicators/transport-emissions-of-greenhouse-gases/transport-emissions-of-greenhouse-gases-12

European Environment Agency. (2021). *Greenhouse gas emissions from transport in Europe*. https://www.eea.europa.eu/ims/greenhouse-gas-emissions-from-transport

European Union. (2019). *Regulation (EU) 2019/1242 of the European Parliament and of the Council* (pp. 202–240). Eurpean Parliament; Council of the European Union. https://eur-lex.europa.eu/eli/reg/2019/1242/oj

Federation of Reinforced Plastics. (2017). *Composites Market Report 2017 The global CF-and CC-Market-Michael Sauer, Michael Kühnel (CCeV) Content*.

Finnveden, G., Hauschild, M. Z., Ekvall, T., Guinée, J., Heijungs, R., Hellweg, S., Koehler, A., Pennington, D., & Suh, S. (2009). Recent developments in Life Cycle Assessment. *Journal of Environmental Management*, *91*(1), 1–21. https://doi.org/10.1016/J.JENVMAN.2009.06.018

Hazell, J. (2017). *Getting it right from the start Developing a circular economy for novel materials*. www.green-alliance.org.uk

Health Organization, W., & Office for Europe, R. (2013). *Health effects of particulate matter*. http://www.euro.who.int/pubrequest

Hermansson, F., Janssen, M., & Svanström, M. (2019). Prospective study of lignin-based and recycled carbon fibers in composites through meta-analysis of life cycle assessments. *Journal of Cleaner Production*, *223*, 946–956. https://doi.org/10.1016/J.JCLEPRO.2019.03.022

Huijbregts, M. A. J., Steinmann, Z. J. N., Elshout, P. M. F., Stam, G., Verones, F., Vieira, M., Zijp, M., Hollander, A., & van Zelm, R. (2017). ReCiPe2016: a harmonised life cycle impact assessment method at midpoint and endpoint level. *International Journal of Life Cycle Assessment*, *22*(2), 138–147. https://doi.org/10.1007/S11367-016-1246-Y/TABLES/2

HYUNDAI Truck & Bus. (n.d.). *XCIENT Fuel Cell*. Retrieved February 16, 2022, from https://trucknbus.hyundai.com/global/en/products/truck/xcient-fuel-cell

International Organization for Standardization. (2009). *ISO - ISO/TS 15869:2009 - Gaseous hydrogen and hydrogen blends — Land vehicle fuel tanks*. Gaseous Hydrogen and Hydrogen Blends — Land Vehicle Fuel Tanks. https://www.iso.org/standard/52871.html

IPCC. (2021). *Climate Change 2021: The Physical Science Basis. Contribution of Working Group I to the Sixth Assessment Report of the Intergovernmental Panel on Climate Change*.

Kim, K. H., Kabir, E., & Kabir, S. (2015). A review on the human health impact of airborne particulate matter. *Environment International*, *74*, 136–143. https://doi.org/10.1016/J.ENVINT.2014.10.005

Langmi, H. W., Engelbrecht, N., Modisha, P. M., & Bessarabov, D. (2022). Hydrogen storage. In *Electrochemical Power Sources: Fundamentals, Systems, and Applications* (pp. 455–486). Elsevier. https://doi.org/10.1016/B978-0-12-819424-9.00006-9

Lee, D. Y., Elgowainy, A., Kotz, A., Vijayagopal, R., & Marcinkoski, J. (2018). Life-cycle implications of hydrogen fuel cell electric vehicle technology for medium- and heavy-duty trucks. *Journal of Power Sources*, *393*, 217–229. https://doi.org/10.1016/J.JPOWSOUR.2018.05.012

Maack, M. (2008). *Generation, of the energy carrier hydrogen in context with electricity buering generation through fuel cells*.

MEADinfo. (2015, August 23). *Material Properties of S355 Steel - An Overview*. https://www.meadinfo.org/2015/08/s355-steel-properties.html

Mehmeti, A., Angelis-Dimakis, A., Arampatzis, G., McPhail, S. J., & Ulgiati, S. (2018). Life Cycle Assessment and Water Footprint of Hydrogen Production Methods: From Conventional to Emerging Technologies. *Environments 2018, Vol. 5, Page 24*, *5*(2), 24. https://doi.org/10.3390/ENVIRONMENTS5020024

Meng, F., Olivetti, E. A., Zhao, Y., Chang, J. C., Pickering, S. J., & McKechnie, J. (2018). Comparing Life Cycle Energy and Global Warming Potential of Carbon Fiber Composite Recycling Technologies and Waste Management Options. *ACS Sustainable Chemistry and Engineering*, *6*(8), 9854–9865. https://doi.org/10.1021/ACSSUSCHEMENG.8B01026/ASSET/IMAGES/ACSSUSCHEMENG.8B01026.SOCIAL.JPEG_V03

Millette, S., Williams, E., & Hull, C. E. (2019). Materials flow analysis in support of circular economy development: Plastics in Trinidad and Tobago. *Resources, Conservation and Recycling*, *150*, 104436. https://doi.org/10.1016/J.RESCONREC.2019.104436

Moberg, Å., Borggren, C., Finnveden, G., & Tyskeng, S. (2010). Environmental impacts of electronic invoicing. *Progress in Industrial Ecology*, *7*(2), 93–113. https://doi.org/10.1504/PIE.2010.036044

Network for Transport Measures. (n.d.). *NTMCalc 4.0*. Retrieved April 26, 2022, from https://www.transportmeasures.org/ntmcalc/v4/basic/index.html#/

Nordelöf, A., Messagie, M., Tillman, A. M., Ljunggren Söderman, M., & van Mierlo, J. (2014). Environmental impacts of hybrid, plug-in hybrid, and battery electric vehicles—what can we learn from life cycle assessment? *International Journal of Life Cycle Assessment*, *19*(11), 1866–1890. https://doi.org/10.1007/S11367-014-0788-0/TABLES/6

Nowakowska-Grunt, J., & Strzelczyk, M. (2019). The current situation and the directions of changes in road freight transport in the European Union. *Transportation Research Procedia*, *39*, 350–359. https://doi.org/10.1016/J.TRPRO.2019.06.037

Righton Blackburns. (2021). *Stainless Steel 1.4571 (316Ti)*.

Sheffield, J. W., Martin, K. B., & Folkson, R. (2014). Electricity and hydrogen as energy vectors for transportation vehicles. In *Alternative Fuels and Advanced Vehicle Technologies for Improved Environmental Performance: Towards Zero Carbon Transportation* (pp. 117–137). Woodhead Publishing. https://doi.org/10.1533/9780857097422.1.117

Shiva Kumar, S., & Himabindu, V. (2019). Hydrogen production by PEM water electrolysis – A review. *Materials Science for Energy Technologies*, *2*(3), 442–454. https://doi.org/10.1016/J.MSET.2019.03.002

Tillman, A.-M., Willskytt, S., Böckin, D., André, H., & Ljunggren, M. (2020). What circular economy measures fit what kind of product? In *Handbook of the Circular Economy* (pp. 327–342). Edward Elgar Publishing. https://doi.org/10.4337/9781788972727.00035

U.S. Department of Energy. (2009). *Energy requirements for hydrogen gas compression and liquefaction as related to vehicle storage needs*. http://www.eere.energy.gov/hydrogenandfuelcells/hydrogen_publications.html#h2_storage

Usai, L., Hung, C. R., Vásquez, F., Windsheimer, M., Burheim, O. S., & Strømman, A. H. (2021). Life cycle assessment of fuel cell systems for light duty vehicles, current state-of-the-art and future impacts. *Journal of Cleaner Production*, *280*, 125086. https://doi.org/10.1016/J.JCLEPRO.2020.125086

Villalonga, S., Nony, F., Magnier, C., Yvernes, J. L., Thomas, C., Delmas, B., & Mazabraud, P. (2009). *Composite 700 bar-vessel for on-board compressed gaseous hydrogen storag*.

Villalonga, S., Thomas, C., Nony, C., Thiebaud, F., Geli, M., Lucas, A., & Knobloch, K. (2019). Applications of full thermoplastic composite for type IV 70 MPa high pressure vessels. *International Conference on Composite Materials*. https://hal.archives-ouvertes.fr/hal-02300516

Viswanathan, B. (2017). Hydrogen Storage. In *Energy Sources* (pp. 185–212). Elsevier. https://doi.org/10.1016/B978-0-444-56353-8.00010-1

Volvo Truck. (n.d.). *Volvo FH Electric*. Retrieved February 16, 2022, from https://www.volvotrucks.com/en-en/trucks/trucks/volvo-fh/volvo-fh-electric.html

Zhang, J., Chevali, V. S., Wang, H., & Wang, C. H. (2020). Current status of carbon fibre and carbon fibre composites recycling. *Composites Part B: Engineering*, *193*, 108053. https://doi.org/10.1016/J.COMPOSITESB.2020.108053

Zhu, J. H., Chen, P. Y., Su, M. N., Pei, C., & Xing, F. (2019). Recycling of carbon fibre reinforced plastics by electrically driven heterogeneous catalytic degradation of epoxy resin. *Green Chemistry*, *21*(7), 1635–1647. https://doi.org/10.1039/C8GC03672A

A LCI Modeling of Comparative LCA Study

This section entails the modelled inventories for the entire study system described in sections 5.2 and 6.4. The bold flows are the reference flows of a process.

A.1 Production Phase

The production phase provides inventories for all the processes involved in modeling the production of the HSSs. First, the modeled inventories for various materials of significance are provided. These materials include the CFRP and specific metals for which Ecoinvent LCI datasets were modified to achieve the required metal grade. The CFRP material is used in the production of the tanks for the CH2 and CCH2 systems, while the metals are used as inputs in various production processes for all HSSs. Second, the inventories for all the production phase processes for the CH2, LH2, and CCH2 systems are given.

A.1.1 Carbon Fibers

The production of carbon fibers was modeled with LCI according to the study by Benitez et al. (2021).

Table A.1. A Suspension polymerization

Flow	**Amount**	**Unit**	**Provider**
Inputs			
acrylic acid	2.83E-02	kg	acrylic acid production, U - RoW
acrylonitrile	3.17E+00	kg	market for acrylonitrile, U - GLO
electricity	7.08E+00	kWh	market for electricity, low voltage, U - DE
heat	3.91E+01	kWh	market for heat, from steam, in chemical industry, U - RER
methyl acrylate	1.42E-01	kg	market for methyl acrylate, U - GLO
water, deionised	2.17E+00	kg	market for water, deionised, U - Europe without Switzerland
Outputs			
Polyacrylonitrile (PAN)	**2.83E+00**	**kg**	

Table A.2. B Spinning dope.

Flow	**Amount**	**Unit**	**Provider**
Input			
compressed air	1.73E-02	Nm3	compressed air production, 800 kPa gauge, >30kW, average generation, U - RER
DMSO recuperated	8.07E+00	kg	C Recuperation DMSO
electricity, low voltage	5.32E-01	kWh	market for electricity, low voltage, U - DE
ethylene glycol	1.81E-03	kg	market for ethylene glycol, U - GLO
methyl acrylate	1.13E-01	kg	market for methyl acrylate, U - GLO
nitrogen, liquid	4.45E-02	kg	air separation, cryogenic, U - RER
Polyacrylonitrile (PAN)	2.83E+00	kg	A Suspension polymerization
steam	3.23E+00	kg	steam production, in chemical industry, U - RER
Output			
Precursor	**1.08E+01**	**kg**	

Table A.3. C DMSO Recuperation.

Flow	Amount	Unit	Provider
Inputs			
Coagulated solution	0.00E+00	kg	
compressed air	2.08E-02	Nm3	compressed air production, 800 kPa gauge, >30kW, average generation, U - RER
dimethyl sulfoxide	2.54E-01	kg	market for dimethyl sulfoxide, U - GLO
DMSO & Water	0.00E+00	kg	
electricity	9.11E-01	kWh	market for electricity, low voltage, U - DE
ethylene glycol	1.96E-02	kg	ethylene glycol production, U - RER
nitrogen	4.34E-02	kg	air separation, cryogenic, U - RER
steam	1.29E+01	kg	steam production, in chemical industry, U - RER
Outputs			
dimethyl sulfoxide	4.44E+00	kg	dimethyl sulfoxide production, U - RER (avoided product)
DMSO	2.50E-01	kg	
DMSO recuperated	**8.07E+00**	**kg**	
Industrial water	5.80E+01	kg	(avoided product)

Table A.4. D Spinning process.

Flow	Amount	Unit	Provider
Inputs			
electricity	1.42E-01	kWh	market for electricity, low voltage, U - DE
ethylene glycol	8.15E-04	kg	market for ethylene glycol, U - GLO
Precursor	1.08E+01	kg	B Spinning dope
Outputs			
Coagulated fiber	**6.56E+00**	**kg**	

Table A.5. E Stretching and washing.

Flow	Amount	Unit	Provider
Inputs			
Coagulated fiber	6.56E+00	kg	D Spinning process
compressed air	3.16E-02	Nm3	market for compressed air, 1000 kPa gauge, U - RER
electricity	1.84E+00	kWh	market for electricity, low voltage, U - DE
Industrial water	4.38E+01	kg	
steam	2.91E+00	kg	steam production, in chemical industry, U - RER
water	1.76E-03	kg	water production, deionised, U - Europe without Switzerland
Outputs			
Coagulated fiber (refined)	**4.38E+00**	**kg**	

Table A.6. F Sizing 1.

Flow	Amount	Unit	Provider
Inputs			
Coagulated fiber (refined)	4.38E+00	kg	E Stretching and washing
compressed air	7.02E-04	Nm 3	market for compressed air, 1000 kPa gauge, U - RER
electricity	1.61E-01	kWh	market for electricity, low voltage, U - DE
Industrial water	3.27E+00	kg	
potassium permanganate	1.12E-01	kg	oxidation of manganese dioxide, U - RER
water	6.56E-01	kg	water production, deionised, U - Europe without Switzerland
Outputs			
PAN fiber (sized)	**4.49E+0 0**	**kg**	
Water	3.15E+00	kg	Elementary flows, Emission to water, ground water

Table A.7. G Drying 1.

Flow	Amount	Unit	Provider
Inputs			
compressed air	1.46E-03	Nm3	market for compressed air, 1000 kPa gauge, U - RER
electricity	1.76E-01	kWh	market for electricity, low voltage, U - DE
PAN fiber (sized)	4.49E+00	kg	F Sizing 1
steam	2.06E+00	kg	steam production, in chemical industry, U - RER
Outputs			
PAN fiber (dried)	**2.77E+00**	**kg**	
Water vapour	1.72E+00	kg	Elementary flows, Emission to air, unspecified

Table A.8. H Relaxation.

Flow	Amount	Unit	Provider
Inputs			
compressed air	6.40E-01	Nm3	market for compressed air, 1000 kPa gauge, U - RER
electricity	3.51E-01	kWh	market for electricity, low voltage, U - DE
ethylene glycol	7.72E-02	g	market for ethylene glycol, U - GLO
PAN fiber (dried)	2.77E+00	kg	G Drying 1
steam	9.13E-01	kg	steam production, in chemical industry, U - RER
Outputs			
PAN fiber (relaxed)	**2.76E+00**	**kg**	

Table A.9. I Sizing 2.

Flow	Amount	Unit	Provider
Inputs			
electricity	7.18E-02	kWh	market for electricity, low voltage, U - KR
ethylene glycol	6.18E-05	kg	market for ethylene glycol, U - GLO
PAN fiber (relaxed)	2.77E+00	kg	H Relaxation
silicone product	1.39E-02	kg	market for silicone product, U - RER
Outputs			
PAN fiber (sized 2)	**2.78E+00**	**kg**	

Table A.10. J Winding 1.

Flow	Amount	Unit	Provider
Inputs			
compressed air	4.24E-01	Nm3	market for compressed air, 1000 kPa gauge, U - RER
electricity	3.11E-01	kWh	market for electricity, low voltage, U - KR
PAN fiber (sized 2)	2.78E+00	kg	I Sizing 2
Outputs			
PAN fiber (winded)	**2.78E+00**	**kg**	

Table A.11. K Unwinding.

Flow	Amount	Unit	Provider
Inputs			
compressed air	1.00E-01	Nm3	market for compressed air, 800 kPa gauge, U - RER
electricity	1.30E-01	kWh	market for electricity, low voltage, U - DE
PAN fiber (winded)	2.78E+00	kg	J Winding 2
water	2.85E-01	kg	market for water, deionised, U - Europe without Switzerland
Outputs			
PAN fiber (unwound)	**2.78E+00**	**kg**	

Table A.12. L1 Exhaust gas treatment.

Flow	**Amount**	**Unit**	**Provider**
Inputs			
Ammonia	1.85E-01	kg	Elementary flows, Emission to air, unspecified
Argon	4.64E-01	kg	Elementary flows, Emission to air, unspecified
Carbon dioxide	1.82E+00	kg	Elementary flows, Emission to air, unspecified
Carbon monoxide	4.86E-01	kg	Elementary flows, Emission to air, unspecified
Cyanide	2.10E+00	kg	Elementary flows, Emission to air, unspecified
electricity	8.44E-01	MJ	market for electricity, low voltage, U - DE
Exhaust gases 1	**3.68E+01**	**kg**	**M Stabilization**
Nitrogen	2.70E+01	kg	Elementary flows, Emission to air, unspecified
Outputs			
Argon	4.64E-01	kg	Elementary flows, Emission to air, unspecified
Carbon dioxide	6.00E+00	kg	Elementary flows, Emission to air, unspecified
Nitrogen	2.74E+01	kg	Elementary flows, Emission to air, unspecified
Water vapour	7.64E+00	kg	Elementary flows, Emission to air, unspecified

Table A.13. L2 Exhaust gas treatment.

Flow	**Amount**	**Unit**	**Provider**
Input			
Air, used	3.53E+01	kg	Elementary flows, Emission to air, unspecified
compressed air	1.00E+00	Nm3	market for compressed air, 800 kPa gauge, U - RER
electricity	2.83E-01	kWh	market for electricity, low voltage, U - DE
Exhaust gases 3	**1.08E+01**	**kg**	**L2.1 Exhaust gases 3**
natural gas liquids	2.06E+00	kg	market for natural gas liquids, U - GLO
NOx retained	1.07E+01	kg	selective catalytic reduction of nitrogen oxides, U - GLO
Oxygen	1.64E+00	kg	Elementary flows, Resource, unspecified
Output			
Carbon dioxide	7.57E+00	kg	Elementary flows, Emission to air, unspecified
Nitrogen	3.71E+01	kg	Elementary flows, Emission to air, unspecified
Nitrogen oxides	1.08E-01	kg	Elementary flows, Emission to air, unspecified
Water vapour	5.11E+00	kg	Elementary flows, Emission to air, unspecified

Table A.14. L2.1 Exhaust gases 3.

Flow	**Amount**	**Unit**	**Provider**
Inputs			
Exhaust gases 2	2.91E+00	kg	O Carbonization (HT)
Exhaust gases 2	7.87E+00	kg	N Carbonization (LT)
Outputs			
Exhaust gases 3	**1.08E+01**	**kg**	

Table A.15. M Stabilization.

Flow	Amount	Unit	Provider
Inputs			
Air, used	3.66E+01	kg	Elementary flows/Emission to air/unspecified
compressed air	1.91E-01	Nm3	market for compressed air, 1000 kPa gauge, U - RER
electricity	1.88E+01	kWh	market for electricity, low voltage, U - DE
natural gas liquids	2.20E-01	kg	market for natural gas liquids, U - GLO
PAN fiber (unwound)	2.78E+00	kg	K Unwinding
Outputs			
Exhaust gases 1	3.68E+01	kg	
Oxygen	3.65E+00	kg	Elementary flows, Resource, in air
PANox (stabilised)	**2.50E+00**	**kg**	

Table A.16. N Carbonization (LT).

Flow	Amount	Unit	Provider
Inputs			
electricity	4.17E+00	kWh	market for electricity, low voltage, U - DE
ethylene glycol	7.82E-04	kg	market for ethylene glycol, U - GLO
nitrogen	6.61E+00	kg	air separation, cryogenic, U - RER
PANox (stabilised)	2.50E+00	kg	M Stabilization
steam	1.86E+00	kg	steam production, in chemical industry, U - RER
Outputs			
Air, used	2.58E+01	kg	Elementary flows, Emission to air, unspecified
Exhaust gases 2	7.87E+00	kg	
PANyc carbonized	**1.25E+00**	**kg**	

Table A.17. O Carbonization (HT).

Flow	Amount	Unit	Provider
Inputs			
electricity, low voltage	8.06E+00	kWh	market for electricity, low voltage, U - DE
ethylene glycol	7.50E-03	kg	market for ethylene glycol, U - GLO
nitrogen, liquid	2.35E+00	kg	air separation, cryogenic, U - RER
PANyc carbonized	1.25E+00	kg	N Carbonization (LT)
Outputs			
Air, used	9.54E+00	kg	Elementary flows, Emission to air, unspecified
Exhaust gases 2	2.91E+00	kg	
PAN fiber nHT	**9.84E-01**	**kg**	

Table A.18. P Electrolysis.

Flow	**Amount**	**Unit**	**Provider**
Inputs			
ammonium bicarbonate	2.12E-02	kg	ammonium bicarbonate production, U - RER
compressed air	2.93E-03	Nm3	market for compressed air, 1000 kPa gauge, U - RER
electricity	2.12E-01	kWh	market for electricity, low voltage, U - DE
ethylene glycol	1.79E-04	kg	ethylene glycol production, U - RER
Industrial water	1.76E-01	kg	
PAN fiber nHT	9.85E-01	kg	O Carbonization (HT)
water	8.86E-05	kg	market for water, deionised, U - Europe without Switzerland
Outputs			
Carbon fiber (n.E.)	**1.01E+00**	**kg**	

Table A.19. Q Washing.

Flow	**Amount**	**Unit**	**Provider**
Inputs			
Carbon fiber (n.E.)	1.01E+00	kg	P Electrolysis
compressed air	5.34E-03	Nm3	market for compressed air, 1000 kPa gauge, U - RER
electricity	4.77E-02	kWh	market for electricity, low voltage, U - DE
Industrial water	4.91E-01	kg	
Outputs			
Carbon fiber (n.W.)	**1.09E+00**	**kg**	

Table A.20. R Drying 2.

Flow	**Amount**	**Unit**	**Provider**
Inputs			
Carbon fiber (n.W.)	1.09E+00	kg	Q Washing
compressed air	0.00E+00	Nm3	market for compressed air, 1000 kPa gauge, U - RER
electricity	1.50E-01	kWh	market for electricity, low voltage, U - DE
steam	9.00E-02	kg	steam production, in chemical industry, U - RER
Outputs			
Carbon fiber (n.D.)	**1.02E+00**	**kg**	
Water vapour	7.64E-02	kg	Elementary flows, Emission to air, high population density

Table A.21. S Sizing 3.

Flow	Amount	Unit	Provider
Inputs			
Carbon fiber (n.D.)	1.02E+00	kg	R Drying 2
compressed air, 1000 kPa gauge	2.00E-03	Nm3	market for compressed air, 1000 kPa gauge, U - RER
electricity, low voltage	2.23E-02	kWh	market for electricity, low voltage, U - DE
epoxy resin insulator, SiO2	1.02E-02	kg	epoxy resin insulator, SiO2 production, U - RER
water, deionised	2.51E-04	kg	market for water, deionised, U - Europe without Switzerland
Outputs			
Carbon fiber (n.S.)	**1.03E+00**	**kg**	

Table A.22. T Drying 3.

Flow	Amount	Unit	Provider
Inputs			
Carbon fiber (n.S.)	1.03E+00	kg	S Sizing 3
compressed air, 1000 kPa gauge	7.80E-04	Nm3	market for compressed air, 1000 kPa gauge, U - RER
electricity, low voltage	4.53E-01	kWh	market for electricity, low voltage, U - DE
steam, in chemical industry	3.06E-02	kg	steam production, in chemical industry, U - RER
Outputs			
Carbon fiber (n.D2)	**1.00E+00**	**kg**	

Table A.23. U Winding 2.

Flow	Amount	Unit	Provider
Inputs			
Carbon fiber (n.D2)	1.00E+00	kg	T Drying 3
compressed air, 1000 kPa gauge	5.85E-02	Nm3	market for compressed air, 1000 kPa gauge, U - RER
electricity, low voltage	5.20E-01	kWh	market for electricity, low voltage, U - DE
Outputs			
Carbon fiber	**1.00E+00**	**kg**	

A.1.2 Metals and Alloys

Three steel grades were required to model the exact metal materials utilized in the production of all HSSs. These steel grades were stainless steel type 316, stainless steel type SS 316 Ti, and the low-carbon steel S 355. The inventories for these metals were developed by modifying the LCI datasets existing in Ecoinvent.

This section presents the material inventory for specific metals. It includes the aluminum process, which was connected to an Ecoinvent process, shown in Table A.24.

Table A.24. Aluminum 6082/61-T6 production.

Flow	**Amount**	**Unit**	**Provider**
Inputs			
aluminium alloy, AlMg3	1.00E+00	kg	aluminium alloy production, AlMg3, U - RER
Outputs			
Aluminium 6082/61-T6	**1.00E+00**	**kg**	

The stainless-steel type 316 was modeled using Ecoinvent production process *steel production, electric, chromium steel 18/8, U – RER.* This type of steel has specific composition requirements which were retrieved from Euro Inox (2007). This type of steel should contain specific chromium, molybdenum, and nickel quantities. While the chromium content was sufficient in the original Ecoinvent process, nickel was only 8% and is required to be between 10 and 13%, and there was no molybdenum which is required to be between 2.2 and 2.5%. The flow which was modified in this process is ferronickel with a 25% nickel content. The nickel was increased to be 11%, which increased the ferronickel from 0.32 to 0.44kg. An additional flow with 0.0235 kg of molybdenum was added. The iron scrap input was also modified by reducing it to balance out the added materials. Since the source process was a production process, the transport needed to be added. The transport flows were sourced and added from the Ecoinvent process *market for steel, chromium steel 18/8, U – GLO.* The added and modified flows can be found in the table below.

Table A.25. SS 316 production.

Flow	**Amount**	**Unit**	**Provider**
Modified inputs			
ferronickel	4.40E-01	kg	market for ferronickel, U - GLO
iron scrap	4.07E-01	kg	market for iron scrap, sorted, pressed, U - RER
Added inputs			
molybdenum	2.35E-02	kg	market for molybdenum, U - GLO
transport, freight train	1.90E-01	t*km	market group for transport, freight train, U - GLO
transport, freight, inland waterways, barge	2.01E-02	t*km	market group for transport, freight, inland waterways, barge, U - GLO
transport, freight, lorry, unspecified	2.07E-01	t*km	market group for transport, freight, lorry, unspecified, U - GLO
transport, freight, sea, bulk carrier for dry goods	4.41E-01	t*km	market for transport, freight, sea, bulk carrier for dry goods, U - GLO
Modified outputs			
Stainless steel 316	**1.00E+00**	**kg**	

The stainless-steel type SS 316 Ti was modified in a similar way as shown in Table A.26. It is based on the Ecoinvent production process *steel production, electric, chromium steel 18/8, U – RER*. In addition to the modifications in Table A.25, primary titanium was added as this steel type contains 0.4 to 0.7% titanium. The average quantity of the required titanium content range was added to the original process, i.e., 0.0055 kg per kg of steel output. The metal composition is retrieved from Righton Blackburns (2021).

Table A.26. SS 316 Ti production.

Flow	Amount	Unit	Provider
Modified inputs			
ferronickel	4.40E-01		market for ferronickel, U - GLO
iron scrap	4.02E-01		market for iron scrap, sorted, pressed, U - RER
Added inputs			
molybdenum	2.35E-02	kg	market for molybdenum, U - GLO
titanium, primary	5.50E-03	kg	market for titanium, primary, U - GLO
transport, freight train	1.90E-01	t*km	market group for transport, freight train, U - GLO
transport, freight, inland waterways, barge	2.01E-02	t*km	market group for transport, freight, inland waterways, barge, U - GLO
transport, freight, lorry, unspecified	2.07E-01	t*km	market group for transport, freight, lorry, unspecified, U - GLO
transport, freight, sea, bulk carrier for dry goods	4.41E-01	t*km	market for transport, freight, sea, bulk carrier for dry goods, U - GLO
Modified outputs			
Stainless steel 316Ti	**1.00E+00**	**kg**	

The inventory for low-carbon steel S 355 was developed based on the Ecoinvent production process *steel production, converter, unalloyed, U – RER*. The material composition for this grade of steel was sourced from MEADinfo (2015). The manganese content is required to be 1.6%. The relevant flow in the original process is ferromanganese with a 74.5% manganese content. This meant the manganese content of the original process is only 0.00447 kg and needed to be increased to 0.016 kg. Therefore, the ferromanganese flow was increased to 0.021477. The added material was balanced out by reducing the pig iron. Additionally, the transport flows were adopted from the process *market for steel, unalloyed, U – GLO*. The modifications and added flows can be found in Table A.27 below.

Table A.27. S 355 production.

Flow	Amount	Unit	Provider
Modified inputs			
ferromanganese	2.15E-02	kg	market for ferromanganese, high-coal, 74.5% Mn, U - GLO
pig iron	8.49E-01	kg	market for pig iron, U - RER
Added inputs			
transport, freight train	1.90E-01	t*km	market group for transport, freight train, U - GLO
transport, freight, inland waterways, barge	2.01E-02	t*km	market group for transport, freight, inland waterways, barge, U - GLO
transport, freight, lorry, unspecified	2.07E-01	t*km	market group for transport, freight, lorry, unspecified, U - GLO
transport, freight, sea, bulk carrier for dry goods	4.41E-01	t*km	market for transport, freight, sea, bulk carrier for dry goods, U - GLO
Modified outputs			
Steel S355 (galavnized and powder coated)	**1.00E+00**	**kg**	

A.1.3 CH2 System

The inventories for all the processes from the production phase of the CH2 System are presented in this appendix. First, the inventories related to the production of tank materials, the tanks and their transport are provided. Second, the production of all other sub-components of the CH2 system are presented. In the end the modeled inventories for the CH2 system assembly are tabled.

Table A.28. Boss production (Volvo).

Flow	**Amount**	**Unit**	**Provider**
Inputs			
Aluminum	1.00E+00	kg	Al 6082/61-T6 production
Outputs			
Boss	**1.00E+00**	**kg**	

Table A.29 and A.30 below show the inner liner and the tank production inventories. These LCI datasets were also sourced from Benitez et al. (2021). The flows in the Tables below were adjusted according to the CFRP content in the CH2 tanks under study.

Table A.29. Inner liner production (Benitez et al., 2021).

Flow	**Amount**	**Unit**	**Provider**
Inputs			
electricity	2.27E+01	kWh	market for electricity, low voltage, U - DE
injection moulding	9.92E+01	kg	injection moulding, U - RER
metal working	1.18E+01	kg	metal working, average for metal product manufacturing, U - RER
natural gas	9.86E+00	kg	market for natural gas, high pressure, vehicle grade, U - GLO
polyethylene	1.10E+02	kg	polyethylene production, high density, granulate, U - RER
Outputs			
Carbon dioxide	2.98E+01	kg	Elementary flows, Emission to air, unspecified
Carbon monoxide	3.24E-02	kg	Elementary flows, Emission to air, unspecified
HDPE liner	**1.18E+02**	**kg**	
Mercury	8.70E-08	kg	Elementary flows, Emission to air, unspecified
Methane	9.18E-03	kg	Elementary flows, Emission to air, unspecified
Nitrogen oxides	1.08E-02	kg	Elementary flows, Emission to air, unspecified
NMVOC	4.32E-03	kg	Elementary flows, Emission to air, unspecified
Sulfur dioxide	2.97E-04	kg	Elementary flows, Emission to air, unspecified

The LCI data for the tank production was also sourced from Benitez et al. (2021). These modelled inventories are provided in Table A.30.

Table A.30. Tank production (Benitez et al., 2021).

Flow	**Amount**	**Unit**	**Provider**
Inputs			
Boss	1.26E+01	kg	Boss production
Carbon fiber	8.06E+02	kg	U Winding 2
compressed air	1.96E+00	m3	market for compressed air, 1000 kPa gauge, U - RER
electricity	1.12E+04	MJ	market for electricity, low voltage, U - DE
epoxy resin	5.38E+02	kg	market for epoxy resin, liquid, U - RER
HDPE liner	1.19E+02	kg	Inner liner production
Outputs			
CH2 tank	**1.48E+03**	**kg**	

The transport inventories for the tanks between its locations of production and assembly of CH2 system are provided in Table A.31. The transport distances were calculated using an online tool (Network for Transport Measures, n.d.)

Table A.31. Tank transport.

Flow	**Amount**	**Unit**	**Provider**
Inputs			
CH2 system tank	1.48E+03	kg	Tank production
transport	3.48E+05	kg*km	transport, freight, lorry 3.5-7.5 metric ton, EURO6, U - RER
Outpus			
Tanks, transported	**1.48E+03**	**kg**	

There were numerous other components which were modelled in the production of a complete CH2 system. These components include frame, instruments, miscellaneous, pipes, valves, and electronics. The modelled inventories for all such components are presented in the below from Table A.32 to Table A.37

Table A.32. Frame production (Volvo).

Flow	**Amount**	**Unit**	**Provider**
Inputs			
Steel	1.00E+01	kg	S 355 production
Outputs			
Frame	**1.00E+01**	**kg**	

Table A.33. Instrument production (Volvo).

Flow	Amount	Unit	Provider
Inputs			
Aluminium 6082/61-T6	2.80E-01	kg	Al 6082/61-T6 production
Stainless steel 316	1.60E-01	kg	SS 316 production
Stainless steel 316Ti	5.60E-01	kg	SS 316Ti production
Outputs			
Instruments	**1.00E+00**	**kg**	

Table A.34. Miscellaneous production (Volvo).

Flow	Amount	Unit	Provider
Inputs			
polypropylene	5.00E-02	kg	market for polypropylene, granulate, U - GLO
Stainless steel	7.00E-01	kg	SS 316 production
Steel	2.50E-01	kg	S 355 production
Outputs			
Miscellaneous	**1.00E+01**	**kg**	

Table A.35. Pipe production (Volvo).

Flow	Amount	Unit	Provider
Inputs			
Stainless steel 316Ti	1.00E+00	kg	SS 316Ti production
Outputs			
Pipes	**1.00E+00**	**kg**	

Table A.36. Valve production (Volvo).

Flow	Amount	Unit	Provider
Inputs			
Aluminium	2.50E-01	kg	Al 6082/61-T6 production
Stainless steel	7.50E-01	kg	SS 316 production
Outputs			
Valves	**1.00E+00**	**kg**	

Table A.37. electronics production.

Flow	Amount	Unit	Provider
Inputs			
electronics, for control units	1.00E+00	kg	electronics production, for control units, U - RER
Outputs			
Electronics	**1.00E+00**	**kg**	

All the manufactured sub-components of the CH2 system were assembled. The modelled inventories for the assembly process are provided in Table A.38

Table A.38. CH2 system assembly.

Flow	Amount	Unit	Provider
Inputs			
Electronics	5.99E+00	kg	Electronics production
Frame	1.12E+03	kg	Frame production
Instruments	1.98E+01	kg	Instrument production
Miscellaneous	1.44E+01	kg	Miscellaneous production
Pipes	3.59E+01	kg	Pipes production
Tanks, transported	1.48E+03	kg	Tanks transport
Valves	3.66E+01	kg	Valves production
Outputs			
CH2 system	**2.70E+03**	**kg**	

The CH2 system after its assembly in was transported to Volvo. The modelled inventories for its transport are provided in Table A.39.

Table A.39. CH2 system, transport.

Flow	Amount	Unit	Provider
Inputs			
CH2 tank system	2.70E+03	kg	CH2 system assembly
transport	3.04E+06	kg*km	transport, freight, lorry 3.5-7.5 metric ton, EURO6, U - RER
Outputs			
CH2 system, transported	2.70E+03	**kg**	

A.1.4 LH2 & CCH2 Systems

This appendix provides the inventories for all the processes involved in production of the LH2 and CH2 systems. A few of the processes, i.e., the production of inner vessel and vacuum layer production were modelled identically between the two systems. Some of the input flows in LH2 and CH2 systems production processes were materials, such as steel grades, whose inventories have been presented in earlier in this appendix.

Table A.40, and Table A.41 present the modeled inventories to produce inner vessel and the vacuum layer.

Table A.40. Inner vessel production (Volvo).

Flow	Amount	Unit	Provider
Inputs			
Stainless steel 316	1.00E+00	kg	SS 316 production
Outputs			
Inner vessel (liner)	**1.00E+00**	**kg**	

Table A.41. Vacuum layer production (Volvo).

Flow	Amount	Unit	Provider
Inputs			
Aluminium 6082/61-T6	1.00E+00	kg	Al 6082/61-T6 production
Outputs			
Vacuum layer	**1.00E+00**	**kg**	

The energy and compressed air input for the LH2 tank production process are based on Benitez et al. (2021). Since the tanks for LH2 system does not contain CFRP, it was roughly assumed that the per kg input of CFRP is replaced with half a kilogram of stainless-steel type 316. The resulting inventory flows can be seen in the table below.

Table A.42. LH2 tank production (Benitez et al., 2021; Volvo).

Flow	Amount	Unit	Provider
Inputs			
Boss	4.49E+00	kg	Boss production
compressed air	2.58E-01	m3	market for compressed air, 1000 kPa gauge, U - RER
electricity	1.48E+03	MJ	market for electricity, low voltage, U - FR
Inner vessel (liner)	3.15E+02	kg	Inner vessel production
Stainless steel 316	3.54E+02	kg	SS 316 production
Vacuum layer	1.33E+01	kg	Vacuum layer production
Outputs			
LH2 tank	**6.87E+02**	**kg**	

Table A.43. LH2 system assembly (Volvo).

Flow	Amount	Unit	Provider
Inputs			
Frame	4.80E+02	kg	Frame production
LH2 tank	6.87E+02	kg	LH2 tank production
transport	1.95E+06	kg*km	transport, freight, lorry 3.5-7.5 metric ton, EURO6, U - RER
Outputs			
LH2 system	**1.17E+03**	**kg**	

The CCH2 tank production was also based on the LCI dataset provided by Benitez et al. (2021). However, compared to the CH2 system, modifications for the additional material inputs needed were made. Table A.44 and Table A.45 below present the modelled inventories for the CCH2 tank production, and CCH2 system assembly.

Table A.44. CCH2 tank production (Benitez et al., 2021; *Volvo).*

Flow	**Amount**	**Unit**	**Provider**
Inputs			
Boss	6.09E+00	kg	Boss production
Carbon fiber	2.78E+02	kg	U Winding 2
compressed air	9.84E-01	m3	market for compressed air, 1000 kPa gauge, U - RER
electricity (per steel)	1.77E+03	MJ	market for electricity, low voltage, U - DE
electricity (per CFRP)	3.87E+03	MJ	market for electricity, low voltage, U - DE
epoxy resin	1.85E+02	kg	market for epoxy resin, liquid, U - RER
Inner vessel (liner)	2.79E+02	kg	Inner vessel production
Stainless steel 316	4.23E+02	kg	SS 316 production
Vacuum layer	1.58E+01	kg	Vacuum layer production
Outputs			
CCH2 tank	**1.19E+03**	**kg**	

Table A.45. CCH2 system assembly (Volvo).

Flow	**Amount**	**Unit**	**Provider**
Inputs			
CCH2 tank	1.19E+03	kg	CCH2 tank production (liquid)
Frame	6.39E+02	kg	Frame production
transport	2.89E+06	kg*km	transport, freight, lorry 3.5-7.5 metric ton, EURO6, U - RER
Outputs			
CCH2 system	**1.82E+03**	**kg**	

A.2 Use Phase

The inventoried datasets for the use phase for all three HSSs are presented in this appendix.

A.2.1 CH2 System

The electricity inputs in the use phase are all based on wind power. The high voltage wind power flow from Ecoinvent was transformed to medium power using Ecoinvent transformation process *electricity voltage transformation from high to medium voltage, U – SE*. The conversion process can be seen in the table below.

Table A.46. Electricity voltage transformation from high to medium voltage, wind power, SE.

Flow	Amount	Unit	Provider
Inputs			
electricity, high voltage	1.01E+00	kWh	electricity production, wind, 1-3MW turbine, onshore, U - SE
Outputs			
electricity, medium voltage (wind power)	**1.00E+00**	**kWh**	

The LCI data for most of the use phase model was sourced from Maack (2008). This includes many use-phase processes, such as production of electrolyzer, hydrogen, and refueling station infrastructure. The modelled inventories for all these processes are given below from Table A.47 to Table A.49.

Table A.47. Electrolyzer production (Maack, 2008).

Flow	Amount	Unit	Provider
Inputs			
acrylonitrile-butadiene-styrene copolymer	5.64E-05	kg	market for acrylonitrile-butadiene-styrene copolymer, U - GLO
aluminium	1.55E-04	kg	market for aluminium, cast alloy, U - GLO
cast iron	4.80E-05	kg	market for cast iron, U - GLO
copper	5.40E-04	kg	market for copper, cathode, U - GLO
glass fibre	1.41E-04	kg	market for glass fibre, U - GLO
nickel	2.82E-03	kg	market for nickel, class 1, U - GLO
nickel	7.05E-04	kg	market for nickel, class 1, U - GLO
nylon 6-6	1.76E-05	kg	market for nylon 6-6, glass-filled, U - RER
polyethylene	1.41E-04	kg	market for polyethylene, low density, granulate, U - GLO
reinforcing steel	1.87E-03	kg	market for reinforcing steel, U - GLO
steel	5.99E-03	kg	market for steel, chromium steel 18/8, U - GLO
synthetic rubber	1.41E-04	kg	market for synthetic rubber, U - GLO
synthetic rubber	3.53E-05	kg	market for synthetic rubber, U - GLO
transport	9.91E-04	t*km	market for transport, freight, lorry 16-32 metric ton, EURO4, U - RER
tube insulation	2.40E-04	kg	market for tube insulation, elastomere, U - GLO
Outputs			
Electrolyzer per kg H_2	**1.00E+00**	**Item(s)**	

The water and electrolyzer inputs of the GH_2 production are based on Maack (2008) and the electricity input was calculated using an efficiency of 80% (Shiva Kumar & Himabindu, 2019).

Table A.48. GH_2 production.

Flow	**Amount**	**Unit**	**Provider**
Inputs			
electricity, medium voltage (wind power)	1.75E+02	MJ	electricity voltage transformation from high to medium voltage, wind power
Electrolyzer per kg H_2	1.00E+00	Item(s)	Electrolyzer production
tap water	1.00E+01	kg	market group for tap water, U - RER
Outputs			
GH_2 from wind power	**1.00E+00**	**kg**	

Table A.49. Fuel Station production (Maack, 2008).

Flow	Amount	Unit	Provider
Inputs for the Compressor			
electricity	7.05E-04	kWh	market for electricity, low voltage, U - SE
ethylene glycol	4.94E-06	kg	market for ethylene glycol, U - GLO
heat	2.54E-03	MJ	heat, from municipal waste incineration to generic market for heat district or industrial, other than natural gas, U - SE
lubricating oil	1.27E-05	kg	market for lubricating oil, U - RER
reinforcing steel	1.75E-03	kg	market for reinforcing steel, U - GLO
steel	1.34E-03	kg	market for steel, chromium steel 18/8, U - GLO
transport	3.62E-04	t*km	market for transport, freight, lorry 16-32 metric ton, EURO4, U - RER
tube insulation	1.06E-05	kg	market for tube insulation, elastomere, U - GLO
Inputs for the Operation (Maintenance)			
electricity	4.23E-02	kWh	market for electricity, medium voltage, U - SE
ethylene glycol	2.96E-04	kg	market for ethylene glycol, U - GLO
heat	1.52E-01	MJ	heat, from municipal waste incineration to generic market for heat district or industrial, other than natural gas, U - SE
lubricating oil	7.62E-04	kg	market for lubricating oil, U - RER
reinforcing steel	5.50E-02	kg	market for reinforcing steel, U - GLO
steel	3.69E-02	kg	market for steel, chromium steel 18/8, U - GLO
transport	2.20E-01	t*km	market for transport, freight, lorry 16-32 metric ton, EURO4, U - RER
Inputs for the Other components			
nitrogen	1.01E-04	kg	market for nitrogen, liquid, U - RER
polypropylene	7.05E-06	kg	market for polypropylene, granulate, U - GLO
reinforcing steel	1.16E-03	kg	market for reinforcing steel, U - GLO
steel	2.85E-04	kg	market for steel, chromium steel 18/8, U - GLO
transport	6.90E-02	t*km	market for transport, freight, lorry 16-32 metric ton, EURO4, U - RER
Inputs for the Storage module			
diesel	6.04E-04	MJ	market for diesel, burned in building machine, U - GLO
electricity	6.77E-04	kWh	market for electricity, medium voltage, U - SE
steel	5.93E-02	kg	market for steel, chromium steel 18/8, U - GLO
transport	5.93E-03	t*km	market for transport, freight, lorry 16-32 metric ton, EURO4, U - RER
Inputs for the Walls and foundation			
diesel	3.02E-02	MJ	market for diesel, burned in building machine, U - GLO
electricity	3.53E-04	kWh	market for electricity, medium voltage, U - SE
flat glass	2.29E-03	kg	market for flat glass, coated, U - RER
gravel	1.27E+00	kg	market for gravel, crushed, U - CH
gypsum fibreboard	7.05E-05	kg	market for gypsum fibreboard, U - GLO
lubricating oil	1.41E-05	kg	market for lubricating oil, U - RER
Occupation	6.44E-03	m2*a	Resource, land
reinforcing steel	6.35E-03	kg	market for reinforcing steel, U - GLO
silica sand	4.06E-02	kg	market for silica sand, U - GLO
transport	1.56E-01	t*km	market for transport, freight, lorry 16-32 metric ton, EURO4, U - RER
Outputs			
Fueling station per kg H_2	**1.00E+00**	**Item(s)**	

Table A.50. Fueling station operation CH2.

Flow	Amount	Unit	Provider
Inputs			
Fueling station per kg H_2	1.00E+00	Item(s)	Fueling station production
GH_2 from wind power	1.00E+00	kg	GH_2 production
electricity, medium voltage (wind power)	2.87E+00	kWh	electricity voltage transformation from high to medium voltage, wind power
Outputs			
GH_2 at Fuel station (880 bar, dispensed)	**1.00E+00**	**kg**	

Table A.51. Use of CH2 System.

Flow	Amount	Unit	Provider
Inputs			
CH2 system, transported	9.26E-03	kg	CH2 system, transport
GH_2 at Fuel station (880 bar, dispensed)	0.00E+00	kg	Fuel station operation CH2
GH_2 at Fuel station (880 bar, dispensed)	4.50E-02	kg	Fuel station operation CH2
Outputs			
CH2 system used	9.26E-03	kg	Shredding CH2 system
Hydrogen delivered to FC	**1.00E+00**	**kg**	

A.2.2 LH2 & CCH2 systems

The modeled inventories for the use phase processes for the LH2 system are presented from Table A.52 to Table A.55. The use phase inventories modeled for the CCH2 system can be viewed in Table A.56, and Table A.57.

Table A.52. Liquefaction

Flow	Amount	Unit	Provider
Inputs			
electricity, medium voltage (wind power)	1.00E+01	kWh	electricity voltage transformation from high to medium voltage, wind power
GH_2 from wind power	1.00E+00	kg	GH_2 production
Outputs			
Liquid GH_2	**1.00E+00**	**kg**	

The fueling station for the LH2 system was modelled slightly different than for the other two systems. The LCI dataset from Maack (2008) was sourced and modified for use. The inputs for the compressor were excluded since liquid hydrogen does not need to be compressed. The modifications can be referred to in the table below.

Table A.53. Fueling station production LH2.

Flow	**Amount**	**Unit**	**Provider**
Removed inputs of the Compressor			
electricity	7.05E-04	kWh	market for electricity, low voltage, U - SE
ethylene glycol	4.94E-06	kg	market for ethylene glycol, U - GLO
heat	2.54E-03	MJ	heat, from municipal waste incineration to generic market for heat district or industrial, other than natural gas, U - SE
lubricating oil	1.27E-05	kg	market for lubricating oil, U - RER
reinforcing steel	1.75E-03	kg	market for reinforcing steel, U - GLO
steel	1.34E-03	kg	market for steel, chromium steel 18/8, U - GLO
transport	3.62E-04	t*km	market for transport, freight, lorry 16-32 metric ton, EURO4, U - RER
tube insulation	1.06E-05	kg	market for tube insulation, elastomere, U - GLO
Modified outputs			
Fueling station per kg LH2	**1.00E+00**	**kg**	

Table A.54. Fueling station operation LH2.

Flow	**Amount**	**Unit**	**Provider**
Inputs			
Liquid GH_2	1.00E+00	kg	Liquification
Fueling station per kg LH2	1.00E+00	item(s)	Fueling station production LH2
Outputs			
Liquid GH_2 at Fuel station (dispensed)	**1.00E+00**	**kg**	

Table A.55. Use of LH2 system.

Flow	**Amount**	**Unit**	**Provider**
Inputs			
LH2 system	3.99E-03	kg	LH2 system assembly
Liquid GH_2 at Fuel station (boiled-off)	4.00E-02	kg	Fueling station operation LH2
Liquid GH_2 at Fuel station (weight-related)	1.94E-02	kg	Fueling station operation LH2
Outputs			
Hydrogen delivered to FC	**1.00E+00**	**kg**	
LH2 system used	3.99E-03	kg	Shredding LH2 system

Table A.56. Fuel station operation CCH2.

Flow	**Amount**	**Unit**	**Provider**
Inputs			
Fueling station per kg H_2	1.00E+00	Item(s)	Fueling station production
Liquid GH_2	1.00E+00	kg	Liquification
electricity, medium voltage (wind power)	4.00E-01	kWh	electricity voltage transformation from high to medium voltage, wind power
Outputs			
Liquid GH_2 at Fuel station (350 bar, dispensed)	**1.00E+00**	**kg**	

Table A.57. Use of CCH2 system.

Flow	**Amount**	**Unit**	**Provider**
Inputs			
CCH2 system	6.25E-03	kg	CCH2 system assembly (compr)
Liquid GH_2 at Fuel station (350 bar, weight-related)	3.04E-02	kg	Fuel station operation CCH2
Liquid GH_2 at Fuel station (350 bar, boiled-off)	1.00E-02	kg	Fuel station operation CCH2
Outputs			
CCH2 system used	6.25E-03	kg	Shredding CCH2 system
Hydrogen delivered to FC	**1.00E+00**	**kg**	

A.3 End of Life Phase

A.3.1 CH2 system

The shredding process for the CH2 system is an adaptation from the Ecoinvent process *treatment of used glider, passenger car, shredding, U – CH.* The table below shows the modifications of the inputs and outputs flows.

Table A.58. Shredding CH2 system.

Flow	**Amount**	**Unit**	**Provider**
Added inputs			
CH2 system used	**1.00E+00**	**kg**	
Removed inputs			
aluminium scrap, post-consumer	-4.18E-03	kg	aluminium scrap, post-consumer, Recycled Content cut-off, U - GLO
copper scrap, sorted, pressed	-6.62E-03	kg	copper scrap, sorted, pressed, Recycled Content cut-off, U - GLO
iron scrap, unsorted	-6.54E-01	kg	iron scrap, unsorted, Recycled Content cut-off, U - GLO
used glider, passenger car	1.00E+00	kg	
Added outputs			
Heavy fragments	4.57E-01	kg	Sorting HF
Light fragments	5.43E-01	kg	Sorting LF
Removed outputs			
residue from shredder fraction from manual dismantling	1.77E-01	kg	market for residue from shredder fraction from manual dismantling, U - RoW
residue from shredder fraction from manual dismantling	2.67E-03	kg	market for residue from shredder fraction from manual dismantling, U - CH
waste plastic, mixture	1.50E-02	kg	market group for waste plastic, mixture, U - RER
waste plastic, mixture	4.52E-04	kg	market for waste plastic, mixture, U - ZA
waste plastic, mixture	4.76E-04	kg	market for waste plastic, mixture, U - IN
waste plastic, mixture	1.21E-01	kg	market for waste plastic, mixture, U - RoW
waste plastic, mixture	1.92E-04	kg	market for waste plastic, mixture, U - PE
waste plastic, mixture	1.15E-03	kg	market for waste plastic, mixture, U - CO
waste plastic, mixture	1.73E-02	kg	market for waste plastic, mixture, U - BR
waste plastic, mixture	8.72E-05	kg	market for waste plastic, mixture, U - CY

Further the sorting processes for the heavy and light fragments were adapted from the Ecoinvent *process treatment of metal scrap, mixed, for recycling, unsorted, sorting, U – Europe without Switzerland.* Table A.59 and Table A.60 below show the modifications which were conducted. The loss of 0.2 kg was applied only for the heavy fragments waste stream.

Table A.59. Sorting HF.

Flow	**Amount**	**Unit**	**Provider**
Added inputs			
Heavy fragments	**1.02E+00**	**kg**	
Removed inputs			
aluminium, in mixed metal scrap	1.02E+00	kg	market for aluminium, in mixed metal scrap, U - Europe without Switzerland
Added outputs			
Aluminium	2.21E-02	kg	
Steel	9.78E-01	kg	
Removed inputs			
aluminium scrap, post-consumer, prepared for melting	1.00E+00	kg	

Table A.60. Sorting LF.

Flow	**Amount**	**Unit**	**Provider**
Added inputs			
Light fragments	**1.00E+00**	**kg**	
Removed inputs			
aluminium, in mixed metal scrap	1.02E+00	kg	market for aluminium, in mixed metal scrap, U - Europe without Switzerland
Added outputs			
CFRP & Plastics	9.96E-01	kg	CFRP & Plastic incineration
Electronics	4.07E-03	kg	Electronics shredding
Removed inputs			
aluminium scrap, post-consumer, prepared for melting	1.00E+00	kg	
municipal solid waste	2.04E-02	kg	market group for municipal solid waste, U - Europe without Switzerland

Table A.61. CFRP & Plastic incineration.

Flow	**Amount**	**Unit**	**Provider**
Inputs			
CFRP & Plastics	**1.00E+00**	**kg**	
Outputs			
waste plastic, mixture	1.00E+00	kg	treatment of waste plastic, mixture, municipal incineration, U - CH

Table A.62. Electronics shredding.

Flow	Amount	Unit	Provider
Inputs			
Electronics	**1.00E+00**	**kg**	
Outputs			
waste electric and electronic equipment	1.00E+00	kg	treatment of waste electric and electronic equipment, shredding, U - GLO

A.3.2 LH2 & CCH2 Systems

The LH2 and CCH2 systems were disposed in the same way. However, due to their different material composition, their sorting processes had different outputs. The tables below show how the CH2 EoL processes were modified to fit the LH2 and CCH2 systems.

Table A.63. Shredding LH2 system.

Flow	Amount	Unit	Provider
Modified inputs			
LH2 system used	**1.00E+00**	**kg**	
Modified outputs			
Heavy fragments	1.00E+00	kg	Sorting HF LH2
Removed outputs			
Light fragments	0.00E+00	kg	Sorting LF

Table A.64. Sorting HF LH2.

Flow	Amount	Unit	Provider
Modified inputs			
Heavy fragments	**1.02E+00**	**kg**	
Modified outputs			
Aluminium	2.59E-02	kg	
Steel	9.74E-01	kg	

Table A.65. Shredding CCH2 system.

Flow	Amount	Unit	Provider
Modified inputs			
CCH2 system used	**1.00E+00**	**kg**	
Modified outputs:			
Heavy fragments	6.10E-01	kg	Sorting HF CCH2 (liquid)
Light fragments	3.90E-01	kg	Sorting LF CCH2 (liquid)

Table A.66. Sorting HF CCH2.

Flow	**Amount**	**Unit**	**Provider**
Modified outputs			
Aluminium	3.00E-02	kg	
Steel	9.70E-01	kg	

B LCI Modeling of the Extended LCA Study

This EoL phase inventories of the CH2 system in the extended LCA study are presented in this appendix from Table B.1 to Table B.7. It includes the modelled inventories for all the CFRP recycling methods which were studied. The recycling methods were modelled according to the inventory data in the study by Meng et al. (2018). For this, it is assumed that the CH2 system is manually dismantled, and its modelled inventories can be seen below in Table B.1 .

Table B.1. Manual dismantling CH2 system HSS.

Flow	**Amount**	**Unit**	**Provider**
Inputs			
CH2 system used	**1.00E+00**	**kg**	
manual treatment facility	1.60E-08	Item(s)	market for manual treatment facility, waste electric and electronic equipment, U - GLO
Outputs			
Flow	Amount	Unit	Provider
Aluminium	1.00E-02	kg	
CFRP	4.97E-01	kg	Mechanical/Pyrolysis/Chemical/Fluidized bed recycling
Electronics	2.00E-03	kg	Electronics shredding
Plastics	4.40E-02	kg	Plastic incineration
Steel	4.47E-01	kg	

Table B.2. Mechanical recycling.

Flow	**Amount**	**Unit**	**Provider**
Inputs			
CFRP	**1.00E+00**	**kg**	
electricity	2.70E-01	MJ	market for electricity, low voltage, U - SE
electricity	4.00E-02	MJ	market for electricity, low voltage, U - SE
transport	2.00E-01	t*km	market for transport, freight, lorry 16-32 metric ton, EURO4, U - RER
Outputs			
Coarse fraction, mechanical	2.85E-01	kg	Incineration coarse CF fragments - CH
Coarse fraction, mechanical	2.85E-01	kg	Landfilling coarse CF fragments
glass fibre (avoided product)	4.30E-01	kg	glass fibre production, U - RER

Table B.3. Incineration coarse carbon fiber fragments.

Flow	**Amount**	**Unit**	**Provider**
Modified inputs			
Coarse fraction, mechanical	**1.00E+00**	**kg**	
Added outputs			
electricity (avoided product)	1.09E+00	MJ	market for electricity, for reuse in municipal waste incineration only, U - SE
heat (avoided product)	7.66E+00	MJ	market for heat, for reuse in municipal waste incineration only, U - SE

Table B.4. Landfilling coarse carbon fiber fragments.

Flow	Amount	Unit	Provider
Inputs			
Coarse fraction, mechanical	**1.00E+00**	**kg**	
transport, freight, lorry 16-32 metric ton, EURO4	1.00E-01	t*km	market for transport, freight, lorry 16-32 metric ton, EURO4, U - RER
Outputs			
inert waste, for final disposal	1.00E+00	kg	treatment of inert waste, inert material landfill, U - CH

Table B.5. Pyrolysis recycling.

Flow	Amount	Unit	Provider
Inputs			
CFRP	**1.00E+00**	**kg**	
electricity	1.37E+01	MJ	market for electricity, low voltage, U - SE
electricity	2.60E-01	MJ	market for electricity, low voltage, U - SE
natural gas	6.21E-01	m3	market for natural gas, low pressure, U - CH
transport	2.00E-01	t*km	market for transport, freight, lorry 16-32 metric ton, EURO4, U - RER
Outputs			
benzene	4.00E-02	kg	
Carbon fibers (avoided product)	4.73E-01	kg	U Winding 2
Char	1.40E-01	kg	
Ethane	2.00E-03	kg	Elementary flows, Emission to air, unspecified
ethyl acetate	1.40E-01	kg	
Methane	3.00E-03	kg	Elementary flows, Emission to air, unspecified
methanol	6.00E-02	kg	
pentane	4.00E-02	kg	
Propene	2.00E-03	kg	Elementary flows, Emission to air, unspecified
Water	3.00E-02	kg	Elementary flows, Resource/in water

Table B.6. Chemical recycling.

Flow	Amount	Unit	Provider
Inputs			
acetic acid	4.50E-01	kg	market for acetic acid, without water, in 98% solution state, U - GLO
CFRP	**1.00E+00**	**kg**	
electricity	6.50E+00	MJ	market for electricity, low voltage, U - SE
electricity	2.60E-01	MJ	market for electricity, low voltage, U - SE
sodium hydroxide	4.00E-02	kg	market for sodium hydroxide, without water, in 50% solution state, U - GLO
transport	2.00E-01	t*km	market for transport, freight, lorry 16-32 metric ton, EURO4, U - RER
water	1.35E+00	kg	market for water, deionised, U - Europe without Switzerland
Outputs			
Carbon fiber (avoided product)	4.79E-01	kg	U Winding 2
epoxy resin, liquid	3.50E-01	kg	

Table B.7. Fluidized bed recycling.

Flow	Amount	Unit	Provider
Inputs			
CFRP	**1.00E+00**	**kg**	
electricity	3.40E+00	MJ	market for electricity, low voltage, U - SE
electricity	2.60E-01	MJ	market for electricity, low voltage, U - SE
natural gas	2.87E-02	m3	market for natural gas, low pressure, U - CH
transport	2.00E-01	t*km	market for transport, freight, lorry 16-32 metric ton, EURO4, U - RER
Outputs			
Carbon dioxide	9.00E-01	kg	Elementary flows, Emission to air, unspecified
Carbon fiber (avoided product)	5.17E-01	kg	U Winding 2
Water	2.30E-01	kg	Elementary flows, Emission to air, unspecified

C Selected LCIA Impact Results

This appendix provides the details of the selected LCIA results for the robustness analyses for the CH2 system and the comparison of the LH2 and CCH2 system to CH2 system. It also presents the LCIA results for the compression or liquefaction of the hydrogen use. Additionally, the results for the variation analyses conducted for the utilization rate of the fueling station for all HSSs is also given.

C.1 CH2 System

The results of various robustness analyses conducted for the CH2 system are presented below from Table C.1 to Table C.5.

Table C.1. LCIA results of the sensitivity analysis for the weight of BoP components.

Indicator	**Baseline**	**BoP high**	**BoP low**	**Unit**
Fine particulate matter formation	3.86E-04	3.91E-04	3.82E-04	kg PM2.5 eq
Global warming	2.68E-01	2.70E-01	2.66E-01	kg CO2 eq
Mineral resource scarcity	5.08E-03	5.23E-03	4.92E-03	kg Cu eq
Terrestrial acidification	8.77E-04	8.84E-04	8.70E-04	kg SO2 eq

Table C.2. LCIA results of the sensitivity analysis for the frame weight.

Indicator	**Baseline**	**Frame high**	**Frame low**	**Unit**
Fine particulate matter formation	3.86E-04	3.91E-04	3.81E-04	kg PM2.5 eq
Global warming	2.68E-01	2.71E-01	2.65E-01	kg CO2 eq
Mineral resource scarcity	5.08E-03	5.15E-03	5.00E-03	kg Cu eq
Terrestrial acidification	8.77E-04	8.84E-04	8.70E-04	kg SO2 eq

Table C.3. LCIA results of the variation analysis of the lifetime of the CH2 tank.

Indicator	**CH2 system 1 tank lifetime**	**CH2 system 2 tank lifetime**	**CH2 system 3 tank lifetime**
Fine particulate matter formation	3.86E-04	3.30E-04	3.10E-04
Global warming	2.68E-01	1.75E-01	1.44E-01
Mineral resource scarcity	5.08E-03	4.97E-03	4.93E-03
Terrestrial acidification	8.77E-04	7.00E-04	6.40E-04

Table C.4. LCIA results of the variation analysis on the location of the CH2 tank production.

Indicator	**Electricity mix DE**	**Electricity mix SE**	**Unit**
Fine particulate matter formation	3.86E-04	3.60E-04	kg PM2.5 eq
Global warming	2.68E-01	2.03E-01	kg CO2 eq
Mineral resource scarcity	5.08E-03	5.07E-03	kg Cu eq
Terrestrial acidification	8.77E-04	7.90E-04	kg SO2 eq

Table C.5. LCIA results for the variation analysis of reducing the electricity input for carbon fiber production.

Indicator	**Baseline**	**25% electricity reduction**	**Unit**
Fine particulate matter formation	3.86E-04	3.80E-04	kg PM2.5 eq
Global warming	2.68E-01	2.49E-01	kg CO2 eq
Mineral resource scarcity	5.08E-03	5.05E-03	kg Cu eq
Terrestrial acidification	8.77E-04	8.50E-04	kg SO2 eq

C.2 HSSs Comparison

The results from Table C.6 to Table C.9 are the comparative LCIA results of the CH2, LH2 and CCH2 systems for four impact categories.

Table C.6. HSS comparison on fine particulate matter formation.

Life cycle phases	**CH2 system**	**LH2 system**	**CCH2 system**
Fine particulate matter formation [kg PM2.5 eq/kg H_2 at FC]			
Production phase			
Tanks	1.20E-04	5.11E-05	9.44E-05
Frame	2.37E-05	1.02E-05	1.40E-05
BoP	9.27E-06	-	-
Total contribution	1.53E-04	6.14E-05	1.08E-04
Use phase			
GH_2 production	1.40E-04	1.80E-04	1.30E-04
GH_2 liqu/compr	3.64E-06	1.68E-05	1.19E-05
Fueling station	8.82E-05	1.10E-04	7.92E-05
Total contribution	2.32E-04	3.07E-04	2.21E-04
EoL phase			
	1.29E-06	2.84E-07	7.53E-07
Total contribution	1.29E-06	2.84E-07	7.53E-07
Total life cycle contribution	**3.86E-04**	**3.68E-04**	**3.30E-04**
BoP Allowance		1.75E-05	5.57E-05

Table C.7. HSS comparison on global warming.

Life cycle phases	**CH2 system**	**LH2 system**	**CCH2 system**
Global warming [kg CO_2 eq/kg H_2 at FC]			
Production phase			
Tanks	1.75E-01	1.54E-02	7.61E-02
Frame	1.11E-02	4.84E-03	6.89E-03
BoP	3.10E-03	-	-
Total contribution	1.89E-01	2.02E-02	8.30E-02
Use phase			
GH_2 production	3.64E-02	4.81E-02	3.27E-02
GH_2 liqu/compr	1.87E-03	8.61E-03	6.09E-03
Fueling station	2.82E-02	3.67E-02	2.54E-02
Total contribution	6.65E-02	9.34E-02	6.41E-02
EoL phase			
	1.22E-02	2.22E-04	6.03E-03
Total contribution	1.22E-02	2.22E-04	6.03E-03
Total life cycle contribution	**2.68E-01**	**1.14E-01**	**1.53E-01**
BoP Allowance		1.54E-01	1.14E-01

Table C.8. HSS comparison for mineral resource scarcity.

Life cycle phases	**CH2 system**	**LH2 system**	**CCH2 system**
Mineral resource scarcity [kg Cu eq/kg H_2 at FC]			
Production phase			
Tanks	2.20E-04	2.04E-03	2.21E-03
Frame	3.89E-04	1.63E-04	2.25E-04
BoP	3.02E-04	-	-
Total contribution	9.11E-04	2.20E-03	2.44E-03
Use phase			
GH_2 production	1.83E-03	2.42E-03	1.65E-03
GH_2 liqu/compr	4.72E-05	2.20E-04	1.56E-04
Fueling station	2.28E-03	2.97E-03	2.05E-03
Total contribution	4.16E-03	5.61E-03	3.86E-03
EoL phase			
	4.00E-06	1.32E-06	2.52E-06
Total contribution	4.00E-06	1.32E-06	2.52E-06
Total life cycle contribution	**5.07E-03**	**7.81E-03**	**6.29E-03**
BoP Allowance		-2.74E-03	-1.22E-03

Table C.9. HSS comparison for terrestrial acidification.

Life cycle phases	**CH2 system**	**LH2 system**	**CCH2 system**
Terrestrial acidification [kg SO_2 eq/kg H_2 at FC]			
Production phase			
Tanks	3.52E-04	6.70E-05	1.86E-04
Frame	3.28E-05	1.42E-05	1.97E-05
BoP	1.36E-05	-	-
Total contribution	3.98E-04	8.13E-05	2.06E-04
Use phase			
GH_2 production	3.60E-04	4.80E-04	3.20E-04
GH_2 liqu/compr	6.50E-06	2.98E-05	2.11E-05
Fueling station	1.09E-04	1.40E-04	9.77E-05
Total contribution	4.76E-04	6.50E-04	4.39E-04
EoL phase			
	3.20E-06	6.82E-07	1.85E-06
Total contribution	3.20E-06	6.82E-07	1.85E-06
Total life cycle contribution	**8.77E-04**	**7.32E-04**	**6.47E-04**
BoP Allowance		1.46E-04	2.31E-04

The tables from Table C.10 to Table C.13 provide the LCIA results when compression or liquefaction of the used hydrogen is added to the modeling of all HSSs.

Table C.10. LCIA results for fine particulate matter formation including liquefaction and compression energy of all hydrogen.

	CH2	**LH2**	**CCH2**	**Unit**
Without add. H_2 compr./liqu	3.86E-04	3.68E-04	3.30E-04	kg PM2.5 eq
With add. H_2 compr./liqu.	7.74E-05	2.86E-04	2.80E-04	kg PM2.5 eq
New total	4.63E-04	6.54E-04	6.10E-04	kg PM2.5 eq

Table C.11. LCIA results for global warming including liquefaction and compression energy of all hydrogen.

	CH2	**LH2**	**CCH2**	**Unit**
Without add. H_2 compr./liqu	2.68E-01	1.14E-01	1.53E-01	kg CO_2 eq
With add. H_2 compr./liqu.	3.97E-02	1.42E-01	1.46E-01	kg CO_2 eq
New total	3.07E-01	2.56E-01	2.99E-01	kg CO_2 eq

Table C.12. LCIA results for mineral resource scarcity including liquefaction and compression energy of all hydrogen.

	CH2	**LH2**	**CCH2**	**Unit**
Without add. H_2 compr./liqu	5.07E-03	7.81E-03	6.29E-03	kg Cu eq
With add. H_2 compr./liqu.	1.00E-03	3.58E-03	3.68E-03	kg Cu eq
New total	6.08E-03	1.14E-02	9.98E-03	kg Cu eq

Table C.13. LCIA results for terrestrial acidification including liquefaction and compression energy of all hydrogen.

	CH2	**LH2**	**CCH2**	**Unit**
Without add. H_2 compr./liqu	8.77E-04	7.32E-04	6.47E-04	kg SO_2 eq
With add. H_2 compr./liqu.	1.38E-04	4.92E-04	5.06E-04	kg SO_2 eq
New total	1.01E-03	1.22E-03	1.15E-03	kg SO_2 eq

Table C.14. LCIA results of the fueling station utilization variation analysis for fine particulate matter formation.

	CH2	**LH2**	**CCH2**	**Unit**
Baseline	4.63E-04	6.54E-04	6.10E-04	kg PM2.5 eq
FS low 1	3.87E-04	5.54E-04	5.41E-04	kg PM2.5 eq
FS low 2	3.81E-04	5.47E-04	5.36E-04	kg PM2.5 eq

Table C.15. LCIA results of the fueling station utilization variation analysis for global warming.

	CH2	**LH2**	**CCH2**	**Unit**
Baseline	3.08E-01	2.56E-01	2.99E-01	kg CO2 eq
FS low 1	2.83E-01	2.24E-01	2.77E-01	kg CO2 eq
FS low 2	2.81E-01	2.22E-01	2.76E-01	kg CO2 eq

Table C.16. LCIA results of the fueling station utilization variation analysis for mineral resource scarcity.

	CH2	**LH2**	**CCH2**	**Unit**
Baseline	6.08E-03	1.14E-02	9.98E-03	kg Cu eq
FS low 1	4.09E-03	8.81E-03	8.19E-03	kg Cu eq
FS low 2	3.95E-03	8.62E-03	8.06E-03	kg Cu eq

Table C.17. LCIA results of the fueling station utilization variation analysis for terrestrial acidification.

	CH2	**LH2**	**CCH2**	**Unit**
Baseline	1.01E-03	1.22E-03	1.15E-03	kg SO2 eq
FS low 1	9.20E-04	1.10E-03	1.07E-03	kg SO2 eq
FS low 2	9.13E-04	1.09E-03	1.07E-03	kg SO2 eq

D LCIA Results for the Extended LCA Study

The LCIA results of the extended study conducted for the CH2 system are given below from Table D.1 to Table D.4. These results are presented for all the recycling methods which were modeled and are distributed according to the life cycle phase. The accounted credits from recycling as well as the net life cycle impacts are also given.

Table D.1. LCIA results for the impact category fine particulate matter formation [kg PM2.5-eq/kg H_2 at FC] comparing CFRP recycling methods.

EoL Methods	Production	Use	EoL	Credit CF	Credit other	Net impact
Cut-off	1.53E-04	2.32E-04	1.29E-06	0.00E+00	0.00E+00	3.81E-04
Mechanical	1.53E-04	2.32E-04	3.92E-07	-7.45E-06	0.00E+00	3.73E-04
Pyrolysis	1.53E-04	2.32E-04	2.13E-06	-7.80E-05	-3.87E-06	3.00E-04
Chemical	1.53E-04	2.32E-04	6.94E-06	-7.89E-05	-1.15E-05	2.96E-04
Fluidized bed	1.53E-04	2.32E-04	4.16E-07	-8.53E-05	0.00E+00	2.95E-04

Table D.2. LCIA impact results for the impact category global warming [kg CO_2-eq/kg H_2 at FC] comparing CFRP recycling methods.

EoL Methods	Production	Use	EoL	Credit CF	Credit other	Net impact
Cut-off	1.89E-01	6.65E-02	1.22E-02	0.00E+00	0.00E+00	2.68E-01
Mechanical	1.89E-01	6.65E-02	4.37E-03	-4.21E-03	0.00E+00	2.56E-01
Pyrolysis	1.89E-01	6.65E-02	4.14E-03	-1.22E-01	-2.62E-03	1.35E-01
Chemical	1.89E-01	6.65E-02	5.27E-03	-1.23E-01	-8.15E-03	1.30E-01
Fluidized bed	1.89E-01	6.65E-02	1.48E-03	-1.33E-01	0.00E+00	1.24E-01

Table D.3. LCIA impact results for the impact category mineral resource scarcity [kg CU-eq/kg H_2 at FC] comparing CFRP recycling methods.

EoL Methods	Production	Use	EoL	Credit CF	Credit other	Net impact
Cut-off	9.11E-04	4.16E-03	4.00E-06	0.00E+00	0.00E+00	5.07E-03
Mechanical	9.11E-04	4.16E-03	1.75E-06	-2.31E-05	0.00E+00	5.05E-03
Pyrolysis	9.11E-04	4.16E-03	1.69E-05	-1.31E-04	-6.00E-06	4.95E-03
Chemical	9.11E-04	4.16E-03	1.86E-05	-1.33E-04	-2.16E-05	4.93E-03
Fluidized bed	9.11E-04	4.16E-03	4.82E-06	-1.43E-04	0.00E+00	4.93E-03

Table D.4. LCIA impact results for the impact category terrestrial acidification [kg SO_2-eq/kg H_2 at FC] comparing CFRP recycling methods.

EoL Methods	Production	Use	EoL	Credit CF	Credit other	Net impact
Cut-off	3.98E-04	4.76E-04	3.20E-06	0.00E+00	0.00E+00	8.83E-04
Mechanical	3.98E-04	4.76E-04	1.74E-06	-2.10E-05	0.00E+00	8.61E-04
Pyrolysis	3.98E-04	4.76E-04	6.38E-06	-2.41E-04	-9.10E-06	6.37E-04
Chemical	3.98E-04	4.76E-04	1.50E-05	-2.43E-04	-2.30E-05	6.29E-04
Fluidized bed	3.98E-04	4.76E-04	1.78E-06	-2.63E-04	0.00E+00	6.19E-04

DEPARTMENT OF TECHNOLOGY MANAGEMENT AND ECONOMICS
DIVISION OF ENVIRONMENTAL SYSTEMS ANALYSIS
CHALMERS UNIVERSITY OF TECHNOLOGY
Gothenburg, Sweden
www.chalmers.se

CHALMERS
UNIVERSITY OF TECHNOLOGY